University of Alberta

Diaspores and degradative abilities of select dematiaceous hyphomycetes

by

Melissa Jane Day

A thesis submitted to the Faculty of Graduate Studies and Research
in partial fulfillment of the requirements for the degree of

Doctor of Philosophy

in

Ecology

Department of Biological Sciences

Fall 2010
Edmonton, Alberta

Examining Committee

Randolph Currah, Biological Sciences, Supervisor

Julia Foght, Biological Sciences, Committee Member

Lynne Sigler, Biological Sciences, Committee Member

Stephen Strelkov, Agriculture, Food, and Nutritional Science, Internal External Examiner

Jocelyn Hall, Biological Sciences, Examining Committee

Robert Blanchette, Plant Pathology, University of Minnesota, External Examiner

“If I have seen further, it is by standing on the shoulders of giants.”
Sir Isaac Newton

This thesis is dedicated to my giants.

Abstract

Dematiaceous hyphomycetes are a taxonomically diverse artificial assemblage of conidial fungi that have dark pigments known as melanins in their walls. Select dematiaceous hyphomycetes from the Coniochaetales, Pleosporales, and Helotiales obtained from arctic and alpine bryophytes and vascular plant roots were chosen for further study. Eight isolates, all from roots of *Saxifraga oppositifolia*, represented a new species of *Monodictys, M. arctica.* This species, characterised by large, darkly pigmented, multicelled, often branching conidia, was most closely related to members of the *Leptosphaeria*, making *M. arctica* potentially the first non-pycnidial anamorph associated with that genus. In alpine glacial forefields, the primary colonisers are bryophytes, which form an organic grout between the rocks. These mosses trap organic particles. Three pleosporalean fungi were isolated from this grout and examined to see if they could degrade moss. All three removed the outer, cellulose rich layer of the cells, but not the inner, polyphenol rich layer. I propose that the mosses disarticulate after degradation and the fragments are trapped in the grout, increasing soil organic matter and aiding pedogenesis. This first soil ostensibly facilitates colonisation by vascular plants, the roots of which are colonised by dark septate endophytes (DSE), a group known for asymptomatically colonising vascular plant roots and thought to be quasi-mycorrhizal. *Cadophora luteo-olivacea, Cadophora melinii, Leptodontidium orchidicola, Phialocephala fortinii* and *Coniochaeta nepalica* were examined for their abilities to degrade moss. All showed that colonisation patterns varied along with the formation of conidia and

sclerotic structures, which could serve as inocula for establishing species of vascular plants. *Cadophora* and *Phialocephala* are delineated by phialide complexity, so I decided traced the origin and evolutionary history of that character on a phylogenetic framework. Based on this reconstruction, phialide complexity is a good character for separating the two genera. I propose that the sclerotium of the outgroup taxon, which develops phialides that produce spermatia, evolved into the phialidic heads of *Phialocephala*, which resemble sclerotia, and then into the solitary phialides of *Cadophora*. Traits in the sexual fungi associated with these asexual taxa support the phylogenetic placement of the asexual fungi.

Acknowledgements
The following people deserve many thanks for their help along the way.

Randy Currah – for being there at every step with guidance, enthusiasm, support, encouragement, and a wealth of knowledge that is truly amazing. And your taste in music is impeccable.

Lynne Sigler, Julia Foght, and Jocelyn Hall – for their insightful comments, helpful suggestions, and advice when I needed it most.

Kay and Andy Day – for going above and beyond the call of parental duty too many times to count by keeping their TV permanently locked to English rugby and Top Gear.

Akihiko Tsuneda and Randy Mandrake – for their expertise in SEM and thin sectioning.

Michael Hertwig-Jaksch – for the Latin diagnosis

MBSU – for help with DNA sequencing.

Karen Romanyk – for help with media, cultures, autoclaves, dishwashers, and endless questions about whether quiz answers deserve part marks.

My friends and family – for putting up with a stressed out grad student.

Members of the Currah, Hall, and LaFarge labs – for help, advice, and friendship. One day, we'll have sushi when it's hot and tea when it's cold.

Marie Davey, Marcie Plishka, Winnie Wang, Yuumi Currah, and Tyler Watson – for moss ID, help in the field, and offering to wrestle a grizzly bear.

ACA Biodiversity, the Government of Alberta, the Department of Biological Sciences, and the Faculty of Grad Studies and Research, Parks Canada– for supplying the money and permit with which to do the research and present the findings at conferences.

Izzy and Ayesha – for reminding me that no matter what I'm doing, there is always time for treats, walkies, tummy rubs, and opening the door for puppy patrols.

Table of Contents

List of Tables

List of Figures

Chapter 1. Introduction

1.1 Selecting target taxa among the dematiaceous hyphomycetes

Dematiaceous hyphomycetes are an artificial assemblage of conidial fungi that have darkly pigmented walls rich in an ill-defined group of indole or phenol polymers referred to as melanins (Butler and Day 1998; Henson et al. 1999). Melanins confer several benefits to fungi including protection from UV radiation, freezing, desiccation, grazing, and enzymatic cell wall degradation (Butler and Day 1998; Jumpponen and Trappe 1998; Henson et al. 1999). The range of ecological advantages gained by melanisation indicates that this feature would be a convergence expected across a broad taxonomic spectrum and, indeed, many lineages, particularly within the Ascomycota, have darkly pigmented hyphae, spores, and fructifications. Examples include many representatives in the Chaetothyriales, Coniochaetales, Helotiales, Pleosporales, Sordariales, and Xylariales. Among these, the Helotiales and Pleosporales are of particular interest because both groups include psychrophilic or at least cold-tolerant representatives that have been reported from cooler habitats such as alpine and arctic regions. In these locations, most dematiaceous hyphomycetes representing the above lineages would be parasites or saprobes of primary producers including vascular plants, bryophytes, and lichens.

This thesis focuses on selected species of dematiaceous hyphomycetes, representing the Pleosporales, Helotiales, and Coniochaetales, and examines both taxonomic and ecological aspects of their biology, especially with respect to their potential roles in arctic and alpine ecosystems. The Order Pleosporales is

characterised by the production of darkly pigmented stromata that develop locules in which bitunicate asci form dark, multicelled ascospores. Anamorphs associated with this order have dematiaceous hyphae and conidia which are single celled, bicelled, or multicelled and which form singly or in acropetally proliferating chains. The Pleosporales are well known as parasites and saprobes of both vascular plants and bryophytes (Davey and Currah 2006). The second group includes the helotialean dark septate endophytes (DSE). The DSE are an artificial assemblage of ascomycetous fungi that live asymptomatically in the roots of vascular plants (Addy et al. 2005). Many DSE belong to the Helotiales, but the Chaetothyriales, Sordariales and perhaps other orders are also represented (Tedersoo et al. 2009). Among the helotialean DSE, conidiogenesis, though uncommon, is usually phialidic. Despite their repeated isolation from roots, the ecological roles of these root endophytes are unclear although there are claims that they play a quasi-mycorrhizal role in host plants (Mandyam and Jumpponen 2005). The third order represented in this thesis is the Coniochaetales (Garcia et al. 2006) and includes species that are saprobes of wood, bark, soil, dung, and bryophytes (Cannon and Kirk 2007; Davey et al. 2010). These mostly perithecial fungi have *Acremonium*-like anamorphs (e.g. *Lecythophora*). Very little is known about their ecology.

At the outset of my investigations, I had access to two large collections of dematiaceous hyphomycetes. The first of these was from roots collected from tundra plants (*Saxifraga oppositifolia*, *Cassiope tetragona*, *Dryas integrifolia,* and *Salix arctica*) on Ellesmere Island and had been prepared by K. Fujimura and

others working out of the University of Northern British Columbia. Although many of these fungi had been partially characterised by DNA sequences, few had been identified and named. I used traditional morphological criteria to identify many of these, including one series that represented an undescribed species of *Monodictys*. The second was a collection of isolates assembled from bryophytes (*Tortella tortuosa, Ditrichum flexicaule, Bryum arcticum,* and *B. angustirete*) and vascular plants (*Saxifraga oppositifolia, Dryas drummondii*) I collected from the outwash plain at the Saskatchewan Glacier in Banff National Park. Unfortunately, much of the latter collection was lost because of a serious mite infestation, but a subset of taxa was rescued and retained.

The form of this thesis therefore was to a degree dictated by the somewhat restricted range of species from these two original collections. With the dematiaceous hyphomycete taxa available, a series of interrelated research projects was designed and these are presented in the following four chapters.

In Chapter 2, I describe a new species in the genus *Monodictys* based on eight darkly pigmented isolates from the roots of *Saxifraga oppositifolia* collected near Alexandra Fiord, Ellesmere Island. All isolates produced multicellular conidia characteristic of *Monodictys*, but these conidia were larger than other species in the genus and were also unique in being branched. The host and habitat were also unusual. To test my hypothesis that these isolates represented a hitherto undescribed species, I followed the development of the conidia and obtained DNA sequence data for phylogenetic analyses. The chapter presents my

argument for recognising *Monodictys arctica* as a new and distinct species allied to *Leptosphaeria* in the Pleosporales.

The overriding objective of the work presented in Chapters 3 and 4 was to determine the potential roles of eight species of dematiaceous hyphomycetes in decomposition of moss gametophytes in arctic and alpine environments. In these habitats, bryophytes are often the first macroscopic plants to colonise mineral soils and their degradation to coarse organic fragments is an important step in the humification of mineral soils – a step that would facilitate the subsequent establishment of vascular plants. In these two chapters, I examine the degradative abilities of eight fungal species when grown *in vitro* on the gametophytes of *Hylocomium splendens*. These species include three pleosporalean fungi (i.e. *Curvularia inaequalis*, *Ulocladium atrum*, and *Chalastospora gossypii*) in Chapter 3, four helotialean fungi and one coniochatealean (*Phialocephala fortinii*, *Cadophora luteo-olivacea*, *Cadophora melinii*, *Leptodontidium orchidicola*, and *Coniochaeta nepalica*) in Chapter 4 For the pleosporalean species, I tested the hypothesis that the three relatively ubiquitous species would be able to degrade the tissues of moss gametophytes and thus contribute to the accumulation of organic materials in mineral alpine soils.

As mentioned above, many isolates of DSE were recovered from the early vascular plant colonisers in the two collections of fungi. DSE have often been thought to play a quasi-mycorrhizal role based on their repeated isolation from vascular plant roots, though experimental evidence for this hypothesis has been ambiguous or lacking (Addy et al. 2005). For the helotialean species, my

objective was similar to that in Chapter 3. Because *P. fortinii*, *C. luteo-olivacea*, and *L. orchidicola* are DSE species, and potentially mycorrhizal with early vascular plant colonists in arctic and alpine successional sequences, I was curious to know if they would degrade bryophyte tissues. I also included *Coniochaeta nepalica* because I had an isolate from alpine bryophytes and because recently another member of the genus has been shown to break down bryophyte tissue (Davey et al. 2010). The results of this work are significant for two reasons. First, successful saprobic growth on coarse organic debris of bryophyte origin by DSE fungi has not been demonstrated previously. Second, saprobic abilities on bryophyte remains would indicate that these fungi might colonise early successional stages and persist in these materials in advance of the arrival of vascular plant hosts.

Chapter 5 represents a second foray into taxonomy (Chapter 2 being the first), but here I tackle a broader question about the relationship of form and function of the conidiogenous apparati in helotialean representatives of the DSE. The genus *Phialocephala* is characterised by the production of large obconic to spherical aggregations of phialides, which resemble sclerotia in size and complexity and in rarely producing conidia in many cases. It is unknown whether the small conidia produced by these species are even viable. The genus most closely related to *Phialocephala* is *Cadophora*, the species of which, in contrast to species in *Phialocephala*, produce phialides that are solitary or in clusters of two or three, and which regularly generate conidia. In this chapter, I explore the idea that the species of these two genera are descended from a sclerotial ancestor, with

species of *Phialocephala* retaining the ancestral sclerotial condition while the species of *Cadophora* have evolved away from the sclerotial habit. I also attempted to relate reproductive morphology in these two broad groups to dispersal biology.

Chapter six presents the conclusions of the thesis, integrating the results and conclusions from the preceding chapters, and suggests directions for future research.

1.2 Literature Cited

Addy, H.D., Piercey, M.M., and Currah, R.S. 2005. Microfungal endophytes in roots. Can. J. Bot. 83: 1-13.

Butler, M.J., and Day, A.W. 1998. Fungal melanins: a review. Can J. Microbiol. 44: 1115-1136.

Cannon, P.F. and Kirk, P.M. 2007. Fungal Families of the World. CABI: UK.

Davey, M.L. and Currah, R.S. 2006. Interactions between mosses (Bryophyta) and fungi. Can. J. Bot. 84: 1509-1519.

Davey, M.L., Tsuneda, A., and Currah, R.S. 2010. Saprobic and parasitic interactions of *Coniochaeta velutina* with mosses. Botany. 88: 258-265

Garcia, D., Stchigel, A.M., Cano, J., Calduch, M., Hawksworth, D., and Guarro, J. 2006. Molecular phylogeny of the *Coniochaetales*. Mycol. Res. 110: 1271-1289.

Henson, J.M., Butler, M.J., and Day, A.W. 1999. The dark side of the mycelium: melanins of phytopathogenic fungi. Annu. Rev. Phytopathol. 37: 447-471.

Jumpponen, A. and Trappe, J.M. 1998. Dark septate endophytes: a review of facultative - biotrophic root-colonizing fungi. New Phytol. 140: 295-310.

Mandyam, K. and Jumpponen, A. 2005. Seeking the elusive function of the root-colonising dark septate endophytic fungi. Stud. Mycol. 53: 173-189.

Tedersoo, L., Pärtel, K., Jairus, T., Gates, G., Põldmaa, K, and Tamm, H. 2009. Ascomycetes associated with ectomycorrhizas: molecular diversity and ecology with particular reference to the Helotiales. Environmental Microbiology. 11: 3166-3178.

Chapter 2. *Monodictys arctica*, a new hyphomycete from the roots of *Saxifraga oppositifolia* collected in the Canadian High Arctic.[1]

2.1 Introduction

The surfaces and cortices of fine roots are usually heavily infected with darkly pigmented, septate hyphae, some of which are easily isolated after surface sterilisation and grow readily in culture (Addy et al. 2005). Among the more common and widely distributed species of these "dark septate endophytes" or DSE are the helotialean anamorphs *Phialocephala fortinii* C.J.K. Wang & H.E. Wilcox, *Leptodontidium orchidicola* Sigler & Currah, and *Scytalidium vaccinii* Dalpé et al.

A large collection of cultures, composed predominantly of DSE fungi, were isolated from the roots of *Cassiope tetragona* (L.) D. Don, *Dryas integrifolia* Vahl., *Salix arctica* Pall., and *Saxifraga oppositifolia* L. collected during the summer of 2000 from Alexandra Fiord, Ellesmere Island, Nunavut, Canada (78° 53'N, 75° 55'W). The plants were collected as part of an experiment to study the effects of passive warming using open-topped chambers (OTCs) on root-associated fungal communities. Among this collection of fungi were numerous representatives of *P. fortinii*, *L. orchidicola*, and *S. vaccinii* along with isolates of other taxa. Eight of the latter, each from separate collections of *S. oppositifolia*, were distinctive in producing irregular, multicelled, darkly pigmented conidia that were assignable to *Monodictys* (anamorphic Dothideales, fide Kirk et al. 2001) but did not match any described species.

[1] A version of this chapter has been published by Day, M.J., Gibas, C.F.C., Fujimura, K.E., Egger, K.N., and Currah, R.S. 2006. *Monodictys arctica*, a new hyphomycete from the roots of *Saxifraga oppositifolia* collected in the Canadian High Arctic. Mycotaxon. 98: 261-272.

Here, I provide a description of *Monodictys arctica* along with a comparison of this new species with similar ones and, using sequence data from the 18s small subunit (SSU) and internal transcribed spacer(ITS) regions on the ribosomal DNA, provide an estimation of its phylogenetic position among related taxa in the Loculoascomycetes (sensu Barr and Huhndorf 2001).

2.2 Materials and Methods

Specimens of *Saxifraga oppositifolia,* from OTCs and ambient plots, were harvested along with surrounding soil, placed in Ziploc® bags and stored at 4°C until processed at the University of Northern British Columbia. Soil was loosened from roots by immersing in water for at least 24 hours at 4°C. Roots were gently cleaned with water and then collected in a 0.5 mm sieve (No. 35 USA standard testing sieve, W.S. Tyler, Inc. Mentor, Ohio, USA). Randomly selected root sections were surface-sterilized with 30% H_2O_2 following Danielson (1984) and placed on modified Melin Norkrans (MMN) agar (Marx 1969) amended with streptomycin sulphate and chlortetracycline. Plates were incubated at room temperature (20–22°C) and isolates were purified by transfer to fresh media. A 0.5 mm plug from each isolate was placed on an MMN agar slant and stored at 4°C until it was sent to the University of Alberta for identification.

Colony characteristics of the new species were based on growth on oatmeal agar [OA; 20 g oatmeal, 20 g Select agar (Invitrogen, Carlsbad, California, USA), 1 L distilled water] and potato dextrose agar (PDA; Difco Bacto). Conidial morphology was examined using an Olympus BX50 microscope

and slide cultures (Kane et al. 1997) mounted in polyvinyl alcohol with acid fuchsin [APVA; 1.66 g polyvinyl alcohol (Sigma Chemicals, Oakville, Ontario, Canada), 10.0 mL lactic acid, 1.0 mL glycerine, 10.0 mL H_2O, 0.02 g acid fuchsin] or 1.5 M KOH. Conidial and conidiophore dimensions are based on 140 and 20 measurements, respectively, and appear in the descriptions as a range. Images of conidia and colonies were prepared using an Olympus DP12 (Olympus Canada Inc, Markham, Ontario, Canada) and an Olympus C60 camera (Olympus Canada Inc, Markham, Ontario, Canada), respectively. Freehand line drawings were made based on observations made with the light microscope.

To obtain the targeted rDNA sequences, cultures were grown on PDA overlaid with a Cellophane™ sheet (UCB Films, Bridgwater, Somerset, UK). Approximately 100 mg of mycelium was scraped off the cellophane and placed in a sterilised mortar containing acid-sterilised sand. Liquid nitrogen was added and the frozen mycelium was ground to a powder with a pestle. The powder was dissolved in 1 mL of 2x CTAB [10 mL 1M Tris pH 8.0, 8 mL 0.25M EDTA, 8.7 g NaCl, 20 mL 10% CTAB (10 g CTAB, 100 mL dH_20), 100 mL dH_20] and 2 μL β – mercaptoethanol and incubated at 65°C for 2 hours. An equal volume of 24:1 chloroform:isoamyl alcohol was added. The tubes were inverted until an emulsion formed and then centrifuged for 20 min at 14 000 rpm at room temperature. The upper DNA-containing layer was collected and purified using a Qiaquick PCR purifying kit (QIAgen Inc., Mississauga, Ontario, Canada). Cleaned extraction products were visualised on a 1% agarose gel stained with ethidium bromide and exposed to UV light.

The target DNA regions, the small subunit rDNA (SSU) and the internal transcribed (ITS) spacer region, consisting of complete ITS 1, 5.8 S, and ITS 2 and partial SSU and LSU DNA, were amplified using primers BMBCR (Lane et al. 1985) and NS8 (White et al. 1990) and BMBCR and ITS 4 (White et al. 1990), respectively. The PCR reaction mixture included 5 μL 10x buffer (500 mM KCl, 100 mM Tris Base pH 8.3), 26 μL distilled water, 3 μL 25 mM $MgCl_2$, 4 μL of dNTP (10 mM of each dNTP), 5 μL of each primer, 1 μL Taq DNA polymerase, and 1 μL of the DNA template. Amplifications were conducted in a GeneAmp PCR System 97000 (PE Applied Biosystems, Foster City, California, USA) with the following program parameters: 94°C for 2 min, 30 cycles of 94°C for 1 min, 55°C for 1 min, 72°C for 2 min, and an extension of 72°C for 7 min and 4°C for 10 min. Amplification products were subjected to electrophoresis on a 1% agarose gel stained with ethidium bromide and visualised under UV light.

The amplicons were purified using a QIAquick PCR purification kit (QIAgen Inc. Mississauga, Ontario, Canada) and both strands were sequenced using the primers BMBCR, ITS1 (White et al. 1990), ITS2 (White et al. 1990), and ITS4 (for the ITS region) and BMBCR, NS1, NS2, NS3, NS4, NS, NS5, NS6, NS7, and NS8 (White et al. 1990) for the SSU region. The sequencing reactions contained a DNA concentration of 50 nmol mL^{-1}, 0.5 μL primer, 2.5 μL sequencing buffer, 1 μL Big Dye v. 3.0 (Applied Biosystems Inc., Foster City, California, USA), and water up to a total of 10 μL. Cycle sequencing reactions were conducted using a GeneAmp PCR System 97000 (PE Applied Biosystems) with the following program parameters: 25 cycles of 94°C for 20 s, 50°C for 2

min, 60°C for 1 min. Sequencing reactions were run on an AB 3100 Genetic Analyzer (Applied Biosystems Inc., Foster City, California, USA). Contigs were examined using Sequencher 4.0.5 (Gene Codes Corp., Ann Arbor, Michigan, USA). A BLAST search was performed in GenBank to find related sequences.

The SSU sequences were used to place the isolates within the Ascomycota. The ITS sequences were used to place the isolates within the genus to which they were most similar according to a BLAST search (Table 2.1). Sequences were manually aligned using Se-Al Carbon version 2.0a11 (http://evolve.zoo.ox.ac.uk). PAUP* (version 4.40b) (Swofford 2003) was used for parsimony analyses of sequences. Gaps were treated as missing. Trees were created under the stepwise addition parameters with tree bisection-reconnection as the branch swapping algorithm. Branch confidence was tested using bootstrap analysis (Felsenstein 1985) with 100 replicates for the ITS tree and 500 replicates for the SSU tree under the same parameters. *Decorospora gaudefroyi* (≡ *Pleospora gaudefroyi*) and *Saccharomyces cerevisiae* were used as outgroup taxa for the ITS tree and SSU trees, respectively.

2.3 Taxonomy

Monodictys arctica M.J. Day & Currah, **sp. nov**. Figs 2.1, 2.2

Mycobank number: MB510336

In OAT et PDA, coloniae floccosae, margines leves, interdum discolorationem brunneam medii causantes. In PDA, colonia 35 mm post 35 dies, primum alba ad pallide brunnea, deinde brunnea post 4 dies et argenteo-grisea post 7 dies. Conidia sessilia et lateralia in hyphis

vegetativis vel ex extremis ramorum orientia, 5–330 μm longitudine, consistent ex cellulis basalibus blastice productis et ex proliferatione distali cellularum, usque ad 24 numero, quae oriunt ex incremento meristematico; imperfecte globosa quando maturant, oblonga, ellipsoidea vel pyriformia vel inaequaliter vel dichotome ramosa, interdum latiora quam longiora, maxime nigrata (melanisata), levia, crassiter tunicata, constricta prope septa, 12–80 × 12–90 μm. Isolata ex radice Saxifragae oppositifoliae ex insula Ellesmere.

Colonies on OAT and PDA floccose with even margins, occasionally causing brown discoloration of medium (Fig. 2.1A). Colony 35 mm after 35 days on PDA, white to light tan at first, becoming brown after four days, and silvery grey after seven days. Conidia sessile and lateral on vegetative hyphae or arising from lateral branches 5–330 μm in length, consisting of a blastically produced basal cell and a distal proliferation of up to 24 cells arising from meristematic growth (Fig. 2.1B); at maturity, roughly globose, oblong, ellipsoidal, or pyriform to irregularly shaped or dichotomously branched (Figs. 2.1 C, D, E), deeply pigmented and appearing olive to dark brown, smooth, thick walled, with constrictions at septa, 20–80 × 12–50 μm when length greater than breadth and 12–67 × 20–90 μm when breadth greater than length.

HOLOTYPE – CANADA. ELLESMERE ISLAND: Alexandra Fiord, Nunavut (78° 53'N, 75° 55'W), ex roots of *Saxifraga oppositifolia*, 17 Jan 2001, UAMH, a dried culture derived from UAMH 10720 - M.J.D. 121 = K.E.F. 1-S1-OTC3-Saop 3.2)

PARATYPES – dried cultures derived from the following cultures and deposited in the UAMH. All from roots of *Saxifraga oppositifolia* collected at the type locality: 18 Sep 2000, UAMH 10718 - = M.J.D. 73 = K.E.F. 1-S4-OTC3-Saop 4.3; 20 Dec 2000, UAMH 10719 - = M.J.D. 86 = K.E.F. 1-S1-C3-Saop 1.2; 16 Nov 2000, UAMH 10721 - = M.J.D. 192 = K.E.F. 1-S4-OTC2-Saop 4.6; 13 Sep 2000, UAMH 10725 - = M.J.D. 217 = K.E.F. 1-S4-OTC3-Saop 2.2; 25 Sep 2000, UAMH 10722 - = M.J.D. 607 = K.E.F. 1-S4-OTC2-Saop 2.2; 13 Oct 2000, UAMH 10723 - = M.J.D. 729 = K.E.F. 1-S4-OTC2-Saop 1.1B; 13 Oct 2000, UAMH 10724 - = M.J.D. 732 = K.E.F. 1-S4-C1-Saop 4.2.

Etymology recognises the collecting locality for the host plant.

2.4 Results

For both the SSU and ITS regions, isolates shared greatest sequence similarity with *Leptosphaeria* species according to BLAST searches of GenBank. Subsequent parsimony analysis of the SSU DNA placed *M. arctica* in the Dothideomycetidae (Fig. 2.3). The SSU tree included 31 taxa and 1022 characters, of which 740 were constant, 98 parsimony uninformative, and 184 parsimony informative. Nineteen most-parsimonious trees were produced for the SSU region. The consistency index (CI) was 0.612, the retention index (RI) 0.753, and the homoplasy index (HI) 0.388. Analysis of the ITS regions of *M. arctica* and *Leptosphaeria* species placed our isolates in the same clade as *L. dryadophila* (Fig. 2.4). The ITS tree included 18 taxa and 600 total characters, 336 of which were constant, 85 parsimony uninformative, and 179 parsimony informative. One

most-parsimonious tree was produced for the ITS region. The CI was 0.579, the RI 0.490, and the HI 0.421.

2.5 Discussion

My isolates are accommodated within *Monodictys* reasonably well on the basis of morphology, even though previous authors have noted that the boundaries among similar genera having pigmented, muriform conidia can be difficult to recognise (Rao and de Hoog 1986; Rodríguez et al. 2001). The genus was erected by Hughes (1958) with *M. putredinis* (Wallr.) S. Hughes as the type species, and is characterised by the production of single, dry, darkly pigmented, multicelled conidia that arise from monoblastic conidiogenous cells. The absence of sporodochia and conidial chains distinguishes members of this genus from developmentally similar taxa (e.g., *Epicoccum* spp., *Alternaria* spp. ,respectively) but the resulting group is heterogeneous and the genus needs re-examination and revision (Rao and de Hoog 1986; Rodríguez et al. 2001). *Monodictys arctica* is distinguished from others in the genus by having smooth, mostly irregularly shaped conidia that are occasionally branched. The conidia of *M. antiqua* (Corda) S. Hughes and *M. lepraria* (Berk.) M.B. Ellis are somewhat similar in being lobed (Ellis 1976) but are larger, up to 75 × 25 μm in *M. lepraria* and 100 × 50 μm in *M. antiqua*.

During conidium development in *M. arctica*, the conidiogenous cell swells and produces a transverse septum (Fig. 2.1 F) that delineates a basal cell (Wang 1990) (Fig. 2.1 G), which in turn produces one or two cells that serve as meristematic initials (Fig. 2.1H). Meristematic initials are subsequently

partitioned by septa that form on irregular, i.e., non-orthogonal, planes of division, but resultant cells ("meristematic cells," Fig. 2.1 I) enlarge so that the component cells of the mature conidium are similar in size. The basal cell persists in the mature conidium and is recognised by being less heavily pigmented than the more distal meristematic portion. This developmental sequence agrees with previous observations made by Hughes (1953) and Ellis (1971) on *M. paradoxa*. By observing longitudinal sections through the conidium, and the subtending conidiophore in *M. paradoxa* (Corda) S. Hughes, using transmission electron microscopy, Wang (1990) determined that conidiogenesis involved percurrent proliferation of the conidiogenous cell, which resulted in the formation of an inconspicuous annellophore. This process was not detected in *M. arctica* using light microscopy. I also did not see evidence of rhexolytic dehiscence or remnants of the conidiogenous cell forming a hilum (Samuels 1980). Further observations using ultrastructural techniques would be useful in clarifying the mode of conidiogenesis in our new species and similar observations across a range of species of *Monodictys* could be of value in clarifying the conceptual limits of the genus.

Analysis of 18S sequences places *M. arctica* within the Dothideomycetidae. Only two other species of *Monodictys*, *M. pelagica* (T. Johnson) E.B.G. Jones and *M. castanea* (Wallr.) S. Hughes, are represented by sequences in GenBank and these show affinities with the Sordariomycetidae. However, links between the Loculoascomycetes (sensu Barr and Huhndorf 2001) and *Monodictys* have been reported. For example, Samuels (1980) observed

conidia resembling *M. putredinis* (Wallr.) S. Hughes developing in cultures derived from ascospores of *Ohleria brasiliensis* (Melanommataceae). Unfortunately, there are no sequences for either *M. putredinis* or *O. brasiliensis* in GenBank.

Phylogenetic analysis of the ITS region suggests that *M. arctica* is quite likely the anamorph of a species of *Leptosphaeria,* a loculoascomycete genus known from a broad range of plants and habitats, but otherwise having pycnidial anamorphs (e.g., in *Coniothyrium* spp., *Diplodina* spp., *Haplosporella* spp., *Phaeoseptoria* spp., *Phoma* spp., *Scolecosporiella* spp., *Septoria* spp., and *Stagonospora* spp.; Dennis 1981; Farr et al. 1989). Pycnidia were not observed in our cultures but conidial development in *Monodictys* resembles stages in the development of pycnidia by *Phoma* and *Asteromella*. Also, the *Monodictys*-like anamorph of *Tubeufia amazonensis* Samuels, Rossman, and E. Müll. (*Tubeufiaceae*) often forms pycnidial locules bearing phialides and single-celled conidia (Samuels 1980). Finally, the formation of pseudoparenchymatous balls, reminiscent of large dictyoconidia, have been associated with the appearance of pycnidia and ascomata in *Leptosphaeria* (Samuels 1980).

The closest genetic match to *M. arctica* (94% similar to the ex-type strain, UAMH 10720) is *L. dryadophila* Huhndorf (≡ *Melanomma dryadis* Johanson). The close genetic similarity between these two species and the similar habitat, i.e., on subfrutescent perennial species native to arctic or alpine habitats, suggest these taxa might be sibling species, but additional data supporting this supposition are missing. For example, it is unknown if *L. dryadophila*, which produces its

ascostromata on the leaves and flowers of *Dryas octopetala* and *D. integrifolia* (Huhndorf 1992; Chlebicki 2002), is systemic and in the roots of these hosts. Furthermore, and as far as I am aware, an anamorph is unknown for *L. dryadophila*. Three other species of *Leptosphaeria*, i.e., *L. brachyasca* Rostr., *L. hyperborea* (Fuckel) Berl. & Voglino, and *L. oreophila* Sacc. (Connors 1967; Farr et al. 1989) have been reported from species of *Saxifraga* but neither cultural nor sequence data are available for these taxa.

Whether *M. arctica* inhabits root cortices in the same relatively harmless manner as other dark septate endophytes such as *Phialocephala fortinii*, *Leptodontidium orchidicola*, and *Scytalidium vaccinii*, all of which were among the isolates examined from the four angiosperm hosts, is unknown. Pattern of occurrence, i.e., in one of four plant species collected from within and outside the OTCs, suggests that host identity had a stronger influence than the experimental treatments. Direct examination of roots of *Saxifraga oppositifolia* infected with *M. arctica* is required to determine the colonisation pattern and whether the fungus is a pathogen or relatively harmless. Furthermore, close inspection of host shoot tissues might indicate the presence of a previously overlooked loculoascomycete teleomorph similar to *Leptosphaeria dryadophila*.

2.6 Literature cited

Addy, H.D., Piercey, M.M., and Currah, R.S. 2005. Microfungal endophytes in roots. Can. J. Bot. 83: 1–13.

Barr, M.E. and Huhndorf, S.M. 2001. Loculoascomycetes. *In* The Mycota VII Systematics and Evolution Part A. *edited by* K. Esser and P.A. Lemke. Springer Press: London (England). 283–305.

Chlebicki, A. 2002. Biogeographic relationships between fungi and selected glacial relict plants. Monographiae Botanicae. 90: 5–230.

Conners, I.L. 1967. An annotated index of plant diseases in Canada and fungi recorded on plants in Alaska, Canada, and Greenland. Canada Department of Agriculture: Canada.

Danielson, R.M. 1984. Ectomycorrhizal associations in jack pine stands in northeastern Alberta. Can. J. Bot. 62: 932–939.

Dennis, R.W.G. 1981. British Ascomycetes. J Cramer: Vaduz (Germany).

Ellis, M.B. 1971. Dematiaceous Hyphomycetes. Commonwealth Mycological Institute: England.

Ellis, M.B. 1976. More Dematiaceous Hyphomycetes. Commonwealth Mycological Institute: England.

Farr, D.F., Bills, G.F., Chamuris, G.P., and Rossman, A.Y. 1989. Fungi on plants and plant products in the United States. APS Press: USA.

Felsenstein, J. 1985. Confidence limits on phylogenies: an approach using the bootstrap. Evolution. 39: 783–791.

Hughes, S.J. 1953. Conidiophores, conidia and classification. Can. J. Bot. 31: 577–659.

Hughes, S.J. 1958. Revisiones Hyphomycetum aliquot cum appendice de nominibus rejiciendis. Can. J. Bot. 36: 727–836.

Huhndorf, S.M. 1992. Systematics of *Leptosphaeria* species found on the Rosaceae. Illinois Natural History Survey. 35: 479–534.

Kane, J., Summerbell, R., Sigler, L., Krajden, S., and Land, G. 1997. Laboratory handbook of dermatophytes. Star Publishing Corp: USA.

Kirk, P.M., Cannon, P.F., David, J.C., and Stalpers, J.A. 2001. Dictionary of the Fungi. 9th Edition. CABI Publishing: UK.

Lane, D.J., Pace, B., Olsen, G.J., Stahl, D.A., Sogin, M.L., and Pace, N.R. 1985. Rapid determination of 16S ribosomal RNA sequences for phylogenetic analysis. Proc. Natl. Acad. Sci., U.S.A. 82: 6955–6959.

Marx, D.H. 1969. The influence of ectotrophic mycorrhizal fungi on the resistance of pine roots to pathogenic infections. I. Antagonism of mycorrhizal fungi to root pathogenic fungi and soil bacteria. Phytopathology. 59: 153–163.

Rao, V. and de Hoog, G.S. 1986. New or critical Hyphomycetes from India. Stud. Mycol. 28: 1–83.

Rodríguez, K., Figueras, M.J., Gené, J., Mercado, A., and Guarro, J. 2001. *Monodictys desquamata*, a new mitosporic fungus from a Cuban rain forest. Nova Hedwigia. 72: 201–207.

Samuels, G.J. 1980. Ascomycetes of New Zealand 1. *Ohleria brasiliensis* and its *Monodictys* anamorph, with notes on taxonomy and systematics of *Ohleria* and *Monodictys*. New Zeal. J. Bot. 18: 515–523.

Swofford, D.L. 2003. PAUP* Phylogenetic Analysis Using Parsimony (*and other methods). Version 4.40b. Sinauer Associates: USA.

Wang, C.J.K. 1990. Ultrastructure of percurrently proliferating conidiogenous cells and classification. Stud. Mycol. 32: 49–64.

White, T.J., Bruns, T., Lee, S., and Taylor, J.W. 1990. Amplification and direct sequencing of fungal ribosomal RNA genes for phylogenetics. *In* PCR protocols: a guide to methods and applications. *edited by* M.A. Innis, D.H. Gelfand, J.J. Sninsky, and T.J. White. Academic Press, Inc: New York (USA). Pp. 315–322.

Table 2.1. Provenance data for species of *Leptosphaeria* and *Decorospora* used in the parsimony analysis of the ITS DNA region.

Species	Genbank Number	Host plant
Decorospora gaudefroyi	AF439451	Not listed
Leptosphaeria biglobosa	DQ133893	*Brassica napus*
L. conferta	AF439459	*Anacyclus radiatus*
L. doliolum	U04207	Not listed
L. dryadophila	AF439461	*Dryas octopetala*
L. maculans	M96384	*Brassica napus*
L. typharum	AF439465	*Typha angustifolia*
Monodictys arctica	EU686521	*Saxifraga oppositifolia*

Figures 2.1 A-I Cultural and morphological features of *M. arctica*.

A. Colony morphology of *Monodictys arctica* isolates after 12 d incubation on PDA andOA. Brown discoloration of medium shown on OA, a) UAMH 10719 on PDA b) UAMH 10720 (ex-type strain) on OA.
B. Globose conidium from a 14 d culture of UAMH 10719 stained in APVA showing the prominent basal cell (*) attached to the conidiogenous cell.
C. Conidium from a 14 d culture of UAMH 10719 stained in APVA showing branches. Conidial breadth is larger than length.
D. Conidium from a 9 d slide culture of UAMH 10720 cleared in 10% KOH showing development of a second conidial branch (arrow) before division of the first branch (*).
E. Conidium from a 7 d slide culture of M.J.D. 727 (from the same root as UAMH 10723) stained with APVA showing development of a second conidial branch (*) after division of the first branch (arrow).
F. Conidium from a 7d slide culture of UAMH 10718 stained in APVA showing a newly formed septum (arrow).
G. Conidium from a 3 d slide culture of M.J.D. 727 (from same root as UAMH 10723) stained in APVA showing a basal cell (BC) protruding from the conidiogenous cell (CC).
H. Branched conidium from a 7d culture of UAMH 10718 stained in APVA showing the meristematic initials (MI) of two branches produced by basal cell (BC).
I. Conidium from a 9 d slide culture of UAMH 10722 cleared in 10% KOH after division of meristematic initial (MC = meristematic cell. BC = basal cell. All bars = 10 μm.

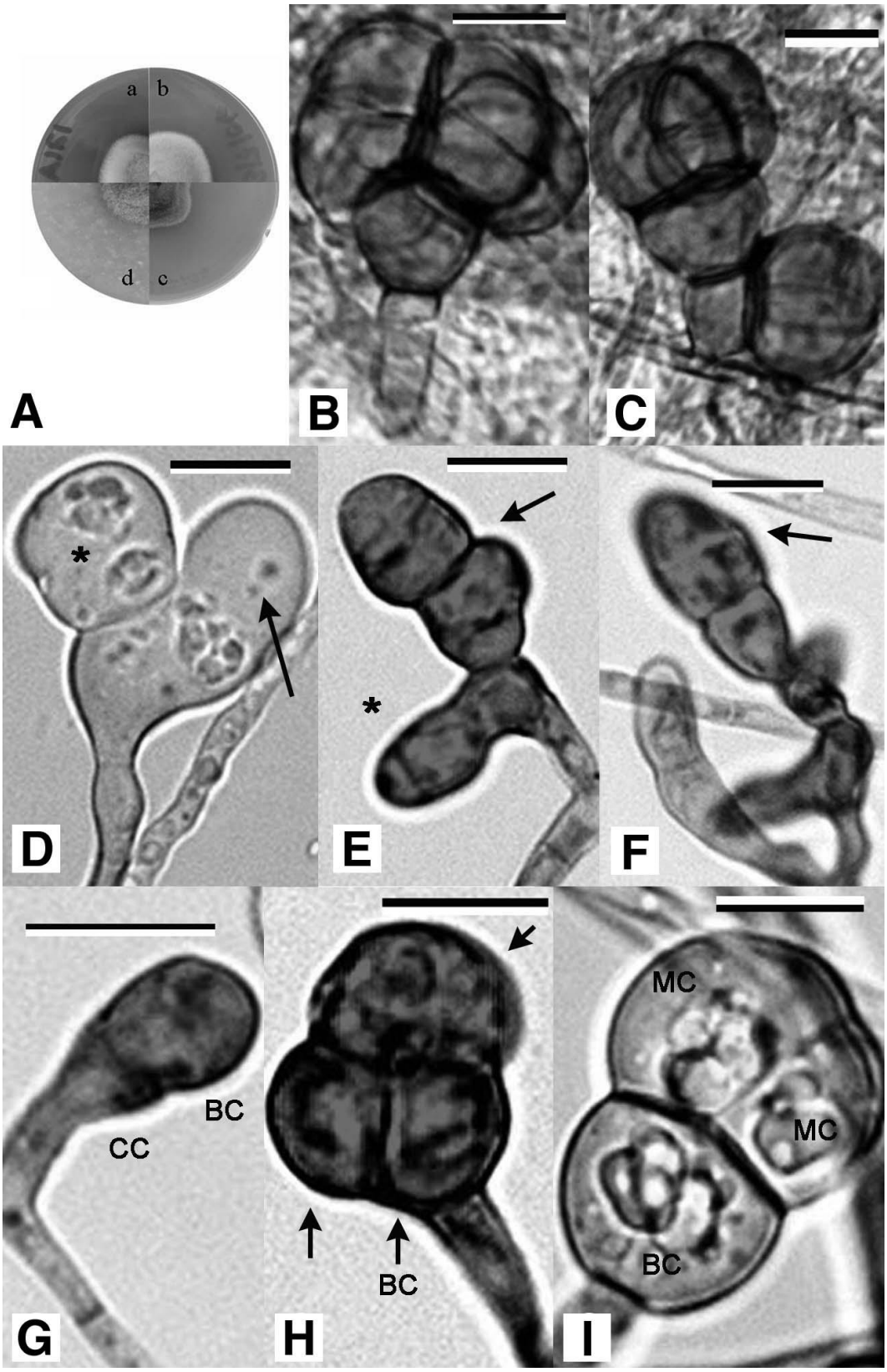
a
b
d
c
A
B
C
D
E
F
G
H
I
*
*
BC
CC
BC
BC
MC
MC

Figure 2.2. Line drawings of conidia of *Monodictys arctica*. Bar = 10μm.

A. Irregularly shaped branched conidium.
B. Branched conidium with second branch just developing.
C. Conidium showing two meristematic initials.
D. Branched conidium with breadth greater than length.
E. Conidium broader than long.
F. Roughly globose conidium.
G. Roughly ellipsoidal conidium.
H. Young, roughly, globose conidium.
I. Young conidium.

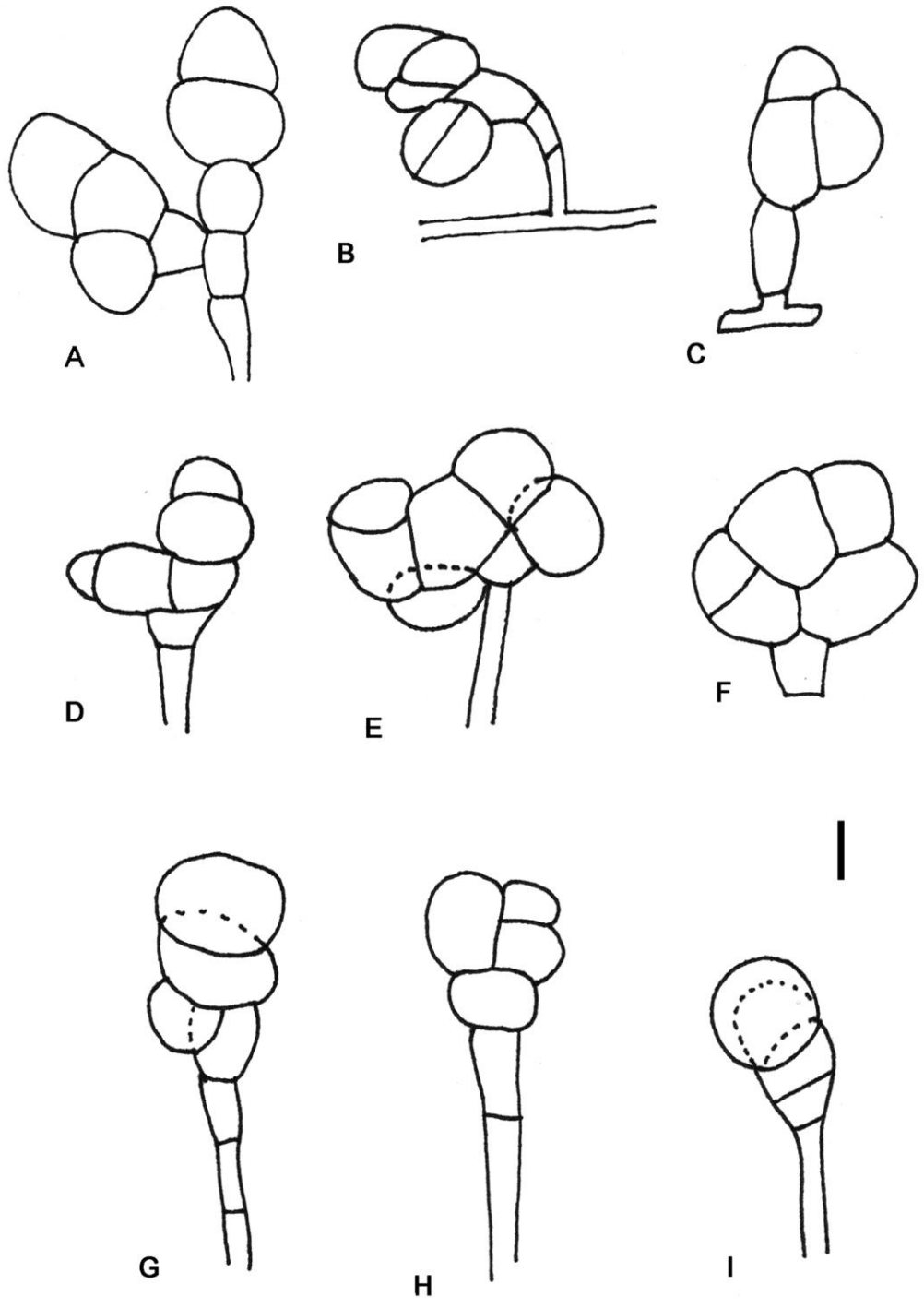
A
B
C
D
E
F
G
H
I

Figure 2.3. One of 19 most parsimonious trees based on an analysis of the small subunit rDNA of *Monodictys arctica* and other ascomycetes. The CI = 0.612, RI = 0.752, and HI = 0.38. The outgroup was *Saccharomyces cerevisiae*. Bootstrap support in percentages (for 500 replicates) is shown on branches where support is greater than 50%. T indicates the type.

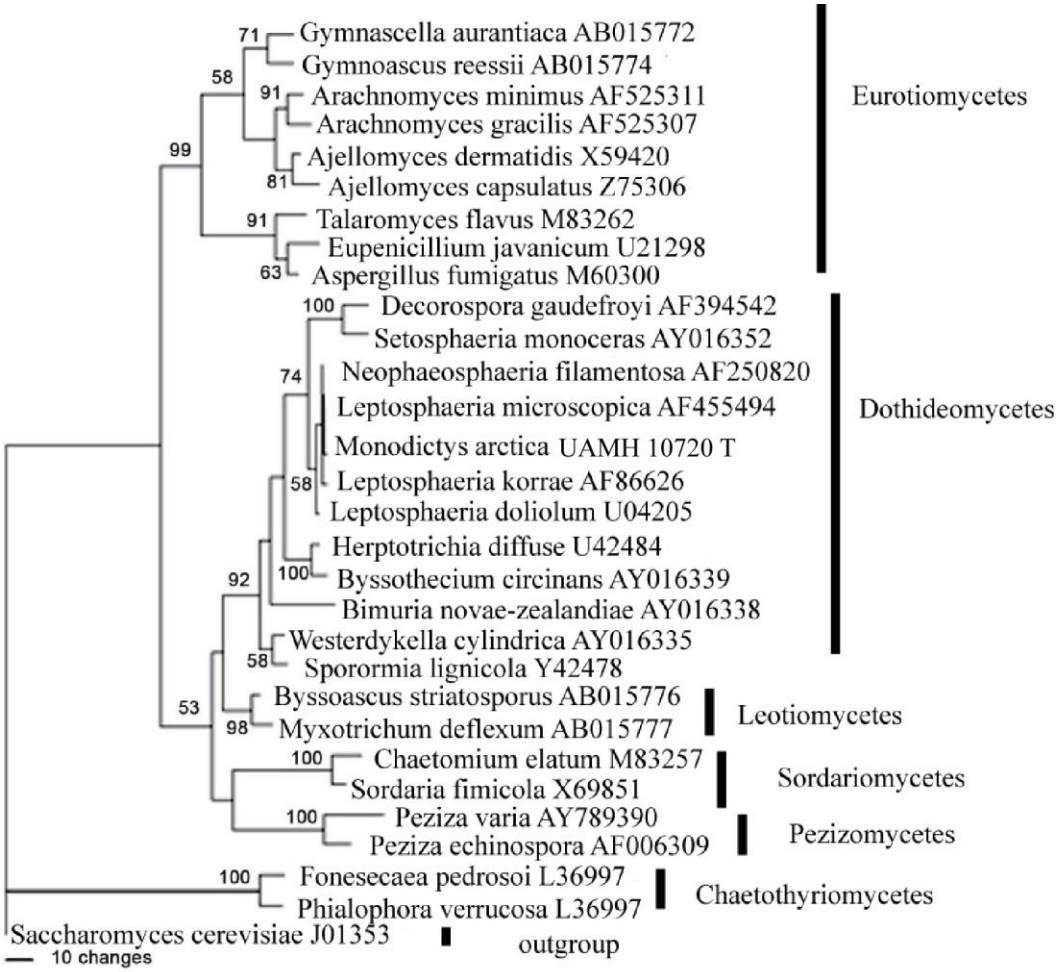
Gymnascella aurantiaca AB015772
Gymnoascus reessii AB015774
Arachnomyces minimus AF525311
Arachnomyces gracilis AF525307
Ajellomyces dermatidis X59420
Ajellomyces capsulatus Z75306
Talaromyces flavus M83262
Eupenicillium javanicum U21298
Aspergillus fumigatus M60300
Eurotiomycetes
Decorospora gaudefroyi AF394542
Setosphaeria monoceras AY016352
Neophaeosphaeria filamentosa AF250820
Leptosphaeria microscopica AF455494
Monodictys arctica UAMH 10720 T
Leptosphaeria korrae AF86626
Leptosphaeria doliolum U04205
Herptotrichia diffuse U42484
Byssothecium circinans AY016339
Bimuria novae-zealandiae AY016338
Westerdykella cylindrica AY016335
Sporormia lignicola Y42478
Dothideomycetes
Byssoascus striatosporus AB015776
Myxotrichum deflexum AB015777
Leotiomycetes
Chaetomium elatum M83257
Sordaria fimicola X69851
Sordariomycetes
Peziza varia AY789390
Peziza echinospora AF006309
Pezizomycetes
Fonesecaea pedrosoi L36997
Phialophora verrucosa L36997
Chaetothyriomycetes
Saccharomyces cerevisiae J01353
outgroup
10 changes

Figure 2.4. The most parsimonious tree based on an analysis of the internal transcribed spacer region of *Monodictys arctica* and members of *Leptosphaeria.* The CI = 0.579, RI = 0.490, and HI = 0.721. The outgroup was *Decorospora gaudefroyi*. Bootstrap support (100 replicates) is shown on branches where support is greater than 50%.

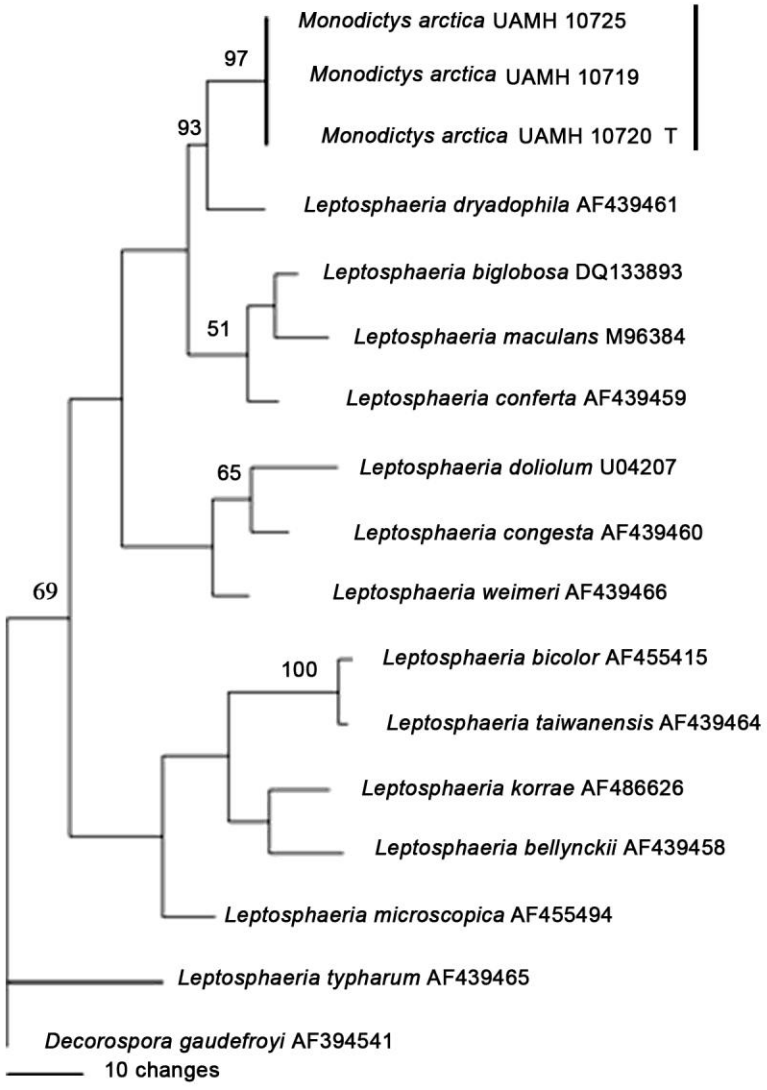
Monodictys arctica UAMH 10725
97
Monodictys arctica UAMH 10719
93
Monodictys arctica UAMH 10720 T
Leptosphaeria dryadophila AF439461
Leptosphaeria biglobosa DQ133893
51
Leptosphaeria maculans M96384
Leptosphaeria conferta AF439459
65
Leptosphaeria doliolum U04207
Leptosphaeria congesta AF439460
69
Leptosphaeria weimeri AF439466
100
Leptosphaeria bicolor AF455415
Leptosphaeria taiwanensis AF439464
Leptosphaeria korrae AF486626
Leptosphaeria bellynckii AF439458
Leptosphaeria microscopica AF455494
Leptosphaeria typharum AF439465
Decorospora gaudefroyi AF394541
10 changes

Chapter 3. Fungal activity on moss gametophytes and its potential role in arctic and alpine pedogenesis.

3.1 Introduction

Rock and gravel debris left in the wake of retreating glaciers can provide a chronosequence for the study of organisms involved in the early stages of pedogenesis and primary succession (Viereck 1966, Chapin et al. 1994). Among the earliest macroscopic primary producers in these areas are moss gametophytes. These minute plants incrementally form dense tufts of stems and leaves that overlie an accumulation of particulates including dead and persistent gametophyte tissues that decay to form a brown, organic "grout" between rocks. This grout acts as a habitat and catchment device for wind and water borne organisms including algae and fungi (Freeman et al. 2009a, b), and organic particulates such as pollen and bits of organic debris. The first seed plants (e.g., *Saxifraga oppositifolia*) in these habitats are often found rooted in this material.

Moss gametophytes produce leaves that are a single cell layer thick along stems that lack lignified vascular tissue and are less than a millimetre in diameter. Cell walls in these plants consist of an outer amorphous layer (Sakar et al. 2009) of cellulose microfibrils, hemicellulose, pectin, and lignin-like compounds (Farmer and Morrison 1964; Erickson and Miksche 1974; Hébant 1977), and an inner layer rich in lignin-like phenolics (Ligrone et al. 2008; Edelmann 1998). The potential role of microbes in the conversion of these materials in the matrix of leaves and stems, and entrained particulates, to a heterogeneous mass of organic material has not been examined, but the abundance and range of hyphal morphologies, distinguished on the basis of hyphal diameter and pigmentation,

and septal morphology that can be detected in grout samples (Day, unpublished data), indicate that fungi are important contributors to this process.

Given the potential significance of fungi in the conversion of moss gametophytes to these early soils, I isolated and identified two of the fungi associated with some grout-forming moss species, *Ditrichum flexicaule* (Schwägr) Hampe and *Tortella tortuosa* (Hedw.) Limpr., and one associated with the common vascular plant cohabitant, *Saxifraga oppositifolia* L. Plants were collected from among the rocks and gravels in the outwash area below a retreating alpine glacier. From a collection of approximately 200 fungi, three common and widespread ascomycetous moulds in the Pleosporaceae, i.e., *Chalastospora gossypii* (Jacz.) U. Braun & Crous, *Curvularia inaequalis* (Shear) Boedijn, and *Ulocladium atrum* Preuss, were identified and selected for *in vitro* studies of their ability to decay moss leaves. Species of the Pleosporaceae are common on the living and dead tissues of plants, including bryophytes (e.g., Davey & Currah 2009), and have deeply melanised cell walls, a property that ostensibly confers protection from the challenges of ultraviolet light and desiccation (Butler & Day 1998) prevalent in exposed alpine habitats.

The objectives of this study were to characterise and compare the degradation process for each fungus using a readily available moss species, *Hylocomium splendens* (Hedw.) Schimp, as the substrate, and to determine which cellular components were readily degraded and which might remain as recalcitrant residue. This latter fraction presumably would be similar in

composition to the characteristic brown organic debris associated with bryophyte grout observed in the field.

3.2 Methods

Plants in grout columns serving as the source of inoculum were collected from the outwash plain below the Saskatchewan Glacier, Banff National Park, Canada in 2006. Specimens were dug out of the coarse till using a sterile trowel, placed intact in a plastic bag, and transported on ice to the laboratory. Moss gametophytes and leaves of vascular plants were washed in several changes of distilled water, cut into pieces, surface sterilised in 1% household bleach, and plated on potato dextrose agar (PDA, Difco Bacto).

From among the fungi isolated, three were selected for further research and deposited in the University of Alberta Microfungus Collection and Herbarium (UAMH). *Curvularia inaequalis* (UAMH 11180) and *Ulocladium atrum* (UAMH 11179) grew from gametophytes of *Ditrichum flexicaule* and *Tortella tortuosa,* respectively. *Chalastospora gossypii* (UAMH 11181) was obtained from the leaves of *Saxifraga oppositifolia.* Provisional identifications were made on the basis of microscopic characters associated with the conidia and conidiophores (measurements were averaged over 10-25 samples) and then supported by sequencing the ITS region of the rDNA of each isolate. DNA sequences were deposited in GenBank.

Extraction, amplification, and sequencing protocols followed Day et al. (2006). Briefly, colonies were grown on PDA over laid with a Cellophane^{TM} sheet (Innovia, Bridgwater, Somerset, UK). Approximately 100 mg of mycelium

was scraped off the sheet and, after freezing with liquid nitrogen, ground with sand using a mortar and pestle. The powder was dissolved in 2x CTAB and 2 μL β mercaptoethanol and incubated at 65°C for 2 hours. An equal volume of 24:1 chloroform: isoamyl alcohol was added. The tubes were centrifuged for 20 min at 14 000 rpm at room temperature. The upper DNA-containing layer was collected and purified using a Qiaquick PCR purifying kit (QIAgen Inc., Mississauga, Ontario, Canada). Cleaned extraction products were visualised on a 1% agarose gel stained with ethidium bromide and exposed to UV light.

The internal transcribed spacer region (ITS), consisting of complete ITS 1, 5.8 S, and ITS 2 and partial SSU and LSU DNA, was amplified using a GeneAmp PCR System 97000 (PE Applied Biosystems, Foster City, California, USA) and the primers BMBCR(Lane et al. 1985) and ITS 4 (White et al. 1990). The PCR reaction mixture included 5 μL 10x buffer (500 mM KCl, 100 mM Tris Base pH 8.3), distilled water (26 μL for *C. inaequalis* and *U. atrum*, 29.5 μL for *C. gossypii*), 25 mM $MgCl_2$ (3 μL for *C. inaequalis* and *U. atrum*, 4 μL for *C. gossypii*), dNTP (10 mM of each dNTP) (4 μL for *C. inaequalis* and *U. atrum*, 1 μL for *C. gossypii*), 5 μL of each primer, Taq DNA polymerase (1 μL for *C. inaequalis* and *U. atrum*, 0.5 μL for *C. gossypii*), and 1 μL of the DNA template. Amplification products were separated using electrophoresis on a 1% agarose gel stained with ethidium bromide and visualised under UV light. The amplicons were purified using a QIAquick PCR purification kit (QIAgen Inc. Mississauga, Ontario, Canada) and both strands were sequenced using the primers BMBCR, ITS1 (White et al. 1990), ITS2 (White et al. 1990), and ITS4. The sequencing

reactions contained a DNA concentration of 100 nmol mL^{-1}, 0.5 μL primer, 2.5 μL sequencing buffer, 1 μL Big Dye v. 3.0 (Applied Biosystems Inc., Foster City, California, USA), and water up to a total of 10 μL. Cycle sequencing reactions were achieved using a GeneAmp PCR System 97000 (PE Applied Biosystems, Foster City, California, USA). Sequencing reactions were run on an AB 3100 Genetic Analyzer (Applied Biosystems Inc., Foster City, California, USA). Sequences were examined using Sequencher 4.0.5 (Gene Codes Corp., Ann Arbor, Michigan, USA) and a BLAST search was performed in GenBank to find related sequences.

Phylogenetic analyses were used to confirm the position of each species in the appropriate taxon and included members of the same species, others in the genus, and selected members of closely related genera (Table 3.1). DNA sequences for the types of *C. inaequalis, C. gossypii,* and *U. atrum* were not available from GenBank so multiple sequences of each species were used. Matrices were manually aligned using SeAl (Version 2.0a11) (Rambaut 1996). Heuristic searches were then completed with maximum parsimony as the optimality criterion using PAUP* 4.0b10 (Swofford 2002). Gaps were treated as missing data. Starting trees were obtained by stepwise addition and taxa were added randomly for 100 replicates. The branch-swapping algorithm was tree bisection-reconnection. Branch confidence was determined by 1000 bootstrap replicates using the same parameters (Felsenstein 1985).

Bayesian posterior probabilities were determined using Mr. Bayes 3.12 (Huelsenbeck & Ronquist 2001; Ronquist & Huelsenbeck 2003). Twenty-four

evolutionary models were compared to determine which best fit each dataset using Mr. Modeltest (Nylander 2004). For *C. inaequalis*, the model was general time reversible with gamma distribution (GTR + G), for *C. gossypii* symmetrical with gamma distribution (SYM+G), and for *U. atrum*, K80 with invariable sites and gamma distribution (K80 + I + G). Two independent Markov Chain Monte Carlo runs were used. For each analysis, 100 000 generations involving 1 hot and 3 cold chains were run and sampling occurred every 100 generations. A burn in of 25% of generations was applied.

To test *in situ* the enzymatic abilities, three replicates per isolate were set up on each of six test media. Inocula were taken from the edge of colonies using the sterilised large end of a Pasteur pipette (5 mm diameter). Uninoculated media served as controls. Plates incubated in the dark at 25ºC. Modified Melin-Norkran's medium (Marx, 1969) (MMN; 1.0 g dextrose, 2.0g malt extract, 1.0g yeast extract, 0.5 g KH_2PO_4, 0.25 g $(NH_4)_2HPO_4$, 0.15 g $MgSO_4 \cdot 7\ H_2O$, 0.05 g $CaCl_2$, 0.025 g NaCl, 0.012g $FeCl_3 \cdot 6H_2O$, 15.0 g Difco agar, 1 L distilled water) was the base medium for the enzymatic tests. Protein degradation was assessed using 120 g L^{-1} gelatin (Sigma Chemical, St. Louis, Missouri) instead of agar in the MMN (Hutchison, 1990). Liquefication of medium was a positive result. Amylase activity was tested on MMN amended with 2.0 g L^{-1} soluble starch (British Drug Company, Poole, England) (Hutchison, 1990). After a five week inoculation period, plates were flooded with an iodine solution (5.0 g KI, 1.5 g I, 100 mL distilled water). A clear halo around the colony indicated that the starch had been digested. Cellulose degradation was assessed by placing a mycelial plug

in a vial containing 5 mL of tap water agar (Select) overlaid with 1 mL of 2% cellulose azure (Sigma Aldrich) in tap water agar. After four weeks, the vials were examined for signs of blue colour in the lower agar layer, indicating the cellulose had been degraded and the azure dye released.

Pectinase activity was examined on MMN with 5.0 g L^{-1} pectin (Sigma Chemicals) (Hutchison, 1990). Five weeks after inoculation, plates were flooded with 1% hexadecyltrimethylammonium bromide. A clear zone around the fungal colony was evidence of pectin degradation. Degradation of insoluble polyphenol compounds was tested on wood guiacol and tannic acid media. Tannic acid medium was made by autoclaving separately 5 g tannic acid (BDH Inc. Toronto, Ontario) in 200 mL distilled water and 15 g malt extract (Difco) and 20 g Difco agar dissolved in 800 mL distilled water. After autoclaving, the two solutions were mixed. Tannic acid medium plates were checked for enzymatic activity after two weeks. A positive test result was indicated by a colour change in the agar from white to brown. The wood guiacol medium was composed of 2 g powdered *Picea glauca* stem wood, 18 g Difco agar, and 1 L distilled water. After autoclaving, the medium was allowed to cool and 100 μL guiacol (Sigma Aldrich) was added. Wood guiacol plates were incubated for 5 weeks and examined for a positive reaction, indicated by the presence of a red halo around the fungal colony.

To determine the nature and extent of degradation caused by each fungus on moss gametophyte tissue, plants of *Hylocomium splendens* were autoclaved for 20 min at 121°C and then dried at 40°C for a week. A small amount (0.05 ± 0.005

g) of this material was placed in a 3x3 cm, 63 µm mesh polyester packet, autoclaved again, and air dried at 40°C for two d. Each replicate consisted of a single packet of moss in a Petri dish containing tap water agar. A 5 mm plug of mycelium, grown on tap water agar, or tap water and yeast extract agar, was placed at the mouth of the polyester packet. Plates were sealed with parafilm and incubated in the dark at room temperature (22ºC) for three months. Each fungal species and one uninoculated control had three replicates for mass loss measurements and one for SEM observations. After three months, three replicates per fungus were dried for a week and then weighed to get the final mass. Percent mass loss was determined for all three dried packets and the average loss for the control treatment was subtracted from the fungal treatments to calibrate against any mass loss due to leakage from the cells. A one-way ANOVA (Excel) was used to determine if there were any differences in mass loss among the three species. As a routine measure, the inoculants were re-isolated from the mesh packets at the end of the incubation period to ensure that cultures had remained true and free of contamination.

Subsamples from four remaining packets were prepared for SEM according to the methods of Tsuneda et al. (1991). Samples were immersed in distilled water for two min, fixed in a 2% glutaraldehyde solution for four h at room temperature, and immersed in a 2% tannic acid-guanidine hydrochloride solution overnight. The following day, the samples were rinsed in dH_2O and postfixed in 2% osmium tetroxide overnight and then dehydrated using an ethanol series (30, 50, 70 , 90, 95, and 100%) with three changes over 20-min intervals

and then dried in amyl acetate (50 and 100%). Samples were critical point dried in Teflon capsules, coated in gold and observed and photographed using a Hitachi S-510 SEM (Hitachi Science Services Systems, Ibaraki, Japan).

3.3 Results

3.3.1 Direct microscopic examination of grout

Excavated grout columns, which consisted of the gametophytes of *Ditrichum flexicaule* and *Tortella tortuosa*, were up to 1 cm in height and composed of a consolidated mass of stems, leaves, and rhizoids that was greenish to olive along the crest and brown and fibrous towards the base. Grout samples held their shape when lifted out from between adjacent stones (Fig 3.1A). Rhizoids were especially abundant in the brown fibrous zone where organic particulates, including pollen grains, algal cells, fungal hyphae and fragmented portions of moss leaves, were also most numerous (Fig 3.1B, C, D). Fungal hyphae and spores were present throughout the vertical column of grout (Fig 3.1D) though they were more prevalent in the brown fibrous zone. *Curvularia inaequalis* and *U. atrum* were isolated from *Ditrichum flexicaule* and *Tortella tortuosa* respectively. Minute tufted plants of *Saxifraga oppositifolia* were common in grout samples. Tufts consisted of crowded persistent, scale-like leaves on short crowded stems and were green above grading to brownish where they were decaying into the grout. Necrotic leaves yielded *Chalastospora gossypii*.

3.3.2 Identification of isolates using microscopic morphology and DNA sequences

Curvularia inaequalis (UAMH 11180) produced conidia on smooth, sometimes asperulate conidiophores (Fig 3.1 E). The isolate was distinguished by its smooth, 3-4 (rarely 5) septate, straight to slightly curved, large (31 x 12.5 μm) brown conidia, in which the second cell is larger than the rest (Fig 3.1 F). Sympodial conidiogenesis resulted in the formation of characteristic palmate configurations of conidia on conidiophores (Fig 3.1 E, F). In all respects, this isolate matched the published description (Ellis 1971). The ITS data set for *C. inaequalis* yielded 774 characters, of which 620 were constant and 69 parsimony informative. Six most parsimonious trees were generated for this analysis with a tree length of 156, a CI of 0.603, and an RI of 0.754 (Fig 3.2). The isolate formed a well supported phylogenetic group with other representatives of *C. inaequalis.*

Conclusive identification of *Ulocladium atrum* (UAMH 11179) was problematic. The isolate produced brown, warty, predominantly spherical to occasionally obpyriform, cruciseptate conidia that were approximately 16 μm in diameter and borne in sympodial clusters (Fig 3 1. G, H). This isolate was morphologically closest to *U. atrum*, although it had conidia that were slightly smaller than the measurements (i.e., on average 18.6 x 16 μm) given by Simmons (1967). The ITS analysis yielded 9700 trees with a length of 212, a CI of 0.774, and an RI of 0.828. Even though the isolate was placed in the genus based on similarity of ITS sequences, there was insufficient variation to determine, phylogenetically at least, whether the isolate represented *U. consortiale, U. capsicum, U. atrum* or *U. curcurbitae* (Fig 3.3). *Ulocladium consortiale* and *U.*

capsicum have smooth rather than roughened conidia (Simmons 1982) and are not a good match. As well as being phylogenetically close to *U. atrum*, *U. curcubitae* is morphologically similar but produces only alternarioid conidia which lack the cruciate septa found in UAMH 11179. The best compromise concerning identification was to label this isolate as *U. atrum.*

Chalastospora gossypii (UAMH 11181) produced oblong, non-septate conidia, averaging 11.5 x 2.5 μm (Fig 3.1 I), which were borne in long, fragile, occasionally branching chains that were easily dislodged and washed off the substrate during preparation for SEM. In all respects, the isolate matched the description given by Ho et al. (1999). The ITS data set for *C. gossypii* yielded 1630 characters, of which 1267 were constant and 81 parsimony informative. In this analysis, 10 000 most parsimonious trees were generated with a length of 117, a CI of 0.872, and an RI of 0.931 (Fig 3.4). UAMH 11181 formed a well-supported phylogenetic group with other representatives of *C. gossypii*.

3.3.3 Enzyme tests and mass loss data

In all three isolates, inoculum was surrounded by a clear halo when plates of MMN with soluble starch were flooded with iodine, and all three liquefied gelatin. Each isolate also liberated the dye from the cellulose azure. None gave a red reaction on wood guiacol but *C. gossypii* and *U. atrum* produced a positive result on the tannic acid medium. Results of other tests varied among isolates (Table 3.2). Fungi formed circular colonies on the TWA and grew over the microfibre packet, colonising the gametophytes as well as the mesh fabric. Percent mass loss values ranged from 9.8% for *C. gossypii* to 12% for *Ulocladium*

atrum (Figure 3.5) but hyphae did not grow across leaf surfaces or form visible mycelium in a single packet in a uniform manner.

3.3.4 SEM observations of decay patterns

The surface of the acuminate, oblong-lanceolate leaves of uninoculated *Hylocomium splendens* (Fig 3.6 A) was generally smooth, although elongate leaf cells, some of which had prominent terminal papilla-like projections, were clearly outlined under a continuous, lacquer-like amorphous layer (Fig 3.6 B). Narrow, branched pseudoparaphylia were abundant along the stem (Fig 3.6 A).

On gametophytes inoculated with *C. inaequalis*, hyphae were abundant on leaf surfaces that had become wavy or puckered rather than smooth and created lines of weakness when the leaf was disturbed (Fig 3.6 C). During early stages of decomposition, the lacquer-like amorphous layer across the surface of the leaf cells and along the junctions between adjacent cells deteriorated (Fig 3.6 D) leaving a fibrillar to membranous residue and exposing parallel longitudinal ridges of the thick, inner layer. Degradation in this manner was more pronounced in the vicinity of multiple hyphae. Simple or dichotomously branched appressoria, and hyphae emerging from leaf cells to form conidiophores, were also abundant (Fig 3.6 E,F,G,H)

Degradation of samples inoculated with *U. atrum* was similar in that the outer amorphous layer became rough and fibrillar on and between adjacent leaf cells (Fig 3.7 A, B) forming voids that coalesced until the outer layerappeared to lift away from the underlying cells which disarticulated (Fig 3.7 B, C, D). As in the decay pattern caused by *C. inaequalis*, the underlying lamellate layer of the

leaf cell walls was exposed as the amorphous layer was eroded, although this was more pronounced in samples inoculated with *U. atrum* (Fig 3.7 E).

Samples inoculated with *C. gossypii* degraded in a similar pattern but erosion of the outer layer proceeded at a faster rate (Fig 3.7 F) in that only traces of the fibrillar material of the outer layer remained between leaf cells after three months of incubation (Fig 3.7 G). The integrity of the inner wall layer appeared unaltered (Fig 3.7 H). Degradation around the raised apices of some moss cells caused them to appear more prominent (Fig 3.7 I). Leaf cells disarticulated once the outer layer had eroded (Fig 3.7 J).

3.4 Discussion

The diversity of hyphal morphologies in the alpine grout samples indicates that a range of fungal species occur in this material. This study focused on only three species in the Pleosporaceae chosen because of their tendency to sporulate abundantly, and because of their melanised hyphae and spores which would allow them to persist among the exposed upper regions of moss gametophytes. These ascomycetous species may be among the earliest fungal colonisers of grout.

Ditrichum flexicaule and *Tortella tortuosa* were among the main bryophyte components of the grout samples collected at the Saskatchewan glacier. Like other mosses, they are poikilohydric and thus well suited to an environment of extreme fluctutations in temperature and moisture. Because it was not feasible to collect sufficient quantities of these tiny plants for *in vitro* assessments of fungal degradative abilities, the abundant circumboreal and circumpolar feather moss, *Hylocomium splendens,* was used instead, and may have a bearing on the

interpretation of the results. The leaves of all three species are unistratose and in both *H. splendens* and *D. flexicaule* leaf cells were elongate with smooth surfaces. In *T. tortuosa,* leaf cells are cuboid and covered with numerous papillose outgrowths of wall material. Patterns of hyphal growth on leaves of *H. splendens* and *D. flexicaule* are probably comparable but may differ on the densely papillose leaves of *T. tortuosa*.

Decomposition of *Hylocomium* leaf tissue was similar for all three fungi, although *C. gossypii* and *U. atrum* degraded the components of the outer wall more rapidly and completely than did *C. inaequalis*. Hyphae grew across the leaf surfaces and into cells often via the formation of appressoria that were sometimes dichotomously branched. Conidiophores and conidia were also produced on the substrate by each of the fungi. Colonised leaves became puckered and fragile as the outer amorphous layer was eroded to reveal a net-like reticulum of cellulose fibrils. As this layer degraded further, the thick inner layer of the cell wall was exposed and at this stage, leaf cells easily disarticulated when disturbed.

Enzymatic tests showed that all three fungi were able to degrade starch, cellulose, and protein, but only *U. atrum* and *C. gossypii* resulted in a reaction when grown on tannic acid media, which indicates the production of some polyphenol oxidases. None, however, gave a positive reaction on the wood guiacol medium indicating an inability to breakdown lignin. This corroborates SEM observations (Fig 3.6 G, 3.7 E, I), that show the thick inner wall of the moss leaf cells, which is rich in lignin-like compounds, was persistent after the outer amorphous layer was eroded. Penetration through the inner layer was often

accomplished through the formation of appressoria, suggesting that the addition of mechanical force may have been necessary to breach this inner wall.

All three fungi broke down materials associated in large part with the outer wall layer, resulting in mass losses ranging from 9.8% for *C. gossypii* to 12% for *U. atrum*. Measurements varied so widely among replicates that statistically significant differences were not detected across the species. Topographic and compositional heterogeneity of whole gametophytes may have led to colonisation patterns in which hyphae accumulate along corridors and in pockets. Similar variations in mass loss data were found during a comparable study of fungal degradation of whole gametophytes of *Sphagnum* inoculated with myxotrichaceous fungi and white rot basidiomycetes (Rice et al. 2006).

Degradation of the outer amorphous layer to leave the inner layer of disarticulating leaf cells results in the formation of a coarse, brownish residue composed of leaf fragments and persistent lignin-like materials. This process is roughly comparable to "brown rot" described in the literature concerning the decay of wood, though there is no evidence here that the pleosporalean fungi were able to remove cellulose from the polyphenol-rich inner cell wall layer. Brown rot of wood caused by certain basidiomycetes involves the dissolution of the cellulose microfibrils embedded in the lignin layer of xylem cell walls and this causes a characteristic shrinkage and cracking. Previous studies with the mold species *Oidiodendron maius* and *Pochonia bulbillosa* in the degradation of *Sphagnum* showed a pattern of degradation in which the amorphous components of the cell wall were eroded to expose the underlying cellulose microfibrils

(Tsuneda et al. 2001) in a pattern reminiscent of a type of wood decay known as "white rot". While the terms white rot and brown rot may not be accurate when describing the decay of moss cells, the range of variation does indicate that the decay of bryophyte tissues by fungi could be just as complex and varied as in the decay of wood (Blanchette 1995). Comparative and standardised studies of bryophyte decay using different species of mosses and fungi would improve our understanding of how these organisms contribute to the humification of moss tissues and early stages of soil formation.

Chalastospora gossypii was isolated from necrotic patches on leaves of *Saxifraga oppositifolia* and was able to erode the outer layer of moss leaf cells. The lesser, but non-significant, percent mass loss caused by *C. gossypii* may be attributed to the fact that its normal host species are vascular plants. Despite a similarity in penetrative and absorptive structures produced by bryophyte and vascular plant pathogens and the previously noted presence of vascular plant pathogens on bryophytes (Davey and Currah 2010), the ability of this fungus to infect and cause necrosis or degradation on both types of hosts has not been examined.

During primary succession, the accumulation of residues derived from bryophyte tissues (Crew et al. 2001), unicellular algae (Freeman et al. 2009b), chytrids (Freeman et al. 2009a), entrained organic particulates such as pollen grains, and the cells of associated decay organisms all contribute to the formation of soil and subsequent establishment byvascular plants. Moss fragments provide a source of nitrogen, phosphorus, sulfur, and trace elements (Chapin et al. 1994,

Coyne & Thompson 2006), contribute to ion exchange capacities, and aid in aggregation and stabilisation (Coyne & Thompson 2006). Microscopic observations of moss gametophytes collected from the Saskatchewan Glacier show that pollen grains of conifers are abundant in the grout column and could serve as an additional source of phosphorus and nitrogen during the degradation of recalcitrant organic residues. Many basidiomycetes involved in the decay of wood parasitise pollen when nutrients are otherwise limiting (Hutchison and Barron 1997). Finally, hyphae growing through the grout column stabilise and anchor friable organic particulates and aid in the creation of soil aggregates (Caesar-TonThat and Cochran 2000; Caesar-TonThat 2002).

The objective of this study was to characterise and compare how three conidial fungi from the Pleosporaceae isolated from the forefield of the Saskatchewan glacier degraded bryophyte tissues. While there were small differences among the three species, *C. inaequalis, U. atrum*, and *C. gossypii* were similar in that, after three months, they had significantly eroded the amorphous surficial and intercellular layers of the unistratose leaves of *Hylocomium splendens*. Cells exposed during this process were surrounded by thick inner walls and these appeared to be resistant to decay. We propose that these polyphenolic-rich, thick walled, brownish cells contribute to the organic debris associated with the lower levels of the grout column and that they are eventually degraded by other fungi, including basidiomycetes, which were well represented in the samples we examined, and other groups, such as dark septate endophytes, which may eventually serve as mycorrhizal partners for vascular

plant colonisers (Addy et al. 2005). More controlled studies of a broader range of fungi are needed to explain how bryophyte tissues and fungi contribute to pedogenesis and patterns of colonisation in primary succession.

3.5 Literature cited

Addy, H.D., Piercey, M.M., and Currah, R.S. 2005. Microfungal endophytes of roots. Can. J. Bot. 83: 1-13.

Blanchette, R.A. 1995. Degradation of the ligninocellulose complex in wood. Can. J. Bot. 73: S999-S1010.

Butler, M.J. and Day, A.W. 1998. Fungal melanins: a review. Can. J. Microbiol. 44: 1115-1136.

Caesar-TonThat, T.C. 2002. Soil binding properties of mucilage produced by a basidiomycete fungus in a model system. Mycol. Res. 106: 930-937.

Caesar-TonThat, T.C. and Cochran, V.L. 2000. Soil aggregate stabilization by a saprophytic lignin-decomposing basidiomycete fungus I. Microbiological aspects. Biol. Fertil. Soils. 32: 374-380.

Chapin, F.S., Walker, L.R., Fastie, C.L., and Sharman, L.C. 1994. Mechanisms of primary succession following deglaciation at Glacier Bay, Alaska. Ecol. Mono. 64: 149-175.

Coyne, M.S. and Thompson, J.A. 2006. Fundamental Soil Science. Thompson Delmar Learning, USA.

Crew, T.E., Kurina, L.M. and Vitousek, P.M. 2001. Organic matter and nitrogen accumulation and nitrogen fixation during early ecosystem development in Hawaii. Biogeochemistry. 52: 259-279.

Davey, M.L. and Currah, R.S. 2009. *Atradidymella muscivora* gen. et sp. nov. (Pleosporales) and its anamorph *Phoma muscivora* sp. nov.: A new pleomorphic pathogen of boreal bryophytes. Am. J. Bot. 96: 1281-1288.

Davey, M.L. and Currah, R.S. 2010. Saprobic and parasitic interactions of *Coniochaeta velutina* with mosses Botany. 88: 259-265.

Day, M.J., Gibas, C.F.C., Fujimura, K.E., Egger, K.N., and Currah, R.S. 2006. *Monodictys arctica*, a new hyphomycete from the roots of *Saxifraga oppositifolia* collected in the Canadian High Arctic. Mycotaxon. 98: 261-272.

Edelmann, H.G., Neinhuis, C., Jarvis, M., Evans, B., Fischer, E., and Barthlott, W. 1998. Ultrastructure and chemistry of the cell wall of the moss *Rhacocarpus pupurascens* (Rhacocarpaceae): a puzzling architecture among plants. Planta. 206: 315-321.

Ellis, M.B. 1971. Dematiaceous hyphomycetes. Commonwealth Mycological Institute: England.

Erickson, M. and Miksche, G.E. 1974. Occurrence of lignin polyphenols in some mosses and liverworts. Phytochemistry. 13: 2295-2299.

Farmer,V.C. and Morrison, R.I. 1964. Lignin in sphagnum and phragmites and in peats derived from these plants. Geochim. Cosmochim. Ac. 28: 1537-1546.

Felsenstein, J. 1985. Confidence limits on phylogenies: an approach using the bootstrap. Evolution. 39: 783-791.

Freeman,K.R., Martin, A.P., Karki, D., Lynch, R.C., Mitter, M.S., Meyer, A.F., Longcore, J.E., Simmons, D.R., and Schmidt, S.K. 2009a. Evidence that chytrids dominate fungal communities in high-elevation soils. P. Natl. Acad. Sci-Biol. 106: 18315-18320.

Freeman, K.R., Pescador, M.Y., Reed, S.C., Costello, E.K., Robeson, M.S. and Schmidt, S.K. 2009b. Soil CO_2 flux and photoautotrophic community composition in high-elevation, 'barren' soil. Environmental Microbiology. 11: 674-686.

Hébant, C. 1977. The conducting tissues of Bryophytes. J. Cramer, Germany.

Ho, M. H-M., Castaneda, R.F., Dugan, F.M., and Jong, S.C. 1999. *Cladosporium* and *Cladophialophora* in culture: description and an expanded key. Mycotaxon. 72: 115-158.

Huelsenbeck, J.P. and Ronquist, F. 2001. MRBAYES: Bayesian inference of phylogeny. Bioinformatics. 1: 754-755.

Hutchison, L.J. 1990. Studies on the systematics of ectomycorrhizal fungi in axenic culture II. The enzymatic degradation of selected carbon and nitrogen compounds. Can. J. Bot. 68: 1522-1530.

Hutchison, L.J. and Barron, G.L. 1997. Parasitism of algae by lignicolous Basidiomycota and other fungi. Can. J. Bot. 75: 1006-1011.

Lane, D.J., Pace, B., Olsen, G.J., Stahl, D.A., Sogin, M.L., and Pace, N.R. 1985. Rapid determination of 16S ribosomal RNA sequences for phylogenetic analysis. Proc. Natl. Acad. Sci., U.S.A. 82: 6955-6959.

Ligrone, R., Carafa, A., Duckett, J.G., Renzaglia, K.S. and Ruel, K. 2008. Immunocytochemical detection of lignin-related epitopes in cell walls in bryophytes and the charalean alga *Nitella* . Plant. Syst. Evol. 270: 257-272.

Marx, D.H. 1969. The influence of ectotrophic mycorrhizal fungi on the resistance of pine roots to pathogenic infections. I. Antagonism of mycorrhizal fungi to root pathogenic fungi and soil bacteria. Phytopathology. 59: 153–163.

Nylander, J.A.A. 2004. MrModeltest v2. Program distributed by the author. Evolutionary Biology Centre, Uppsala University.

Rambaut, A. 1996. Se-Al: Sequencing alignment editor [online]. Available at http://evolve.zoo.ox.ac.uk.

Rice, A.V., Tsuneda, A. and Currah, R.S. 2006. *In vitro* decomposition of *Sphagnum* by some micro fungi resembles white rot of wood. FEMS Microbiol. Ecol. 56: 372-382.

Ronquist, F. and Huelsenbeck, J.P. 2003. MRBAYES 3: Bayesian phylogenetic inference under mixed models Bioinformatics. 19: 1572-1574.

Sakar, P., Boseneaga, E., and Auer, M. 2009. Plant cell walls throughout evolution: towards a molecular understanding of their design principles. J. Exp. Bot. 60: 3615-3635.

Simmons, E.G. 1967 Typification of *Alternaria, Stemphylium,* and *Ulocladium*. Mycol. Res. 59: 67-92.

Simmons, E.G. 1982. *Alternaria* themes and variations (11-13). Mycotaxon. 14: 44-57.

Swofford, D.L. 2002. PAUP* Phylogenetic analysis using parsimony (* and other methods). Version 4. Sunderland. Sinauer and Associates.

Tsuneda, A., Maekawa, N., Ohira, I., and Furukawa, I. 1991. Incipient decay of *Quercus serrata* sapwood by *Lentinus edodes* and its inhibition by an antagonistic hyphomycete, *Leptodontidium elatius.* Can. J. Bot. 69: 2797–2825.

Tsuneda, A., Thormann, M.N., and Currah, R.S. 2001. Modes of cell-wall degradation of *Sphagnum fuscum* by *Acremonium* cf. *curvulum* and *Oidiodendron maius.* Can. J. Bot. 79: 93-100.

Viereck, L.A. 1966. Plant succession and soil development on gravel outwash of the Muldrow Glacier, Alaska. Ecol. Mono. 36: 181-199.

White, T.J., Bruns, T., Lee, S., and Taylor, J.W. 1990. Amplification and direct sequencing of fungal ribosomal RNA genes for phylogenetics *In* PCR protocols: a guide to methods and applications *edited by* M.A. Innis, D.H. Gelfand, J.J. Sinisky, and T.J. White. Academic Press, Inc, USA. pp 315-322.

Table 3.1. GenBank accession numbers for taxa used in the phylogenetic analyses.

Species	GenBank Accession Number
Alternaria alternata	FJ545250
Alternaria alternata	AF347031
Alternaria brassicae	DQ156344
Alternaria brassicola	AY781077
Alternaria carotiincultae	EU136640
Alternaria cheiranthi	AF229457
Alternaria conjuncta	AF392988
Alternaria conjuncta	FJ266475
Alternaria crassa	AF229464
Alternaria daturicola	AY372685
Alternaria dauci	EU807869
Alternaria japonica	AY781079
Alternaria oregonensis	AY762947
Alternaria palandui	DQ323702
Alternaria petroselini	EU807868
Alternaria radicina	EU807870

Alternaria selini	AF229455
Alternaria smyrnii	AF229456
Alternaria triticina	AY762948
Alternaria triticina	AY714476
Chalastospora cetera	FJ839607
Chalastospora ellipsoidea	FJ839608
Chalastospora gossypii	AY251081
Chalastospora gossypii	AF393680
Chalastospora gossypii	AF393715
Chalastospora gossypii	AF393714
Chalastospora gossypii	AF393713
Chalastospora gossypii	AF393722
Chalastospora gossypii	AF393721
Chalastospora gossypii	FJ839609
Chalastospora gossypii	FJ839610
Chalastospora gossypii	FJ839615
Chalastospora gossypii	FJ839614

Chalastospora gossypii	FJ839612
Chalastospora gossypii	AY251079
Chalastospora gossypii var. *polymorpha*	AY251080
Chalastospora obclavata	FJ839616
Curvularia affinis	EF187909
Curvularia affinis	AF071335
Curvularia brachyspora	AF212308
Curvularia clavata	AF071336
Curvularia cymbopogonis	AF163079
Curvularia eragrostidis	AF163077
Curvularia geniculata	AB245085
Curvularia gladioli	AF071337
Curvularia gudauskasii	AF071338
Curvularia heteropogonicola	AF163080
Curvularia inaequalis	AF313409
Curvularia inaequalis	AM924157
Curvularia inaequalis	AY941256

Curvularia inaequalis	AF120261
Curvularia inaequalis	AF163081
Curvularia intermedia	AF163078
Curvularia oryzae	AF163083
Curvularia panici	AB164703
Curvularia trifolii	EF600959
Curvularia trifolii	AF212310
Curvularia trifolii	AF455446
Dothidea hippophaeos	AF022763
Dothidea sambuci	AY883094
Lewia ethzedia	AF392987
Lewia ethzedia	AY278833
Phaeosphaeriopsis musae	DQ885894
Pleospora alfalfae	AY329171
Ulocladium atrum	AY625072
Ulocladium atrum	AY372683
Ulocladium botrytis	AY625070

Ulocladium capsici	AY762940
Ulocladium consortiale	AY278837
Ulocladium cucurbitae	EU330457
Ulocladium cucurbitae	FJ266483
Ulocladium cucurbitae	AY762941
Ulocladium obovoideum	AY762942

Table 3.2. *In vitro* enzymatic abilities of *Curvularia inaequalis*, *Ulocladium atrum*, and *Chalastospora gossypii*. - = negative reaction, + = positive reaction

	Soluble polyphenols	Cellulose	Pectin	Starch	Insoluble polyphenols	Protein
Curvularia inaequalis	-	+	-	+	-	+
Ulocladium atrum	+	+	-	+	-	+
Chalastospora gossypii	+	+	+	+	-	+

Figure 3.1. Alpine grout and fungi present in or isolated from *Ditrichum flexicaule* [*Curvularia inaequalis* (UAMH 11180)], *Tortella tortuosa* [*Ulocladium atrum* (UAMH 11179)], and *Saxifraga oppositifolia* [*Chalastospora gossypii* (UAMH 11181)].

A. Partially excavated moss grout columns (arrow heads) up to 1 cm in height. Grout is dense and fibrous and keeps its shape (*) when adjacent rocks (arrows) are removed. Bar = 2 cm.
B. Abundant rhizoids (arrowhead) in the brown fibrous zone where organic particulates (arrow) are also numerous. Fungal hyphae (H) are abundant. Direct mount in distilled water. Bar = 30 μm.
C. Moss fragments (arrow) are abundant in the rhizoids (arrowheads). Direct mount in distilled water. Bar = 80 μm.
D. A diversity of fungal hyphae (H) are present in this vertical column of grout. Arrow highlights stem of moss gametophyte. Direct mount in distilled water. Bar = 30 μm.
E. *Curvularia inaequalis* with a single conidium (arrowhead) on a conidophore that is exiting the gametophyte (arrow) of *Hylocomium splendens*. Bar = 6.5 μm.
F. The smooth, 3-4 (rarely 5) septate, straight to slightly curved dark conidia of *Curvularia inaequalis*. The material is mounted in polyvinyl alcohol (PVA) and shows the characteristic palmate configuration of conidia (arrow head) on the conidiophore (arrow). Bar = 33 μm.
G. *Ulocladium atrum* with warty, occasionally obpyriform (arrowhead) conidia on the conidiophore (arrow). Bar = 12.5 μm.
H. *Ulocladium atrum* with dark, warty, predominantly spherical, cruciseptate conidia borne in sympodial clusters. Direct mount in APVA. Bar = 33 μm.
I. *Chalastospora gossypii* with oblong, non-septate conidia (arrow) borne in a fragile branched chains (arrowhead). Material mounted in PVA. Bar = 15 μm.

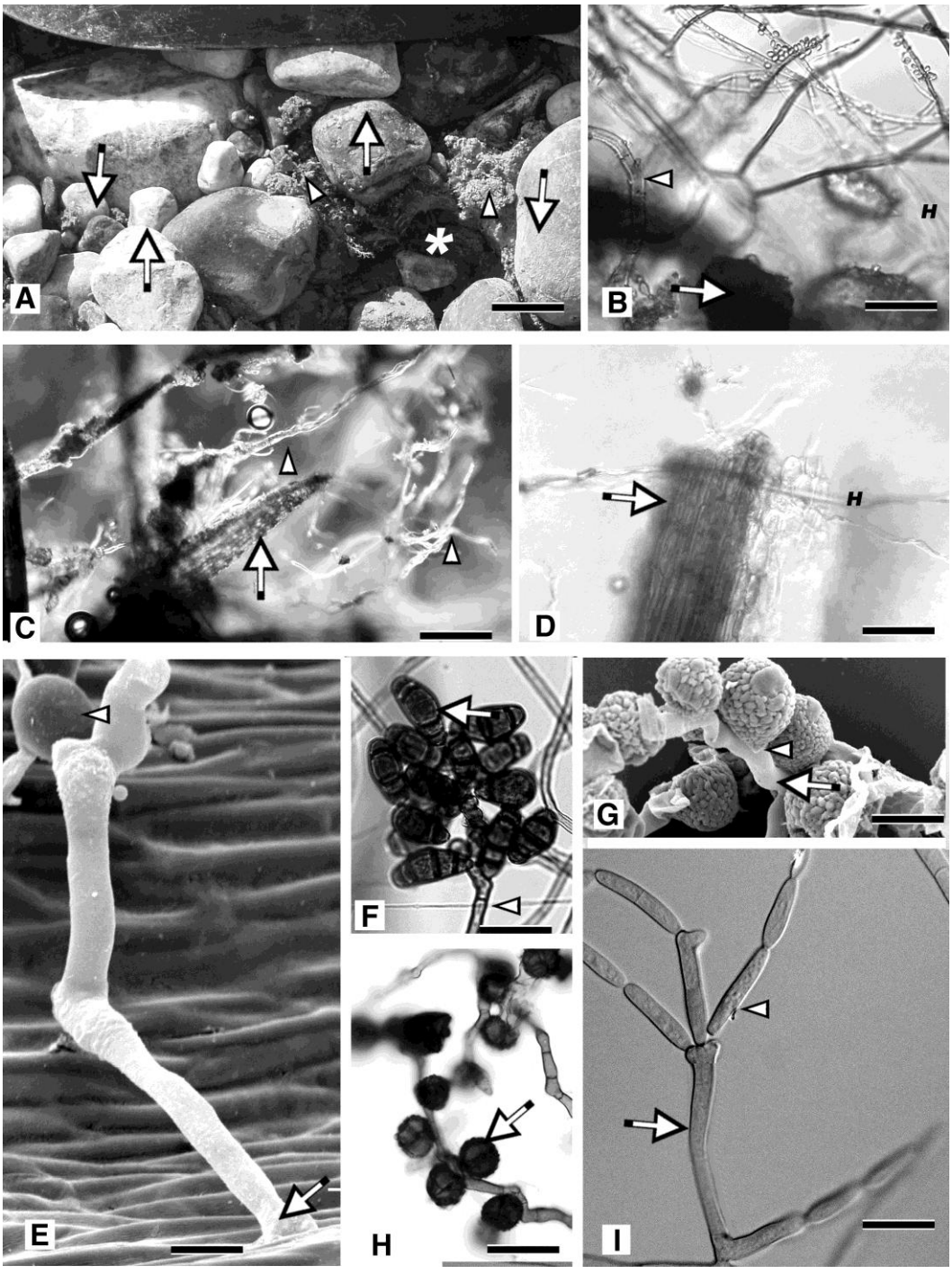
A
B
H
C
D
H
E
F
G
H
I

Figure 3.2. One of 6 most parsimonious trees showing the placement of *Curvularia inaequalis* UAMH 11180. Branches in bold have both bootstrap support and Bayesian posterior probabilities greater than 70%.

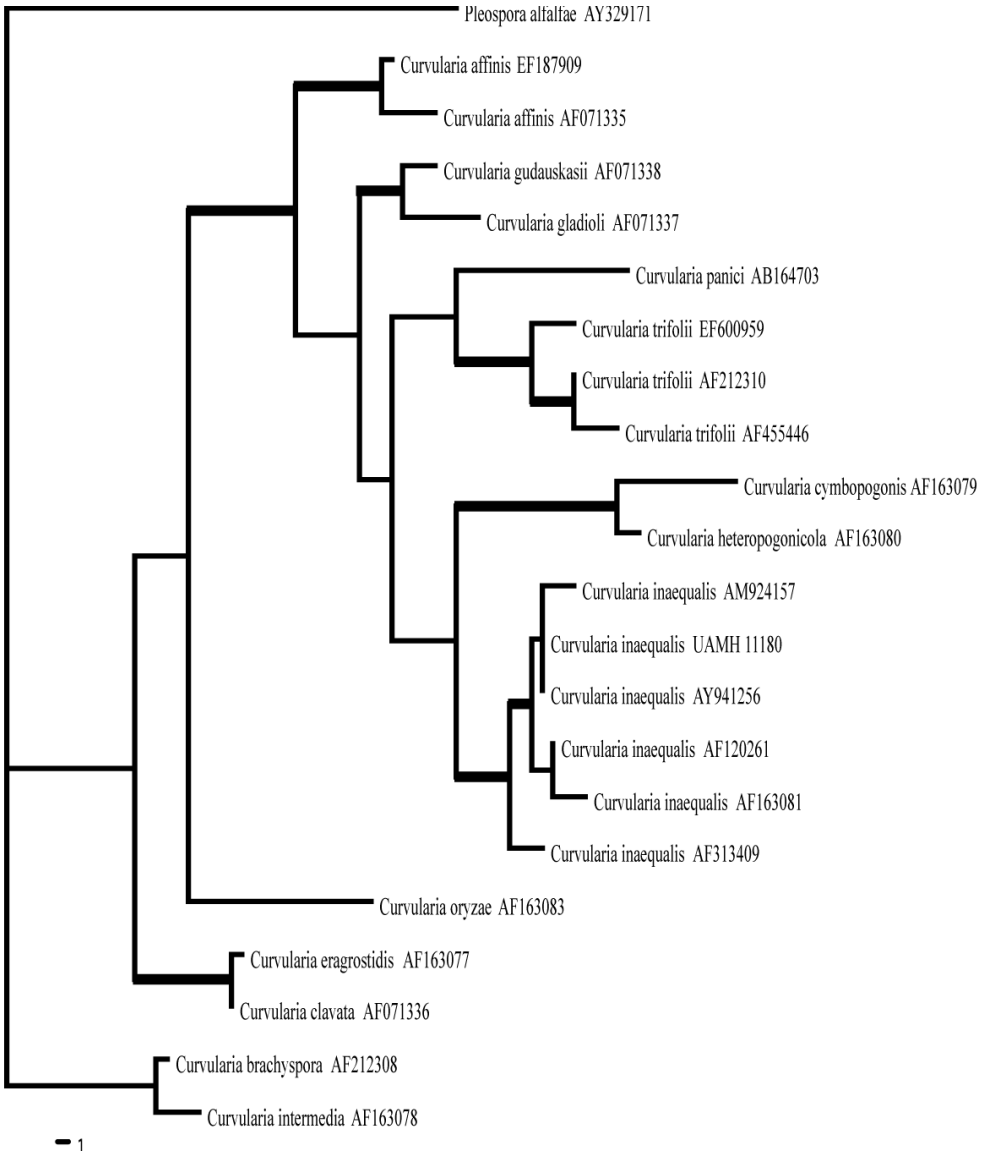
Pleospora alfalfae AY329171
Curvularia affinis EF187909
Curvularia affinis AF071335
Curvularia gudauskasii AF071338
Curvularia gladioli AF071337
Curvularia panici AB164703
Curvularia trifolii EF600959
Curvularia trifolii AF212310
Curvularia trifolii AF455446
Curvularia cymbopogonis AF163079
Curvularia heteropogonicola AF163080
Curvularia inaequalis AM924157
Curvularia inaequalis UAMH 11180
Curvularia inaequalis AY941256
Curvularia inaequalis AF120261
Curvularia inaequalis AF163081
Curvularia inaequalis AF313409
Curvularia oryzae AF163083
Curvularia eragrostidis AF163077
Curvularia clavata AF071336
Curvularia brachyspora AF212308
Curvularia intermedia AF163078
1

Figure 3.3. One of 9700 most parsimonious trees based on ITS analysis showing the placement of *Ulocladium atrum* UAMH 11179. Branches in bold have both bootstrap support and Bayesian posterior probabilities greater than 70%. Note the clade of *Ulocladium capsici, U. consortiale, U. cucurbitae, U. atrum,* and UAMH 11179 leaves the identity of UAMH 11179 unresolved.

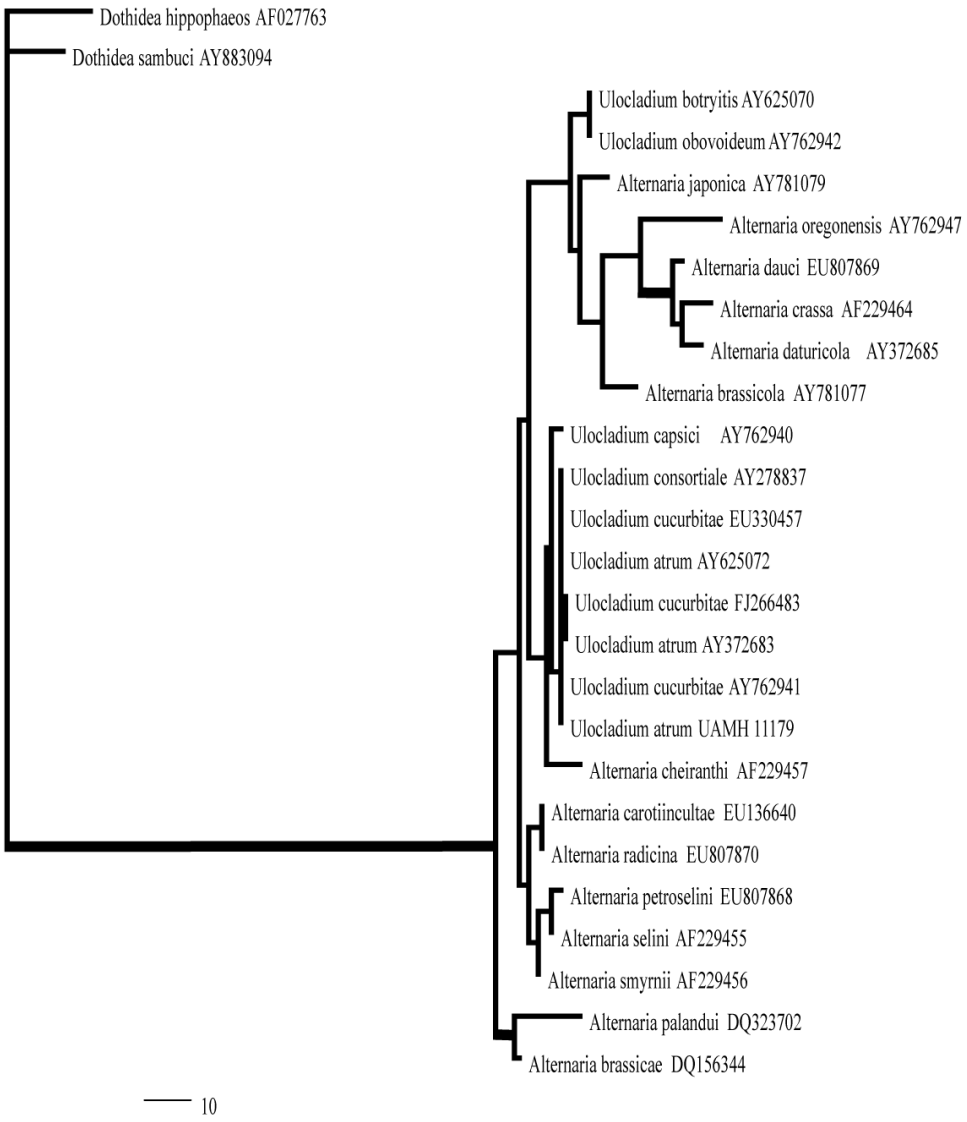
Dothidea hippophaeos AF027763
Dothidea sambuci AY883094
Ulocladium botryitis AY625070
Ulocladium obovoideum AY762942
Alternaria japonica AY781079
Alternaria oregonensis AY762947
Alternaria dauci EU807869
Alternaria crassa AF229464
Alternaria daturicola AY372685
Alternaria brassicola AY781077
Ulocladium capsici AY762940
Ulocladium consortiale AY278837
Ulocladium cucurbitae EU330457
Ulocladium atrum AY625072
Ulocladium cucurbitae FJ266483
Ulocladium atrum AY372683
Ulocladium cucurbitae AY762941
Ulocladium atrum UAMH 11179
Alternaria cheiranthi AF229457
Alternaria carotiincultae EU136640
Alternaria radicina EU807870
Alternaria petroselini EU807868
Alternaria selini AF229455
Alternaria smyrnii AF229456
Alternaria palandui DQ323702
Alternaria brassicae DQ156344
10

Figure 3.4. One of 10 000 most parsimonious trees showing the placement of *Chalastospora gossypii* UAMH 11181. Branches in bold have both bootstrap support and Bayesian posterior probabilities greater than 70%.

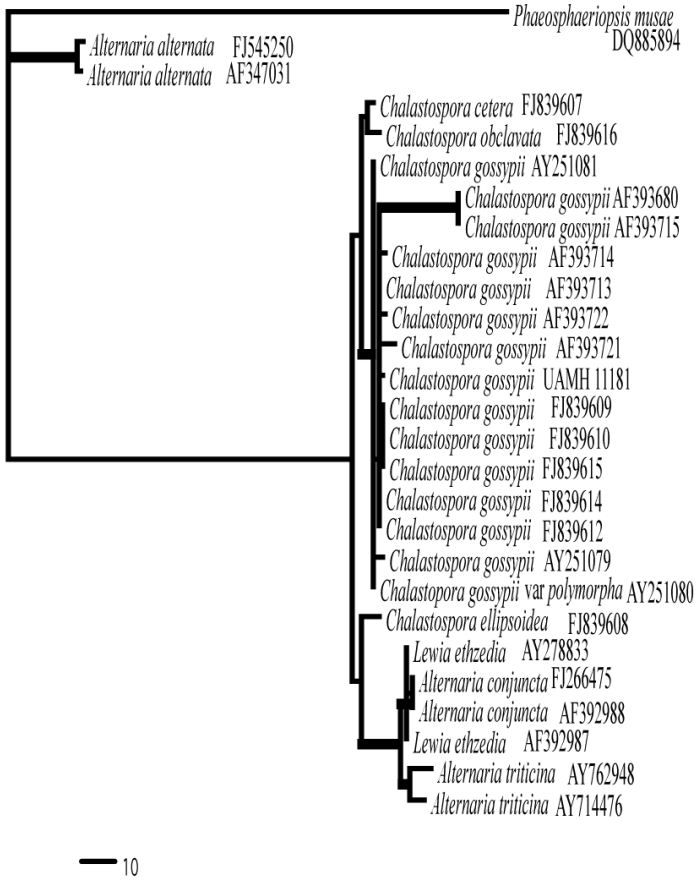
Phaeosphaeriopsis musae DQ885894
Alternaria alternata FJ545250
Alternaria alternata AF347031
Chalastospora cetera FJ839607
Chalastospora obclavata FJ839616
Chalastospora gossypii AY251081
Chalastospora gossypii AF393680
Chalastospora gossypii AF393715
Chalastospora gossypii AF393714
Chalastospora gossypii AF393713
Chalastospora gossypii AF393722
Chalastospora gossypii AF393721
Chalastospora gossypii UAMH 11181
Chalastospora gossypii FJ839609
Chalastospora gossypii FJ839610
Chalastospora gossypii FJ839615
Chalastospora gossypii FJ839614
Chalastospora gossypii FJ839612
Chalastospora gossypii AY251079
Chalastopora gossypii var polymorpha AY251080
Chalastospora ellipsoidea FJ839608
Lewia ethzedia AY278833
Alternaria conjuncta FJ266475
Alternaria conjuncta AF392988
Lewia ethzedia AF392987
Alternaria triticina AY762948
Alternaria triticina AY714476
10

Figure 3.5. Percent mass loss of gametophytes of *Hylocomium splendens* inoculated with *Curvularia inaequalis*, *Ulocladium atrum*, and *Chalastospora gossypii* for three months. Three replicates were examined per species. These values are corrected against the control. There are no statistically significant differences among the average percent mass losses caused by the three species.

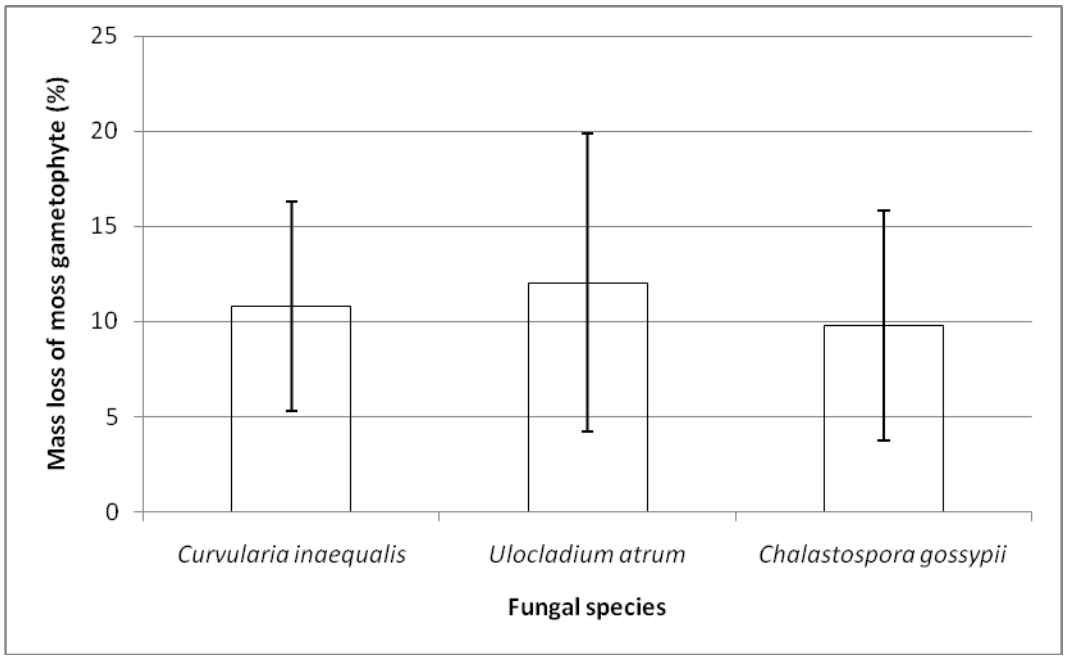
25
20
15
10
5
0
Mass loss of moss gametophyte (%)
Curvularia inaequalis
Ulocladium atrum
Chalastospora gossypii
Fungal species

Figure 3.6. Gametophytes of *Hylocomium splendens* uninoculated (A and B) and inoculated with *Curvularia inaequalis* UAMH 11180 (C-H).

A. Unistratose acuminate, oblong-lanceolate leaves (arrowheads) of uninoculated *Hylocomium splendens* showing narrow branched pseudoparaphylia (arrow) which are abundant along the stem. Bar = 200 μm.
B. Surface of the uninoculated *Hylocomium splendens* leaves showing elongate leaf cells, some of which have prominent terminal papilla-like projections (arrowheads). Note the continuous, lacquer-like amorphous layer. Bar = 25 μm.
C. Abundant inoculated hyphae on puckered leaf surfaces (arrows) Note the line of weakness along adjoining cells after three months incubation (arrowhead). Bar = 7 μm.
D. Appressoria (arrows) on the leaf surface. The lacquer-like amorphous layer along the junctions between cells deteriorates (arrowheads) leaving a fibrillar to membranous residue. Bar = 7 μm.
E. Conidiophores, sometimes asperulate (arrowhead), and conidia (arrow) on the substrate. Bar = 12.5 μm.
F. Hypha growing across the leaf surface and into cells (arrowhead). Bar = 12.5 μm.
G. The lacquer-like amorphous layer has been removed exposing a fibrillar to membranous residue and the parallel longitudinal ridges (arrows) of the thick inner lamellate layer. Note the hole through the inner layer made by a hypha (arrowhead). Bar = 2.5 μm.
H. Dichotomously branched appressorium (arrowhead) surrounded by pronounced degradation and fibrillar to membranous residue (arrow). Bar = 3.3 μm.

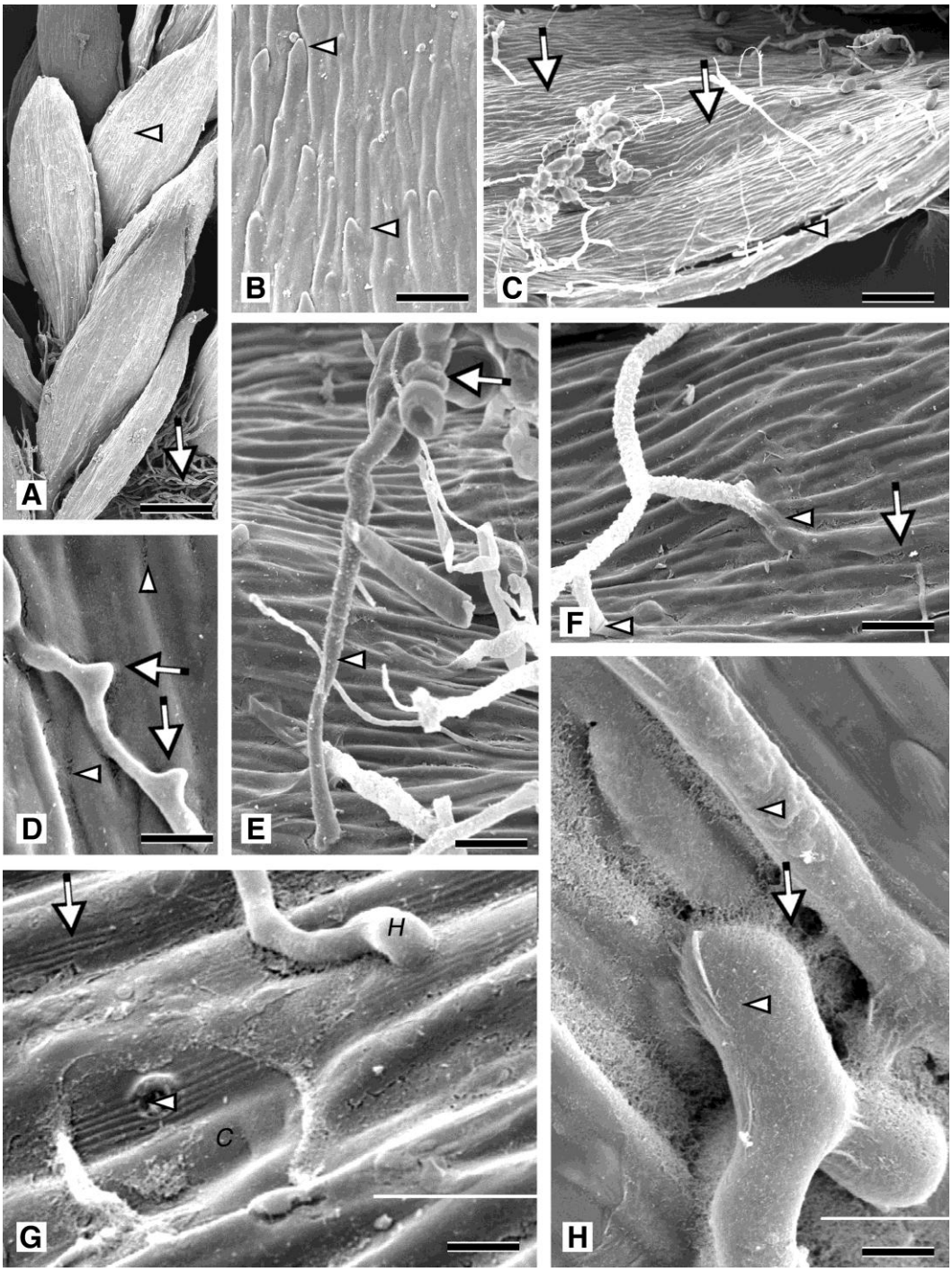
A
B
C
D
E
F
G
H
C
H

Figure 3.7. Decomposition of *Hylocomium splendens* leaves by *Ulocladium atrum* UAMH 11179 (A-E) and *Chalastospora gossypii* UAMH 11181 (F-I). J – *Tortella tortuosa* leaf collected from site.

A. Degradation of samples showing the outer amorphous layer becoming rough and fibrillar (arrowhead) between adjacent leaf cells. Bar = 5 μm.
B. Note voids (arrow heads) formed between adjacent cells. Bar = 2.5 μm.
C. *Ulocladium atrum* causing the outer layer (arrowhead) to lift away from the underlying cells. Note the hypha in the junction between elongate leaf cells (arrow). Bar = 7 μm.
D. Voids (arrowhead) in the vicinity of hyphae (arrow). Bar = 2.5 μm.
E. Degradation caused by *Ulocladium atrum* is more pronounced than that caused by *Curvularia inaequalis*. Note the presence of *Ulocladium atrum* hypha (arrow) and the lifting of the entire outer cell wall layer (arrowheads). Bar = 7 μm.
F. Degradation has caused the outer cell wall layer to lift away, exposing the underlying layer. Note the fibrillar residue in the junctions between cells (arrow heads). Bar = 5 μm.
G. Decomposition left fibrillar residue (arrowheads), revealing parallel longitudinal ridges of the thick inner lamellate layer (arrows). Bar = 3.3 μm.
H. Degradation caused by the fungus (arrows) is most prominent in the vicinity of multiple hyphae (arrow heads). Bar = 3.3 μm.
I. Traces of fibrillar remains of outer layer (arrow) after degradation. Note the raised apices of some leaf cells (*). Bar = 7 μm.
J. *Tortella tortuosa* leaf collected from grout sample. Note the break between cells (arrowheads). Bar = 30 μm.

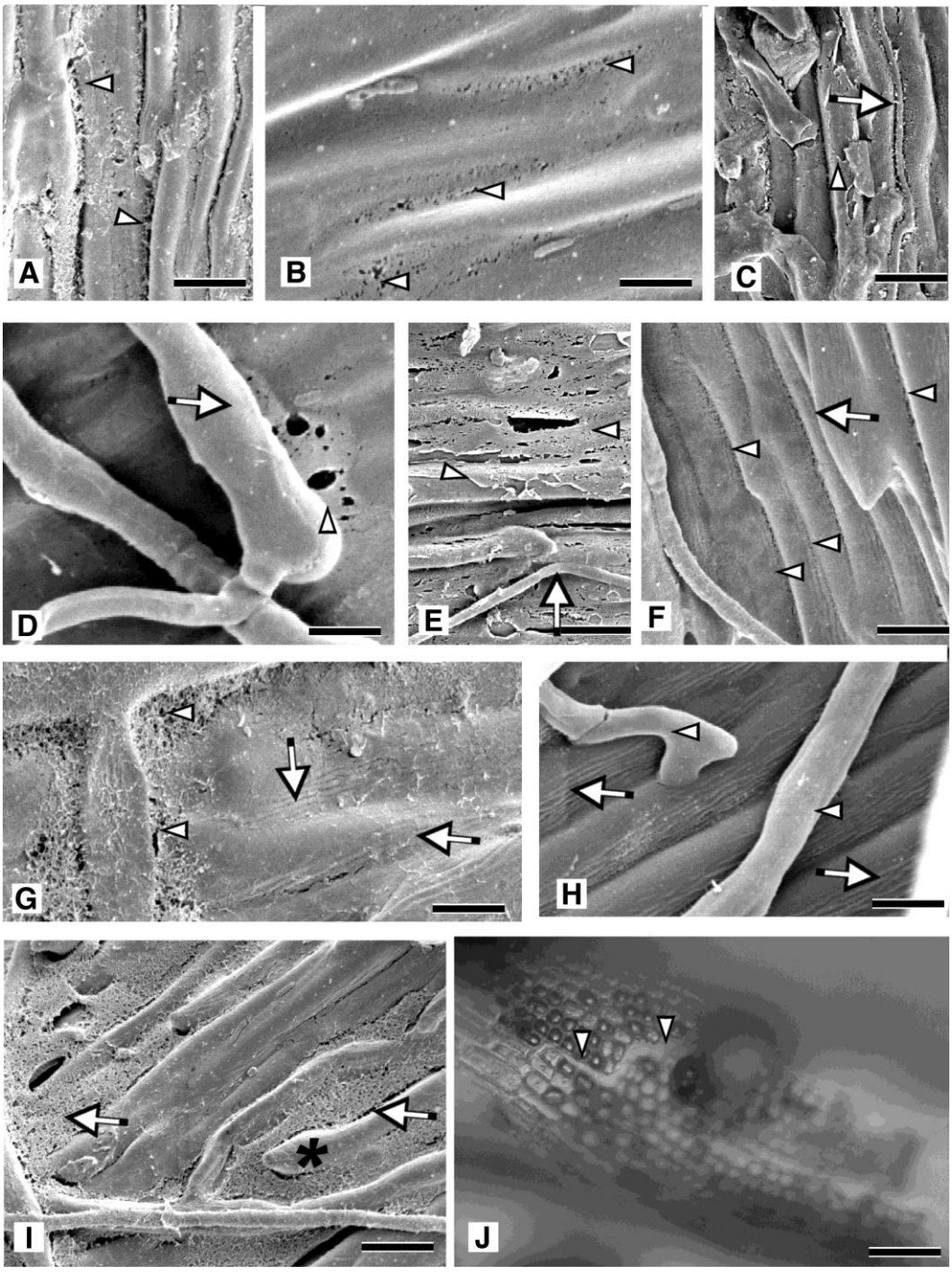
A
B
C
D
E
F
G
H
I
J

Chapter 4. Role of selected DSE species and other hyphomycetes as saprobes on moss gametophytes.

4.1 Introduction

The accumulation of organic debris from the fungal breakdown of bryophyte tissues in arctic and alpine habitats ostensibly facilitates the establishment of pioneer plants, the roots of which are also commonly colonised by dark septate endophytic fungi (DSE) (Currah and Van Dyk 1986; Bledsoe et al. 1990; Treu et al. 1996; Väre et al. 1996; Addy et al. 2005). Species included among the DSE are ascomycetous microfungi that are readily isolated from host roots and grow well when cultured on routine laboratory media. This indicates that these fungi are saprobic, at least to some extent, but quasi-mycorrhizal roles have also been attributed to the DSE (Mandyam and Jumpponen 2005). In most cases the endorhizal phase consists of hyphae and sometimes microsclerotia in the cortices of roots but one common representative, *Phialocephala fortinii*, has been shown to form ectomycorrhizas when inoculated onto host species (Currah et al. 1993; Fernando and Currah 1996; Jumpponen et al. 1998). Reports of most DSE from materials other than roots are uncommon (Menkis et al. 2004) and as a result it is not known if these fungi can or do establish in advance of the arrival of a suitable host, as saprobic associates of bryophyte debris, for example, or if rooted host plants would be a precondition for their colonisation.

Controlled studies of the growth and effects of DSE fungi introduced as inoculants on various plant hosts have been reported (Wang and Wilcox 1985; O'Dell et al. 1993; Fernando and Currah 1996) but data concerning the degradative potential of DSE species are less common and have been derived

entirely from crude enzymatic tests using a limited number of species i.e., *P. fortinii, P. sphaeroides, Cadophora finlandica* and *Leptodontidium orchidicola* (see Mandyam and Jumpponen 2005). The potential role of DSE in the humification of bryophyte tissues prompted me to examine the saprobic ability of selected DSE species (*Cadophora luteo-olivacea, Leptodontidium orchidicola,* and *Phialocephala fortinii*) and two known saprobes (*Cadophora melinii* and *Coniochaeta nepalica*) to degrade intact dead tissues of a locally abundant bryophyte, *Hylocomium splendens*. Resultant data, derived from crude enzymatic profiles and scanning electron microscopic observations, were assembled to provide insight concerning the potential role of DSE as saprobes fungi on bryophytes and vascular plants, respectively, in arctic and alpine environments.

4.2 Methods

Provenance data for isolates examined (*Cadophora luteo-olivacea, C. melinii, Coniochaeta nepalica, Leptodontidium orchidicola,* and *Phialocephala fortinii*) are given in Table 4.1.

4.2.1 Enzyme tests

To test *in vitro* enzymatic abilities, three replicates per isolate were set up on six test media following the procedure in Chapter 3. Inocula were taken from colonies using the sterilised large end of a Pasteur pipette (5 mm diameter). Uninoculated media served as controls. Modified Melin-Norkran's medium (Marx, 1969) (MMN; 1.0 g dextrose, 2.0 g malt extract, 1.0 g yeast extract, 0.5 g KH_2PO_4, 0.25 g $(NH_4)_2HPO_4$, 0.15 g $MgSO_4 \cdot 7\ H_2O$, 0.05 g $CaCl_2$, 0.025 g NaCl,

0.012g $FeCl_3 \cdot 6H_2O$, 15.0 g Difco agar, 1 L distilled water) was the base medium for five of these tests. The sixth used water agar (WA) (12 g Difco agar, 1 L distilled water) as a base. Gelatin degradation was assessed using 120 g L^{-1} gelatin (Sigma Chemical, St. Louis, Missouri) instead of agar in the MMN (Hutchison 1990). Liquefication of the medium indicated the protein had been digested. Amylase activity was tested on MMN amended with 2.0 g L^{-1} soluble starch (British Drug Company, Poole, England) (Hutchison 1990). After a five week inoculation period, plates were flooded with an iodine solution (5.0 g KI, 1.5 g I, 100 mL distilled water) and a clear halo around the colony indicated that the starch had been digested.

Pectinase activity was examined on MMN plates amended with 5.0 g L^{-1} pectin (Sigma Chemicals) (Hutchison, 1990) that were flooded with 1% hexadecyltrimethylammonium bromide five weeks after inoculation. A clear zone around the fungal colony was evidence of pectin degradation. Degradation of insoluble and soluble polyphenol compounds was tested on wood guiacol [2 g powdered *Picea glauca* stem wood, 18 g Difco agar, 1 L distilled water, 100 μL guiacol] and tannic acid [5 g tannic acid (BDH Inc. Toronto, Ontario) 15 g malt extract (Difco), 20 g agar (Difco), 1 L distilled water] media respectively. Wood guiacol plates were incubated for five weeks and examined for a positive reaction, indicated by the presence of a red halo around the fungal colony. Tannic acid medium plates were checked for enzymatic activity after two weeks. A positive test result was indicated by a colour change in the agar from white to brown. All enzymatic tests were conducted at 25 °C in the dark. Cellulose degradation was

assessed by placing a mycelial plug in a vial of WA overlaid with a layer of WA containing 2% cellulose azure (Sigma Aldrich). After two weeks, the vials were checked for blue dye in the lower layer, indicating that the cellulose had been broken down.

4.2.2 Mass loss tests

Mass loss determinations were made according to the procedure in Chapter 3. Briefly, *Hylocomium splendens* gametophytes were placed in two deep glass Petri dishes and autoclaved for 60 minutes at 121°C, dried at 40°C for a week, and placed in 3x3 cm, 63 µm mesh, polyester packets sealed on three sides with the remaining side open. Each packet contained 0.05 g ($\pm$ 0.005 g) of gametophyte tissue (stems, leaves, pseudoparaphyllia, etc.). Packets were autoclaved as above and dried for two days. Each replicate comprised a single packet on a WA base in a 60 mm Petri dish. A 5 mm plug of mycelium on potato dextrose agar (Difco Bacto) was placed on the agar at the mouth of the polyester packet. Plates were sealed with parafilm and incubated at room temperature in the dark for three months. Four replicates were prepared for each fungal species. Uninoculated packets served as controls. Three replicates were used for mass loss measurements and one for SEM observations. No attempt was made to remove the surface hyphae. After three months, the moss packet was dried for a week, and then the gametophytes weighed to get the final mass. Percent mass loss was calculated for each packet and then adjusted to correct for mass loss in the control treatment. Averages and standard deviations were calculated. A one-way ANOVA (Excel Software, Microsoft, Seattle, U.S.A.) was used to determine

differences in mass loss among the five species. As a routine measure, the inoculants were re-isolated from the gametophytes at the end of the incubation period to ensure that cultures had remained free of contamination.

4.2.3 SEM

One packet from each treatment was set aside to prepare subsamples for SEM according to the methods of Tsuneda et al. (1991). Subsamples were immersed in distilled water for two min, fixed in a 2% glutaraldehyde solution overnight, immersed in a 2% tannic acid-guanidine hydrochloride solution, rinsed in dH_2O, postfixed in 2% osmium tetroxide overnight and dehydrated using an ethanol series (25, 50, 75, 90, 95, and 100%). Once ethanol was replaced with amyl acetate (50 and 100%) samples were critical point dried in Teflon capsules, coated in gold, and observed and photographed using a Hitachi S-510 SEM (Hitachi Science Services Systems, Ibaraki, Japan).

Subsamples of control gametophytes and of those inoculated with *L. orchidicola, P. fortinii, C. melinii,* and *C. luteo-olivacea* were fixed in FAA (50 mL ethanol, 5 mL acetic acid, 10 mL 40% formaldehyde, 35 mL water) for one week. Following ethanol dehydration, gametophytes were embedded in paraffin, and 5 µm sections were prepared. Sections were stained using Safranin O (Sigma Aldrich), counterstained with Fast Green F (Sigma Aldrich), and mounted using DPX mountant (Sigma Aldrich). Images of the thin sections were taken with a DP-12 digital camera on an Olympus BX50 (Olympus Canada Inc, Markham, Canada) microscope.

4.3 Results

4.3.1 Enzyme tests

Mycelial plugs of all isolates had a halo when the amylase medium was flooded, induced the formation of a brown pigment on the tannic acid medium, liquefied the gelatin, and released blue dye from the cellulose azure medium (Table 4.2). None produced a halo around the colony when the pectinase medium was flooded (Table 4.2). Only *P. fortinii* and *L. orchidicola* induced the formation of a red pigment on the wood guiacol medium (Table 4.2).

4.3.2 Mass loss tests

All fungi grew over the bryophyte tissue, in most cases covering at least part of the gametophyte with a thick mycelium and two species, *Coniochaeta nepalica* and *C. melinii*, sporulated. Average mass lost from inoculated samples ranged from 2.8% (*L. orchidicola*) to 3.5% *(P. fortinii*), but there were no statistically significant differences among any of the fungi (Fig 4.1).

4.3.3 SEM and LM observations

The acuminate, lanceolate-oblong leaves of the control treatment were smooth and unpuckered and pseudoparaphylia were present on the stems (Fig 4.2 A). Leaf surfaces were covered with a smooth, lacquer-like layer and cell apices were occasionally raised (Fig 4.2 B).

Hyphae of *Coniochaeta nepalica* were abundant on the leaf surface where they formed a loosely interwoven layer of thin to broad filaments that were sometimes aggregated into strands (Fig 4.2 C). Branching patterns and direction of growth were random and conidia were abundant (Fig 4.2 C). Leaves so

colonised were puckered rather than smooth, and the junctions between cells were more pronounced with the outer amorphous layer eroded away (Fig 4.2 D). Sharply defined, circular bore holes that penetrated the wall into the cell lumen were common (Fig 4.2 D). Leaf cells had numerous small fissures and voids in the outer wall layers, especially along junctions between adjacent cells (Fig 4.2 E).

Under SEM, the hyphae of *P. fortinii* were sparse, consistent in diameter, and generally oriented parallel to the long axis of leaf cells, which were sharply delineated from each other (Fig 4.2 F). Erosion of the outer amorphous layer was most pronounced along the junctions between hyphae and the leaf surface (Fig 4.2 F). The amorphous material and the cellulose microfibrils of the outer layer of leaf cells were simultaneously removed, giving the edges a ragged rather than fibrillar appearance (Fig 4.2 G). Bore holes were absent but LM examination of sectioned gametophytes showed that hyphae had gained entry to the cells of both leaves and stems (Fig 4.3 A). Hyphae were more prevalent in stems and particularly abundant in tissue adjacent to leaf axils (Fig 4.3 B) where aggregations of pigmented globose cells formed structures resembling sclerotia (Fig 4.3 B).

Observations using SEM showed hyphae of *L. orchidicola* were abundant, somewhat variable in diameter to often toruloid, and randomly oriented over the surface of leaves, which were wavy and puckered (Figs 4.3 C, D). Coaxial aggregations of hyphae forming slender strands were common. Degradation was most pronounced in the junctions between leaf cells and along the margins of

hyphae (Fig 4.3 F). Erosion of the outer amorphous layer on the leaf cells exposed cellulose microfibrils, giving the cells a fibrillar appearance (Fig 4.3 F). The thicker inner layer of the moss leaf cells was not broken down, although a parallel arrangement of low ridges on the outer face of this layer was evident (Fig 4.3 F).

By LM, pigmented toruloid hyphae ramified through the lumen of contiguous stem cells, passing from one cell to the next often through narrow end walls (Fig 4.3 F). The thick walled cells of some hyphae in the stem were swollen and formed chains of monilioid cells. Cell walls in the stem were thin and had large voids, often with ragged edges. Groups of moniloid cells were present in the stem (Fig 4.3 F). Sharply defined, circular boreholes occurred on both the lateral and end walls and ranged in diameter from 2-6 μm (Fig 4.3 F). Fungal hyphae were present in some of the holes in the lateral cell walls.

Hyphae of *C. luteo-olivacea* were randomly oriented to form a loose mycelial network including prominent coaxial aggregations among the leaves and stems of gametophytes (Fig 4.4 A). Degradation was visible primarily in the junctions between cells and along the hyphal margins (Fig 4.4 B). The amorphous fraction and cellulose microfibrils of the outer cell wall layer were simultaneously removed, giving it a fibrillar appearance, though it otherwise remained intact (Fig 4.4 B). The thicker inner layer was not broken down by the fungus though it was penetrated. Hyphae stained readily with fast green and had heavily colonised the lumen of leaf cells (Fig 4.4 C). Hyphae were absent in stem

tissue. Numerous, sharply defined circular boreholes, 1.6-5 μm in diameter, pierced the lateral walls (Fig 4.4 C) but otherwise the cell wall remained intact.

Hyphae of *C. melinii* were abundant on the surface of the gametophyte, oriented in no apparent pattern over the leaf surface (Fig 4.4 D). Conidia were numerous (Fig 4.4 E). General thinning of the amorphous layer occurred and leaf surfaces were wavy and puckered (Fig 4.4 E). Degradation of cell wall layers was otherwise minimal (Fig 4.4 E). Evidence of intracellular penetration was not observed in either stem or leaf cells.

4.4 Discussion

All fungi grew well on the packets of *Hylocomium splendens* indicating an ability to degrade or utilise at least some of the macromolecules associated with the gametophyte tissues. Patterns of colonisation varied considerably among isolates, with *Coniochaeta nepalica*, *L. orchidicola*, and *C. luteo-olivacea* exhibiting the most pronounced disruption of the substrate and *P. fortinii* and *C. melinii* the least. The significance of these differences in the context of the niche these species are thought to occupy is discussed below.

Coniochaeta nepalica, described originally from soil in Nepal (Minoura et al. 1977), is reported here bryophytes (*Bryum pallescens*) for the first time but, because my isolate did not fruit in culture and was identified entirely on the basis of ITS sequence similarity and anamorph characters, its identification could be considered tentative in the absence of teleomorphic features. Gochenaur (1984) observed ascomata of *Coniochaeta nepalica* in agar cultures after 14 days, so in this respect my isolate is unusual. My isolate (UAMH 11129) formed an

extensive mycelial network over the gametophyte and broke down the outer, cellulose-rich cell wall layer, but not the inner layer rich in polyphenols. The pattern of degradation under SEM was congruent with the *in vitro* enzyme test results, which were positive for cellulases and negative for insoluble polyphenol oxidases. Gochenaur (1984) reported that multiple isolates of this species obtained from podzolic soils associated with oak were able to hydrolyse a wide range of substrates, including cellulose, but polyphenolics were not tested. A second species in this genus, also isolated from bryophytes, *Coniochaeta velutina*, grew as a weak parasite on *Funaria hygrometrica* in axenic culture and was shown to degrade the cell walls of its host (Davey et al. 2010). Both *C. velutina* and *C. nepalica* produced conidia of their corresponding *Lecythophora* states on gametophytes (see Fig 4 C). *Coniochaeta velutina* also produced ascomata (30-40 days post inoculation) on living *F. hygrometrica* (Davey et al. 2010). Ready growth of *Coniochaeta nepalica* in culture, reports of its isolation from soil, including the type locality in Nepal, and the origin and ability of our isolate to degrade bryophyte tissues suggests that this species is at least a potentially competent saprobe in postglacial alpine habitats.

Phialocephala fortinii and *Leptodontidium orchidicola* are among the most frequently reported species in the DSE (Addy et al. 2005). The type of *L. orchidicola* formed an extensive mycelium over the tissue surface, causing exfoliation of the outer layer of the cell wall, and the formation of bore holes through the inner layer. In contrast, on samples inoculated with *P. fortinii*, hyphae were sparse and tended to grow along the junctions of adjacent leaf cells

parallel to their long axes. The outer amorphous layer of the cell walls merely thinned, and there were no signs of perforation of the inner wall layers. However, both fungi did gain entry to the interior of cells in stem and leaf tissue. In material inoculated with *L. orchidicola*, cell wall erosion was extensive and hyphae grew throughout the gametophyte. In comparison, and despite a positive reaction on the cellulose azure, *P. fortinii* caused relatively little degradation of the cellulose rich layer of the moss cell wall and this was localised to the point of contact between hyphae and the bryophyte cell surface. Positive reactions on the wood guiacol and tannic acid media might have predicted an ability to break down the thick inner layer, rich in lignin-like compounds, but there was no evidence of this in material observed by either SEM or LM. These observations corroborate those of Currah and Tsuneda (1993) who found that, despite positive *in vitro* results for polyphenol oxidases, four strains of *P. fortinii* did not decay xylem. Reactions of tannic acid and wood guiacol media may be too coarse to predict potential to degrade all types of lignin and lignin-like macromolecules. Caldwell et al. (2000) also examined the enzymatic abilities of this species and found that multiple isolates were able to degrade cellulose, polyphenols, starch, lipids, pectin, xylan, protein, and RNA, but so far, the abilities of *P. fortinii* to degrade these substances *in situ* have not been examined.

The growth pattern response of *P. fortinii* to topographic features, i.e., the grooves between cells of moss leaves, shown here, or along the epidermal cells of roots (Currah et al. 1993), suggests a foraging behaviour that is independent of the vitality of substrate. A hypha growing along the long axis of a leaf or root will

eventually reach a node or branch root and the disrupted or weakened cells in the vicinity of these structures where leaking nutrients can be absorbed or access gained through ruptured walls. On the inoculated gametophytes, microsclerotia developed in the vicinity of the leaf axils. Currah et al. (1993) observed that *P. fortinii* frequently formed large microsclerotia in tissues surrounding the point of emergence of branch roots in *Rhododendron brachycarpum* and similar structures in roots colonized by *L. orchidicola* have been observed by Fernando and Currah (1996).

Both *Phialocephala fortinii* and *Leptodontidium orchidicola* have been suspected of forming mycorrhiza-like associations with their hosts, although there is probably more evidence that these fungi are parasites or weak pathogens (Wang and Wilcox 1985; O'Dell et al. 1993; Stoyke and Currah 1993; Fernando and Currah 1996) with *Leptodontidium orchidicola* being the more aggressive (virulent) of the two (Peterson et al. 2008). Results reported here, including identical enzymatic profiles and the production of sclerotic clumps of cells in dead tissues of *Hylocomium splendens*, suggest the two are capable saprobes and can form perennating structures in non-living tissues of plants, at least in the absence of competitors. It seems plausible that these DSE fungi could establish and persist in bryophyte detritus and in the absence of vascular plants. *Phialocephala fortinii* has been reported from wood (Menkis et al. 2004) and soil but never from unvegetated arcticor alpine soil, though most surveys of these areas have a category for unnamed DSE, which might include this species (Bissett and Parkinson 1979a, b, c; Bledsoe et al. 1990; Väre et al. 1992; Treu et al. 1996).

The pattern of degradation caused by *C. luteo-olivacea* was similar to that caused by *L. orchidicola* in that both removed the outer cell wall layer, but degradation caused by *C. luteo-olivacea* was localised around cell junctions and along hyphae. Unlike samples inoculated with *L. orchidicola* and *P. fortinii*, hyphae of *C. luteo-olivacea* were not found in the stem cells. Both *L. orchidicola* and *C. luteo-olivacea* extensively colonised leaf cells and formed bore holes of approximately the same size in the cell walls. *Cadophora luteo-olivacea* did not form structures resembling sclerotia in bryophyte tissues, and in this respect differed from *P. fortinii* and *L. orchidicola*. Intraradical sclerotia have not been reported in roots colonised by *C. luteo-olivacea* but detailed studies of the growth and morphology of this fungus in roots have not been found. *Cadophora luteo-olivacea* was originally described from waste water (van Beyma 1940) and has since been reported from soils, feathers, wood and bryophytes (see Blanchette et al. 2004), and recently from the roots of *Gutierrezia sarothrae* (Kageyama et al. 2009). Inoculation of this fungus onto leek plants showed an increase in shoot mass, leading Kageyama et al. (2009) to suggest the fungus was beneficial to the host plant; however, hyphae were not found in the roots when examined by LM and the mechanism causing increased shoot growth was not determined.

Cadophora melinii was first isolated from wood pulp in 1934 by Nannfeldt. Since then, it has been reported from wood and wood chips (Schol-Schwarz 1970), and cooling towers (Morrell and Smith 1988). Shefferson et al. (2005) reported the species, or phylogenetically close affiliates, from the mycorrhizas of orchids. My enzymatic tests revealed that *C. melinii* can degrade

cellulose *in vitro* and investigations into fungi growing on cooling towers has shown that isolates identified as *C. melinii* are capable of degrading the cellulose in wood to cause a soft rot pattern (Morrell and Smith 1988); however, my isolate (CBS 268.33) did not degrade the cellulose in the cell walls of *H. splendens*.

The degradation caused by *Coniochaeta nepalica*, *L. orchidicola*, and *C. luteo-olivacea* was similar to that caused by some pleosporalean fungi in that only the outer layer of the cell wall was removed, leaving behind the lignin-rich inner layer (Chapter 3). The peeling of this layer caused by *L. orchidicola* was similar to that caused by *Ulocladium atrum* and *Chalastospora gossypii* (Chapter 3). In contrast, myxotrichaceous fungi exhibited a pattern of decay more typical of white rot basidiomycetes in which both the cellulose and lignin-like layers were removed (Rice et al. 2006). It is possible, however, that the type of moss used as substrate may affect degradation patterns. The myxotrichaceous fungi were grown on *Sphagnum*, the leaves of which comprise numerous thick-walled, dead cells specialized for holding water (similar to the tracheary elements of wood) interspersed with thin-walled living cells, while the pleosporalean fungi were grown on *H. splendens*, in which leaves comprise a more or less homogenous layer of chlorophyllous cells. Comparisons of the effects of the same fungi across a range of bryophyte species would allow assessment of the effect host type on fungal decomposition patterns.

Mass loss values among the packets across all the species were inconsistent although at least one packet in each set had a mass loss that exceeded the control. *Phialocephala fortinii* and *C. luteo-olivacea* both had higher mean

percent loss than *L. orchidicola*, but in *P. fortinii* only one of three packets lost mass while all three did so when inoculated with *L. orchidicola*. The variability in mean mass loss values has been seen in other studies using moss gametophytes as the test substrate (Rice et al. 2006; Chapter 3) and may be due possibly to the heterogeneity of this substrate. Mass loss experiments using wood (e.g. Held et al. 2006) and vascular plant leaves (e.g. Thormann et al. 2004) have shown less variation perhaps because the substrate materials have a larger mass and less surface area and small variations in mass lost would not have a big impact on the results. It is also easier to remove fungal mycelia from the surface of bulkier substrates and reduce variability due to fungal biomass.

In conclusion, my observations indicate that all of the species examined would be able grow as saprobes to some extent on organic particulates derived from bryophytes, and could therefore be part of a bank of endophytes in place ready to colonise post-glacial vascular plant pioneer species. *Leptodontidium orchidicola* and *Phialocephala fortinii* formed sclerotium-like structures in shoot tissues which presumably would allow them to persist and disperse in windblown or water borne gametophyte fragments. *Cadophora melinii* and *Coniochaeta nepalica* were able to form conidia on this substrate and so would be able to disseminate from colonised materials. *Cadophora luteo-olivacea* did not sporulate or form sclerotia and may require different substrata or a longer incubation time for propagules to develop. At any rate, all species may persist as hyphal fragments in or on relatively decay-resistant bryophyte detritus and have the potential to also contribute to the humification of these materials.

4.5 Literature Cited

Addy, H.D., Piercey, M.M., and Currah, R.S. 2005. Microfungal endophytes in roots. Canadian Journal of Botany. 83: 1–13.

Bissett, J. and Parkinson, D. 1979a. Distribution of fungi in some alpine soils. Canadian Journal of Botany. 57: 1609-1629.

Bissett, J. and Parkinson, D. 1979b. Fungal community structures in some alpine soils. Canadian Journal of Botany. 57: 1630-1641.

Bissett, J. and Parkinson, D. 1979c. Functional relationships between soil fungi and environmental in alpine soils. Canadian Journal of Botany. 57: 1642-1659.

Blanchette, R.A., Held, B.W., Jurgens, J.A., McNew, D.L., Harrington, T.C., Duncan, S.M., and Farrell, R.L. 2004. Wood-destroying soft rot fungi in the historic expedition huts of Antarctica. Applied and Environmental Microbiology. 70: 1328-1335.

Bledsoe, C., Klein, P., and Bliss, L.C. 1990. A survey of mycorrhizal plants on Truelove Lowland, Devon Island, N.W.T., Canada. Canadian Journal of Botany. 68: 1848-1856.

Caldwell, B.A., Jumpponen, A., and Trappe, J.M. 2000. Utilization of major detrital substrates by dark-septate, root endophytes. Mycologia. 92: 230-232.

Currah, R.S. and Van Dyk, M. 1986. A survey of some perennial vascular plant species native to Alberta for occurrence of mycorrhizal fungi. Canadian Field Naturalist. 100: 330-342.

Currah, R.S. and Tsuneda, A. 1993. Vegetative and reproductive morphology of *Phialocephala fortinii* (Hyphomycetes, *Mycelium radicis atrovirens*) in culture. Transactions of the Mycological. Society of Japan. 34: 345-356.

Currah, R.S., Tsuneda, A., and Murakami, S. 1993. Morphology and ecology of *Phialocephala fortinii* in roots of *Rhododendron brachycarpum*. Canadian Journal of Botany. 65: 2473-2482.

Davey, M.L., Tsuneda, A., Currah, R.S. 2010. Saprobic and parasitic interactions of *Coniochaeta velutina* with mosses. Botany. 88: 258-265.

Fernando, A.A. and Currah, R.S. 1996. A comparative study of the effects of the root endophytes *Leptodontidium orchidicola* and *Phialocephala fortinii*

(Fungi Imperfecti) on the growth of some subalpine plants in culture. Canadian Journal of Botany. 74: 1071-1078.

Gochenaur, S.E. 1984. *Coniochaeta nepalica*, a common Long Island soil fungus. Mycotaxon. 19: 85-92.

Held, B.W., Jurgens, J.A., Duncan, S.M., Farrell, R.L., and Blanchette,R.A. 2006. Assessment of fungal diversity and deterioration in a wooden structure at New Harbor, Antarctica. Polar Biology. 29: 526-531.

Hutchison, L.J. 1990. Studies on the systematics of ectomycorrhizal fungi in axenic culture. II. The enzymatic degradation of selected carbon and nitrogen compounds. Canadian Journal of Botany. 68: 1522-1530.

Jumpponen, A., Mattson, K., and Trappe, J.M. 1998. Mycorrhizal functioning of *Phialocephala fortinii* with *Pinus contorta* on glacier fore front soil: interactions with soil nitrogen and organic matter. Mycorrhiza. 7: 261-265.

Kageyama, S.A., Mandyam, K.G., and Jumpponen, A. 2008. Diversity, function and potential applications of root-associated endophytes. *In* Mycorrhiza State of the Art Genetics and Molecular Biology, Ecofunction, Biotechnology, Eco-Physiology, Structure and Systematics. *Edited by* A. Varma. Springer Berlin Heidelberg, USA, pp 29-57.

Mandyam, K. and Jumpponen, A. 2005. Seeking the elusive function of the root-colonising dark septate endophytic fungi. Studies in Mycology. 53: 173-189.

Marx, D.H. 1969. The influence of ectotrophic mycorrhizal fungi on the resistance of pine roots to pathogenic infections. I. Antagonism of mycorrhizal fungi to root pathogenic fungi and soil bacteria. Phytopathology 59: 153–163.

Menkis, A., Almer, J., Vasiliauskas, R., Lygis, V., Stenlid, J., and Finlay, R. 2004. Ecology and molecular characterization of dark septate fungi from roots, living stems, coarse and fine woody debris. Mycological Research 108: 965-975.

Minoura, K., Morinaga, T., and Muroi, T. 1977. Some Ascomycetes isolated from soil of Nepal III. Transactions of the Mycological Society of Japan. 18: 119-124.

Morrell, J.J. and Smith, S.M. 1988. Fungi colonizing redwood in cooling towers: identities and effects on wood properties. Wood Fiber Science. 20: 243-249.

O'Dell, T.E., Massicotte, H.B., and Trappe, J.M. 1993. Root colonization of *Lupinus latifolia* Agardh. and *Pinus contorta* Dougl. by *Phialocephala fortinii* Wang and Wilcox. New Phytologist. 124: 93-100.

Peterson, L.R., Wagg, C., and Paulter, M. 2008. Associations between microfungal endophytes and roots: do structural features indicate function? Botany. 86: 445-456.

Rice, A.V., Tsuneda, A., and Currah, R.S. 2006. *In vitro* decomposition of *Sphagnum* by some micro fungi resembles white rot of wood. FEMS Microbiology Ecology. 56: 372-382.

Schol-Schwarz, M.B. 1970. Revision of the genus *Phialophora* (Moniliales). Persoonia. 6: 59-94.

Shefferson, R.P., Weiß, M., Kull, T., and Taylor, D.L. 2005. High specificity generally characterizes mycorrhizal association in rare lady's slipper orchids, genus *Cypripedium*. Molecular Ecology. 14: 613-626.

Stoyke, G. and Currah, R.S. 1993. Resynthesis in pure culture of a common subalpine fungus-root association using *Phialocephala fortinii* and *Menziesia ferruginea* (Ericaceae). Arctic Alpine Research. 25: 189-193.

Thormann, M.N., Bayley, S.E., and Currah, R.S. 2004. Microcosm tests of the effects of temperature and microbial species number on the decomposition of *Carex aquatilis* and *Sphagnum fuscum* litter from southern boreal peatlands. Canadian Journal of Microbiology. 50: 793-802.

Treu, R., Laursen, G.A., and Stephenson, S.L. 1996. Mycorrhizae from Denali National Park and Preserve, Alaska. Mycorrhiza. 6: 21-29.

Tsuneda, A., Maekawa, N., Ohira, I., and Furukawa, I. 1991. Incipient decay of *Quercus serrata* sapwood by *Lentinus edodes* and its inhibition by an antagonistic hyphomycete, *Leptodontidium elatius*. Canadian Journal of Botany. 69: 2797–2825.

Van Beyma thoe Kingma. F.H. 1940. Beschreibung einiger neuer pilzarten aus dem Centraalbureau voor Schimmelcultures, Baarn (Nederland). Antoine van Leeuwenhoek Journal of Microbiology. 6: 263-290.

Väre, H., Vestberg, M., and Eurola, S. 1992. Mycorrhiza and root associated fungi in Spitsbergen. Mycorrhiza. 1: 93-104.

Wang, C.J.K. and Wilcox, H.E. 1985. New species of ectendomycorrhizal and pseudomycorrhizal fungi: *Phialophora finlandia, Chloridium paucisporum,* and *Phialocephala fortinii*. Mycologia. 77: 951-958.

Table 4.1. Provenance data for selected species used in the moss decomposition study. CBS = Centraalbureau voor Schimmelcultures, UAMH = University of Alberta Microfungus Collection and Herbarium.

Species	Herbarium accession number	Source	Country
Cadophora luteo-olivacea	CBS 141.41	Waste water	Sweden
Cadophora melinii	CBS 268.33	Wood pulp	Sweden
Coniochaeta nepalica	UAMH 11229	*Bryum pallescens* gametophytes	Canada
Leptodontidium orchidicola	UAMH 5422	*Platanthera hyperborea* roots	Canada
Phialocephala fortinii	UAMH 11228	*Salix arctica* roots	Canada

Table 4.2. *In vitro* enzymatic abilities of *Cadophora luteo-olivacea*, *Cadophora melinii*, *Coniochaeta nepalica*, *Leptodontidium orchidicola*, and *Phialocephala fortinii*. + = a positive reaction. – = a negative reaction.

	Starch	Soluble polyphenols	Insoluble polyphenols	Protein	Pectin	Cellulose
Cadophora luteo-olivacea	+	+	-	+	-	+
Cadophora melinii	+	+	-	+	-	+
Coniochaeta nepalica	+	+	-	+	-	+
Leptodontidium orchidicola	+	+	+	+	-	+
Phialocephala fortinii	+	+	+	+	-	+

Figure 4.1. Percent mass loss of gametophytes of *Hylocomium splendens* inoculated with *Cadophora luteo-olivacea*, *Cadophora melinii*, *Coniochaeta nepalica*, *Leptodontidium orchidicola*, and *Phialocephala fortinii* after incubation for three months. Three replicates were used per species. These values are corrected against the control. There are no statistically significant differences among the average percent mass losses of each of the five species. Bars indicate standard deviation.

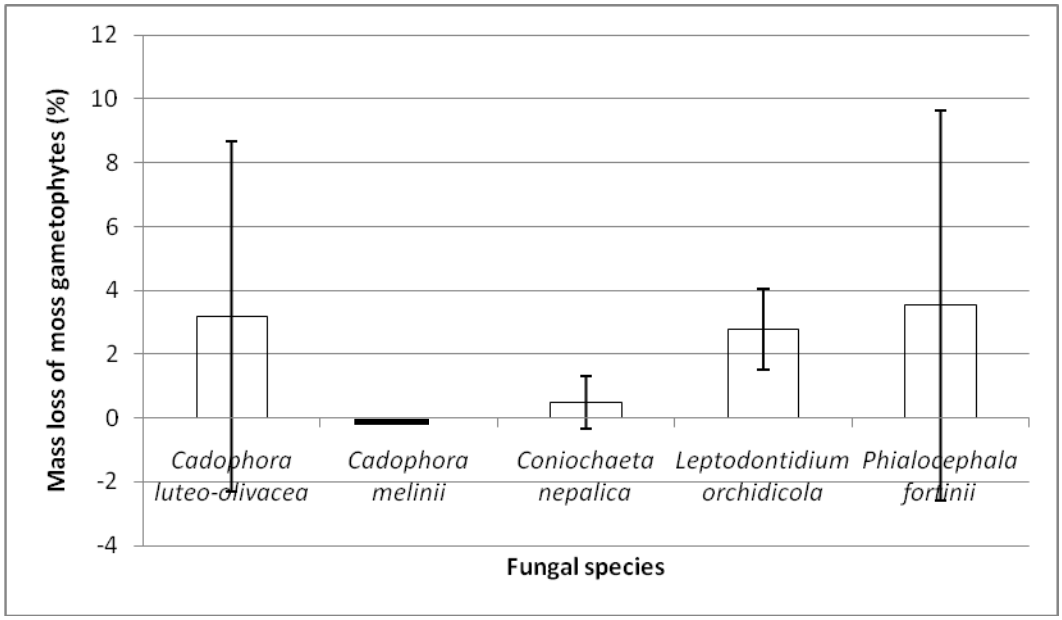
12
10
8
6
4
2
0
-2
-4
Mass loss of moss gametophytes (%)
Cadophora luteo-olivacea
Cadophora melinii
Coniochaeta nepalica
Leptodontidium orchidicola
Phialocephala fortinii
Fungal species

Figure 4.2. Uninoculated *Hylocomium splendens* gametophytes (A-B) and gametophytes inoculated with *Coniochaeta nepalica* (C-E), and *Phialocephala fortinii* (F-G) and incubated for 3 months.

A. Smooth, unpuckered, acuminate, oblong-lanceolate leaves (arrow) with pseudoparaphylia (arrowhead). Bar = 200 μm.
B. A lacquer-like amorphous layer covers the leaf surface. Note the raised cell apices (arrowheads). Bar = 25 μm.
C. Hyphae form a loosely interwoven layer of thin to broad filaments on the leaf surface. Bar = 33 μm.
D. Leaves are puckered and junctions between cells are more pronounced. Circular, sharply defined boreholes (arrowheads) penetrate the wall. Bar = 5μm.
E. Leaf cells have small fissures and voids (arrows) in the outer cell wall layer in the junctions between the cells. Note the conidium (arrowhead). Bar = 2.5μm.
F. The sparse hyphae are consistent in diameter and generally oriented parallel to leaf cells. Erosion of outer amorphous layer is more pronounced along hyphae (arrowheads). Bar = 10 μm.
G. The amorphous material and cellulose microfibrils of the outer cell wall layer are simultaneously removed (arrowheads), giving the junction between hypha and cell wall a ragged appearance. Bar = 2.5 μm.

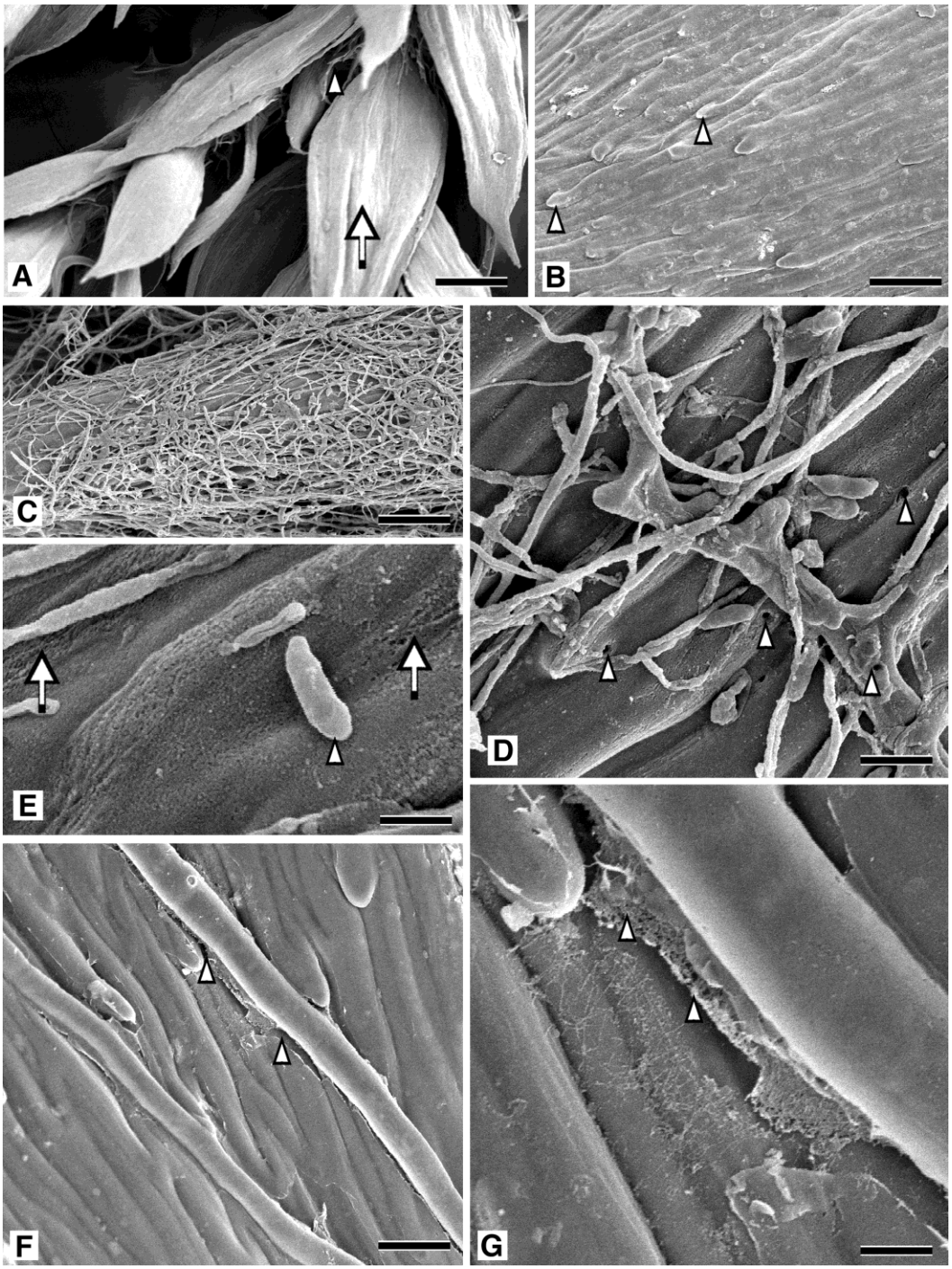
A
B
C
D
E
F
G

Figure 4.3. Light (A, B, F, and G) and scanning electron microscope (C, D, and E) observations of *Phialocephala fortinii* (A-B) and *Leptodontidium orchidicola* (C-H) on *Hylocomium splendens* gametophytes.

A. An oblique section through stem and leaves showing that hyphae form aggregations of pigmented globose cells (arrowhead) that resemble sclerotia. Note leaf (arrow) coming from leaf axil. S refers to the moss stem. Bar = 26 μm.
B. A glancing section across stem at the node showing hyphae are particularly abundant in tissue adjacent to the leaf axils (arrow). Note leaf (L) and stem tissue (arrowhead) in axil. Bar = 26 μm.
C. Abundant hyphae of *Leptodontidium orchidicola* on a gametophyte leaf. Bar = 200 μm.
D. Toruloid hyphae (arrows) grow above wavy and puckered leaf surface. Bar = 5 μm.
E. A longitudinal section through the leaf showing degradation is most pronounced in cell junctions and along hyphal margins (arrowheads). The inner cell wall layer is not broken down though a parallel arrangement of ridges (*) is visible under the outer layer. Note hyphae (arrows). Bar = 33 μm.
F. A longitundinal section through the leaf showing toruloid hyphae (arrows) ramify through the lumen of stem cells, passing from one cell to the next through narrow end walls (arrowhead). Bar = 26 μm.
G. Groups of monilioid cells (arrowhead) are present in the stem. Sharply defined, circular boreholes (arrows) occur on lateral walls. Bar = 33 μm.

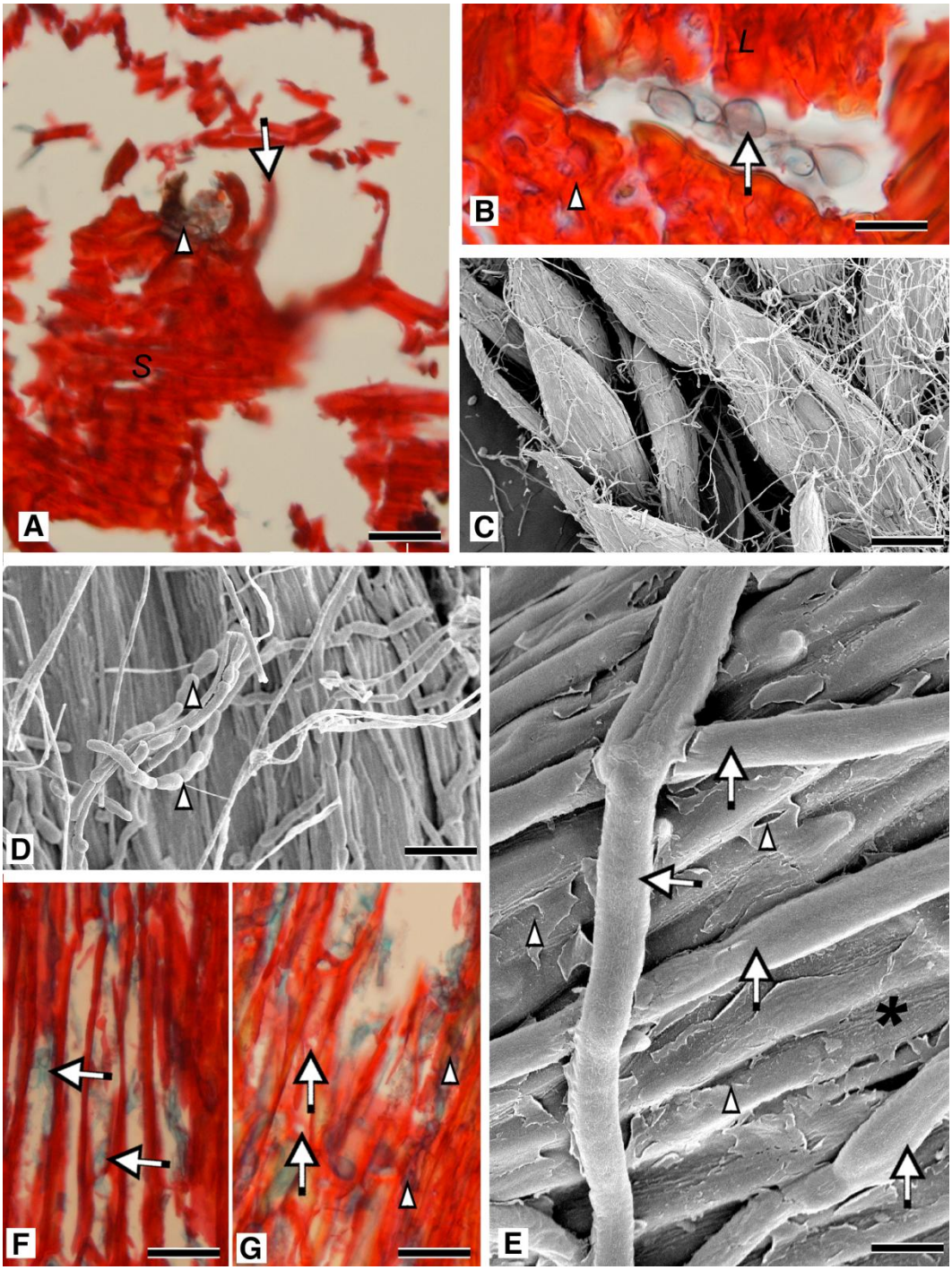
A
S
B
L
C
D
E
*
F
G

Figure 4.4. Colonisation and degradation of *Hylocomium splendens* by *Cadophora luteo-olivacea* (A-C) and *Cadophora melinii* (D-E).

A. Hyphae of *Cadophora luteo-olivacea* are numerous and form a loose mycelial network over leaves. Bar = 125 μm.
B. Degradation is visible in the junctions between cells and at hyphal margins (arrowheads). Note hypha exiting the leaf (*). Bar = 10 μm.
C. A longitudinal section through the leaf showing hyphae, readily stained with fast green, heavily colonise the cell lumen. Note the sharply defined, circular boreholes (arrows). Bar = 33 μm.
D. Hyphae are abundant on the leaf surface in a random orientation. Bar = 600 μm.
E. Conidia (arrowheads) are numerous. Despite general thinning of the amorphous layer and wavy, puckered leaves, no degradation occurred. Bar = 60 μm.

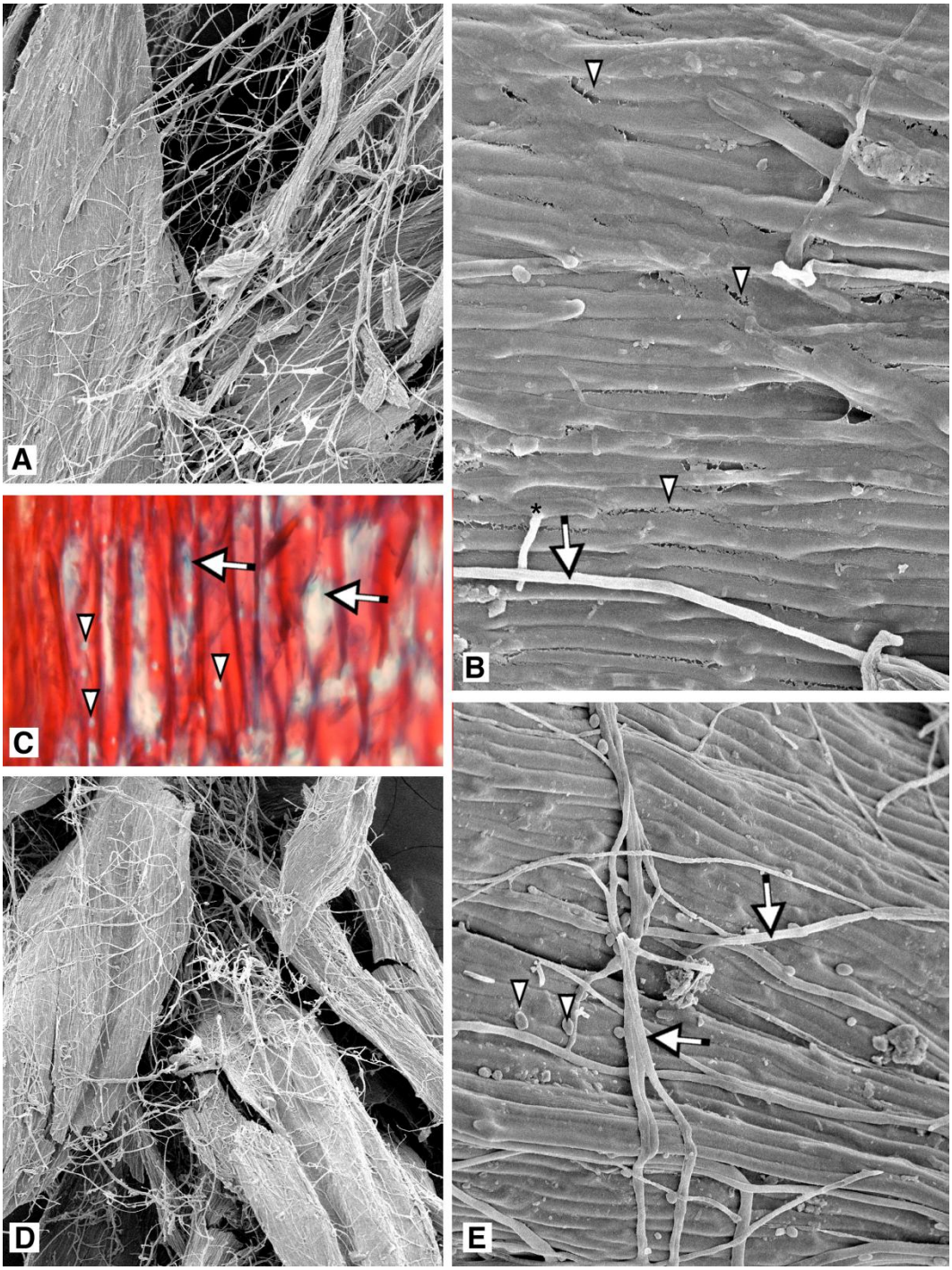
A
B
C
D
E

Chapter 5. Phialide arrangement and character evolution in the helotialean anamorph genera *Cadophora* and *Phialocephala*.

5.1 Introduction

Members of the genera *Cadophora* and *Phialocephala* produce hyphae with melanised walls, phialidic conidial states, and are common associates of living plants or their remains. Several species, e.g. *Phialocephala fortinii* s.l. and *Cadophora finlandica*, are known primarily as isolates obtained from living roots and belong to a group of fungi known informally as the "dark septate endophytes" or DSE (Wang and Wilcox 1985). Others, such as *Cadophora hiberna* and *Phialocephala lagerbergii*, are best known as isolates from wood and wood pulp (Melin and Nannfeldt 1934; Bills 2004). *Cadophora gregata* causes brown stem rot of cultivated beans (Kobayashi et al. 1979). The two genera are generally distinguished from each other based on complexity of branching associated with phialide production: the phialides of *Cadophora* typically occur singly or in groups of two or three, while in *Phialocephala* they form in larger groups that may be diffuse or form dense obconic to spherical clusters. However, variation within and among isolates in the number and distribution of phialides, and intermediate forms, cause problems both in the recognition of the limits of the two taxa and in routine identification.

Cadophora Lagerberg and Melin was erected in 1927 with *C. fastigiata* as the type to encompass dematiaceous hyphomycetes producing solitary phialides with distinct hyaline collarettes. Shortly thereafter, similarities in phialide morphology were the basis for designating *Cadophora* a synonym of *Phialophora* (Conant 1937). Much later, the affiliation of *C. fastigiata* (and others) with

teleomorphs in the Helotiales, rather than the Chaetothyriales where the type of *Phialophora* (*P. verrucosa*) is affiliated, became the basis for reinstating *Cadophora* as a distinct genus (Gams 2000), a decision subsequently supported by analyses of rDNA sequences (Harrington and McNew 2003). Few direct links to teleomorph states have been made although *Mollisia dextrinospora* was reported to have a *Cadophora*-like anamorph (Greenleaf and Korf 1980) and phylogenetic analysis shows that the relationship between many species in *Cadophora* and *Mollisia* is close (Harrington and McNew 2003).

Phialocephala Kendrick was erected during a revision of the "*Leptographium* complex" with *P. dimorphospora* as the type (Kendrick 1961). As in *Cadophora*, species of *Phialocephala* are dematiaceous and produce phialides with distinct hyaline collarettes; however, *Phialocephala* differs in bearing phialides in large heads or at least branched clusters. In some instances (e.g. *P. compacta*), clusters are so densely branched and sporulate so sparingly or infrequently that they bear a striking similarity to sclerotia. Furthermore, in species such as *P. fortinii*, the minute spores resemble spermatia more than conidia. The teleomorph of *P. dimorphospora* is unknown but phylogenetic analyses of rDNA indicate that its affinities (and those of *P. scopiformis, P. urceolata, P. fortinii, P. compacta, P. repens, P. lagerbergii, P. botulispora, P. glacialis,* and *P. sphaeroides*) are with the Helotiales (Wilson et al. 2004; Grünig et al. 2009; Wang et al. 2009). Species named in *Phialocephala* and representing the Sordariales (e.g. *P. humicola*), Chaetothyriales (e.g. *P. fluminis*) and Ophiostomatales (e.g. *P. fusca, P. xalapensis*) based on rDNA sequences indicate

that the genus as currently circumscribed is problematic (Grünig et al. 2002; Jacobs et al. 2003). Another issue in the delineation of *Phialocephala* concerns the inclusion of species that have phialides that are loosely distributed along a conidiophore or in very small clusters, and thus appear similar to *Cadophora*, e.g. *P. urceolata* and *P. lagerbergii*.

A third, but non-phialidic dematiaceous, root-endophytic taxon, *Leptodontidium orchidicola* (Currah et al. 1987), is phylogenetically close to the types of *Cadophora* and *Phialocephala* (Wilson et al. 2004). This species forms minute, globose to tear-drop shaped solitary conidia laterally on undifferentiated hyphae or in small terminal clusters. Conidia are unusual in that they rarely secede, making the placement of this species in *Leptodontidium* unsatisfactory (Currah et al. 1987). *Leptodontidium orchidicola* is also phylogenetically distant from the type (*L. elatius*) based on analyses of rDNA.

Given that patterns in the number and arrangement of phialides appear to reflect generic boundaries among some of the phylogenetically related species in *Cadophora*, *Phialocephala,* and *L. orchidicola,* we explored the notion that these characters might be significant in terms of adaptive advantage and evolutionary polarity in these taxa. Among the Helotiales, the biology of the agricultural pathogen *Sclerotinia sclerotiorum*, and its immediate relatives, are among the most intensely studied representatives of the order. These fungi produce sclerotia as overwintering structures associated with or within various organs of the host, e.g, stems, leaves, bulbs, etc. Sclerotia can germinate to reinfect its host or produce minute spores (microconidia) which form from phialides that develop

within or over the surface of the sclerotium and function as spermatia rather than conidia in the transfer of gamete nuclei to receptive hyphae, which are early stages in the formation of an ascocarp and sexual reproduction.

The morphological similarity between the sclerotium-like conidiogenous apparatus of some species of *Phialocephala* and the spermatogenous sclerotia of certain Sclerotiniaceae suggested the possibility of parallel functionality if not homology. I speculated that an increase in size of spermatia or microconidia over time to become functional conidia would allow these structures to replace the perennating and disseminative functions of the sclerotium, which would then decline in complexity through redundancy. This paradigm suggests that the reproductive morphology of *Phialocephala*, with its complex heads of branches, multiple phialides and minute conidia would be basal relative to the much reduced (more derived) conidiogenous apparatus of *Cadophora* and *Leptodontidium*, which have much fewer (or no) phialides but larger conidia. A corollary to this hypothesis would be that anamorphic complexity could be explained on the basis of adaptive responses to challenges associated with dispersal and perennation.

5.2 Methods

5.2.1 Taxonomic sampling and phylogenetic analysis

Twenty-five fungal isolates were selected, representing helotialean members of *Cadophora* and *Phialocephala* as well as species of *Meliniomyces*, *Chloridium paucisporum, Leptodontidium orchidicola,* and anamorphic species of *Mollisia* (Table 1). Where possible, sequences based on the ex-type strains were

used. rDNA sequences [internal transcribed spacer regions (ITS)] were available from GenBank for all taxa. Three different data sets were analysed: 1) 57 taxa to place the focal species within the Helotialies, hereafter referred to as the Helotiales data set; 2) a reduced data set of 30 species to determine the relationships among target species and putatively related teleomorphs; and 3) 26 taxa, representing the taxa for which I was able to score morphological data and which would allow me to test whether there is a correlation between phylogenetic relationship and phialide number and arrangement by performing an ancestral character reconstruction using named (and unnamed) species in *Phialocephala, Cadophora* and *Leptodontidium*. Dataset two allowed me to determine if there were any patterns in the sexual states that might explain the phylogenetic placement of the asexual focal taxa. The three matrices were manually aligned using SeAl (verison 2.0a11) (http://evolve .zoo.ox.ac.uk). A heuristic search was done using maximum parsimony as the optimality criterion using PAUP* 4.0b10 (Swofford 2002). Gaps were treated as missing data. Starting trees were obtained by stepwise addition. Taxa were added randomly for 100 replicates. The branch-swapping algorithm was tree bisection-reconnection. Confidence in the resultant trees' branches was determined by 1000 bootstrap replicates using the same parameters (Felsenstein 1985).

Bayesian posterior probabilities for the branches were calculated using Mr. Bayes 3.12 (Huelsenbeck and Ronquist 2001; Ronquist and Huelsenbeck 2003). Mr. Modeltest determined which of 24 evolutionary models best fit each matrix (Nylander 2004). For the first analysis, the model was GTR + I + G. For

the second, it was SYM + I + G. For the third, it was SYM + G. Two independent Markov Chain Monte Carlo runs were used, 10 000 000, 1 000 000, and 100 000 generations respectively, involving 1 hot and 3 cold chains which were sampled every 100 generations. For all Bayesian analyses, prior probabilities were flat weighted and parameters estimated A burn in of 25% of generations was applied.

5.2.2 Ancestral character reconstruction

Anamorphic target taxa were scored for having reduced phialides (Figs 5.1 A, 5.2 F, G), solitary phialides (Figs 5.1 B, 5.2A, B, C) or multiple phialides (Figs 5.1 C, 5.2 E, H) based on information obtained from published descriptions and images (Table 5.2). I surmised that the indehiscent conidia in *L. orchidicola* (Fig 5.2 J, K), and the short, swollen lateral pegs in species of *Meliniomyces variabilis, Mel. bicolor*, and *Mel. vraolstadiae*, could be interpreted as reduced or non-functional phialides. Phialides occurring singly or in small loose clusters (of two to four) were considered solitary and those in larger groups and borne on loose or compact aggregations of branches were considered multiple. Ancestral character states were inferred on a parsimony and Bayesian framework using Mesquite (Maddison and Maddison 2006) and SIMMAP (Bollback 2006) respectively. SIMMAP estimates the posterior probabilities of ancestral states at each node. Topologies and branch lengths from 75 000 trees from the Baysian analysis integrated phylogenetic uncertainty into the analysis, while allowing the rates of character evolution to vary, integrated mapping uncertainty. Character states were unordered and changes between states were considered equally likely. The

proportion likelihood of each state at a given node was calculated for the Bayesian analysis (Table 5.3). Because changes in the position of taxa on the maximum parsimony trees did not affect the overall evolutionary pattern of phialide complexity, a single tree was chosen to be representative.

5.3 Results

5.3.1 Phylogenetic analysis

The first analysis, which placed the target taxa within the Helotiales, yielded a total of 2120 characters, of which 990 were constant and 404 parsimony informative. A maximum parsimony search yielded six most parsimonious trees (Fig 5.3). The tree length was 2311, consistency index (CI) 0.395, and retention index (RI) 0.593. In the second analysis, in which sequence data of both anamorphic and teleomorphic species were compared, alignment of the ITS yielded 1472 total characters, of which 988 were constant and 268 parsimony informative. Eleven most parsimonious trees were produced with a tree length of 1186, a CI of 0.655, and an RI of 0.677 (Fig 5.4). In the third analysis, in which sequence data of only anamorphic species were compared, alignment yielded a total of 1283 characters, 941 of which were constant and 216 parsimony informative. Five most parsimonious trees were produced with a tree length of 681, a CI of 0.561, and an RI of 0.722 (Fig 5.5).

In the analysis of the Helotiales (Fig 5.3), I recovered a well-supported clade (>70% MP bootstrap, >90% Bayesian posterior probablilities) that included the focal taxa. *Phialocephala virens* was not part of this clade, nor did it form a clade with other taxa in my analyses. It also appeared to be outside the

Dermateaceae (Fig 5.3). *Phialocephala virens* is also unusual in the genus in producing green colonies and having phialides in solitary, multiple heads, and verticillately whorled arrangements (Siegfried et al. 1992). Because of these phylogenetic and morphological anomalies, *P. virens* was deemed beyond the limits of this study and was not considered further.

Leptodontidium boreale and *L. elatius* formed a well supported group with *Hyphodiscus hymenophila* and its *Cadophora*-like anamorph *Catenulifera rhodogena*. *Leptodontidium orchidicola* was included in Clade D with *C. luteo-olivacea, C. gregata, C. melinii, C. malorum,* and *C. fastigiata*, rather than with other members of *Leptodontidium*.

In the remaining two analyses, four clades were consistently derived. Clade A consisted of *P. scopiformis, M. cinerella, P. urceolata, C. hiberna,* and *P. sphaeroides* (Fig 5.5) and, when teleomorphic species were included, *M. fusca, M. cinerea* and *M. minutella* (Fig 5.4); however, there was no bootstrap or Bayesian support for this clade. Clade B, consisting of *P. fortinii, P. compacta, P. repens, P. lagerbergii, P. botulispora, P. dimorphospora,* and *P. glacialis,* received high bootstrap and Bayesian support (Fig 5.4). When the teleomorphic species were included in the analysis, *Phaeomollisia piceae* was also part of this clade (Fig 5.4). Clade C received high bootstrap and Bayesian support in all three analyses and comprised *Mel. variabilis, Mel. bicolor, Mel. vraolstadiae, Chloridium paucisporum,* and *Cadophora finlandica* (Fig 5.5). Clade D, encompassing *L. orchidicola, M. "rhizophila", C. luteo-olivacea, C. gregata, C.*

malorum, C. fastigiata, C. melinii, and *M. dextrinospora*, received high bootstrap and Bayesian support in all three analyses (Fig 5.5).

Ancestral character state reconstruction showed similar trends in both maximum parsimony (Fig 5.6) and Bayesian (Fig 5.7) reconstructions. All species in clades A and B have multiple phialides and those in clade D have single phialides, with the exception of *L. orchidicola* and *M. "rhizophila"* in which phialides are reduced (Figs 5.6, 5.7). Species in clade C have phialides that are reduced, single, or multiple (Figs 5.6, 5.7), but all arise from a basal node in the tree where ancestral states are single.

5.4 Discussion

The foregoing analyses provided a strong framework on which to test the hypothesis that reduced or solitary-to-few phialides, characteristic of *L. orchidicola* and species of *Cadophora* respectively, represented derived features relative to the more basal condition of producing large sclerotium-like clusters of phialides characteristic of most helotialean species assignable to *Phialocephala*. Analyses of anamorphic taxa yielded four clades, three of which had strong bootstrap and Bayesian support (Fig 5.5). Clade A included *P. scopiformis, M. cinerella, P. urceolata, C. hiberna,* and *P. sphaeroides*. Conidiogenous structures in these species range from globose heads (*P. sphaeroides*), diffuse arrangements of branches along a central axis (*P. urceolata* and the anamorph of *M. cinerella*) and clustered phialides on synnemata (*C. hiberna, P. scopiformis*). Conidiogenous structures of species in clade B, i.e., *P. fortinii, P. compacta, P. repens, P. lagerbergii, P. botulispora, P. dimorphospora,* and *P. glacialis*, are

more uniform and consist of mostly obconic aggregates of multiple phialides. Dimensions of phialides and conidia overlap among the species in clades A and B although none has conidia longer than 4 microns (Fig 5.8). The teleomorphic species associated with the clades differed in that species with hyaline ascospores and named in *Mollisia*, i.e., *M. cinerella, M. cinerea, M. melaleuca, M. minutella*, and *M. fusca,* were included in clade A, and *Phaeomollisia picea,* with its distinctive darkly pigmented ascospores, was included in clade B.

Cadophora hiberna was erected to encompass isolates of a winter-fruiting hyphomycete that produced large, penicillately branched heads of multiple phialides arising from either sporodochia on wood or synnemata on agar (Bills, 2004), but its complex branching conidiophores and relatively short conidia (Fig. 5.8) indicate a closer relationship with *Phialocephala*. These morphological characteristics, along with the close phylogenetic position of *C. hiberna* with *P. urceolata* and *P. scopiformis* in Clade A, support the following taxonomic recombination.

Phialocephala hiberna (Bills) M.J.Day and Currah comb. nov.

≡ *Cadophora hiberna* Bills
Bills, G.F. 2004. *Cadophora hiberna* sp. nov., a winter-fruiting helotialean anamorph from wood of *Robinia pseudoacacia* and forest soil. *In* Fungi in Forest Ecosystems: Systematics, Diversity and Ecology. Ed. C.L. Cripps. Pg 115.

Clade D, consisting of *L. orchidicola, M. "rhizophila", C. luteo-olivacea, C. gregata, C. fastigiata, C. malorum*, *C. melinii*, and *M. dextrinospora*, had high bootstrap and Bayesian support. A search for corroborating morphological features reveals that species in clade D form solitary phialides and produce

conidia that are substantially larger, i.e., > 4 μm in length (Fig 7), in comparison to the clustered phialides and short conidia characteristic of species in clades A and B.

The strongly supported position of *L. orchidicola* among species of *Cadophora* in Clade D prompted further consideration of the globose to teardrop shaped indehiscent conidia. In comparing the position of these structures and of phialides in other species of *Cadophora*, it seems plausible at least that the non-seceding conidia of *Leptodontidium orchidicola* could represent aborted or non-functional phialides rather than conidia. Similar structures are produced along with normal phialides by *C. luteo-olivacea* (Fig 1G). These interpretations, along with the close phylogenetic position of *L. orchidicola* with *Cadophora species* including the type in Clade A, support the following taxonomic recombination.

Cadophora orchidicola (Sigler and Currah) M.J.Day and Currah.

≡ *Leptodontidium orchidicola* Sigler and Currah comb. nov.
Currah, R.S., Sigler, L., and Hambleton, S. 1987. New records and new taxa of fungi from the mycorrhizae of terrestrial orchids of Alberta. Canadian Journal of Botany. 65: 2473.

Clade C had very high bootstrap and Bayesian support and encompassed *C. finlandica, Chloridium paucisporum, Mel. variabilis, Mel. vraolstadiae,* and *Mel. bicolor*, a clade previously recognized with varying composition by Grünig et al. (2002); Hambleton and Sigler (2005) and generally including *Rhizoscyphus ericae* (≡ *Hymenoscyphus ericae*). The genus *Melinomyces* was erected to encompass the fungi formerly known as "variable white taxon" (Hambleton and Sigler 2005). These fungi, isolated from roots, are sterile and produce mycelium

on agar cultures that is variable in pigmentation and often white. Instead of conidia, these species produce short, peg-like appendages (Hambleton and Sigler 2005). *Chloridium paucisporum*, originally isolated from *Pinus resinosa,* produces long, thin, solitary phialides and large globose conidia and bears only superficial resemblance to the type of *Chloridium* (i.e., *C. viride*), which produces percurrent phialides. Although sequence data for *C. viride* are not accessioned in GenBank, other members of the genus are and these are associated with the Chaetothyriales. *Chloridium paucisporum* needs recombining, but, as the species is known only from the type collection, I suggest that redisposition should wait until more isolates have been examined.

Species of *Mollisia* are found in Clades A, B and D, making the genus paraphyletic. Clade A includes *M. cinerea, M. cinerella, M. minutella,* and *M. fusca,* Clade B contains *Phaeomollisia piceae*, and Clade D *M. "rhizophila"* and *M. dextrinospora.* The monotypic *Phaeomollisia* differs from species of *Mollisia* in having darkly pigmented ascospores (Grünig et al. 2009). Teleomorph species in clades A and B, species of *Mollisia* and *Phaeomollisia*, have small asci that do not extend beyond the tips of the paraphyses. The anamorphs in both clades have large conidiogenous apparati and small conidia, i.e., belong to *Phialocephala*. Re-examination of drawings of the "*Phialophora*-like" anamorph of *Mollisia cinerella* (Le Gal and Mangenot 1961) shows multiple phialides branching from a single conidiophore and this reinforces my contention that *Mollisia* species with small asci, a characteristic of *M. cinerella*, are likely to have *Phialocephala* states. In contrast, the species of *Mollisia* in clade D have larger asci and ascospores and

shorter paraphyses (Table 4) along with anamorphs with mostly solitary conidiogenous cells and larger conidia, i.e., belong to *Cadophora*. This pattern holds for a unique isolate of *Cadophora orchidicola*, which has produced a teleomorph labeled *Mollisia "rhizophila"* (Skinner 2007) and the putative link between *Mollisia dextrinospora* and its "*Phialophora*-like" anamorph (Greenleaf and Korf 1980) that consists of single phialides. Based on my re-examination of the original drawing in Greenleaf and Korf, I conclude that this anamorph is a *Cadophora.* Anamorph morphology is clearly a useful source of characters for resolving some of the taxonomic issues associated with the many species of *Mollisia*.

In my analyses and according to both maximum parsimony and Bayesian ancestral character reconstructions, the plesiomorphic state is the production of closely packed groups of phialides, which is characteristic of the outgroup, *Sclerotinia sclerotiorum* and of *Phialocephala* species positioned in Clades A and B. The apomorphic state is represented by the production of reduced phialides, which arose in the ancestor to Clade C and in the most recent common ancestor to *M. "rhizophila"* and *L. orchidicola*. A single reversion to the plesiomorphic state may have occurred in *C. finlandica*. An additional state, solitary phialides, evolved twice, once in the ancestor to Clade D and once in the fungus named *Chloridium paucisporum*.

In the Sclerotiniaceae, some species, e.g., *S. sclerotiorum*, produce dense clusters of phialides on or in persistent melanized sclerotia that form in organs of the infected host. Given the assumption that this type of sporogenic structure

represents an ancestral state within the Helotiales, the complex heads of phialides produced by species of *Phialocephala* might be interpreted as small spermatogenous sclerotia. The heads of densely packed phialides in *P. compacta* exemplify this similarity particularly well (Fig. 5.2 D) because subtending branches are closely packed and darkly pigmented and give rise to minute spores. These sclerotium-like heads also break off easily (Fig. 5.2 H) from the subtending conidiophore increasing the potential of each unit becoming a diaspore. The conidia produced across the genus are small and relatively infrequent, and although there is no evidence that they would be better considered spermatia, there is also no evidence that they function as conidia.

With this model in mind, it appears as though members of *Cadophora* have undergone a reduction in phialide complexity in that they produce solitary to few phialides that do not form in compact clusters. Here, sclerotium-like heads may have been made redundant through an increase in conidial size and frequency. A further reduction in phialide complexity may be represented in the hypothesised aborted phialides of species of *Meliniomyces* and *L. orchidicola*.

Sclerotia serve well in the recurrent colonization of a substrate or host in a given area, as for example the seasonal flush of feeder roots in perennial plants from one year to the next. But while macroscopic sclerotia, such as those formed by *Sclerotinia,* serve as sources of infection in croplands (Willets and Wong 1980) and can be easily monitored, the minute phialidic sclerotia of *P. fortinii* and others, have not been identified *in situ*. Presumably species of *Cadophora* are more reliant on dispersal by conidia although in this regard, it is must be pointed

out that very little is known about the life history of these species. *L. orchidicola* clearly forms intraradical sclerotia in the roots of its hosts (Fernando and Currah 1996) and other root associated *Cadophora* species may be found to do so as well.

In summary, the hypothesis advanced here, concerning single vs. multiple phialide arrangements in *Cadophora* and *Phialocephala*, was challenged using data obtained from limited analyses of a single ribosomal gene. My analyses not only provide some rationale for the diversity of diaspores in DSE and related taxa, but also show that the distribution of anamorphic features is a valuable source of characters for sorting out problems associated with the taxonomically unwieldy genus *Mollisia*. More rigorous tests of my hypothesis may be derived from the analysis of genes directly related to phialidic conidiogenesis. For example, in *Penicillium* and *Aspergillus*, three genes implicated in the transition from multiple to single phialides are *medusa*, *brlA*, and *stuA*. A mutation in the *medusa* gene pathway has been shown to increase the number of metulae, and consequently the number of phialides, in a single conidiogenous head (Timberlake 1990; Adams et al. 1998) while mutations in the *brlA* and *stuA* genes decreased the number of phialides produced (Prade and Timberlake 1993; Adams et al. 1998). Given that the genes controlling conidiogenesis appear to be conserved across the filamentous fungi (Roncal and Ugalde 2003), sequence comparisons of one or more these genes would be useful in elucidating the evolution of phialide arrangement in *Cadophora* and *Phialocephala* and the relationship of this phenomenon to the biology of the species of *Mollisia* and related inoperculate discomycetes.

5.5 Literature Cited

Adams, T.H., Wieser, J.K., and Yu, J-H. 1998. Asexual sporulation in *Aspergillus nidulans.* Microbiology and Molecular. Biology Review. 62: 35-54.

Bills, G.F. 2004. *Cadophora hiberna* sp. nov., a winter-fruiting helotialean anamorph from wood of *Robinia pseudoacacia* and forest soil. *In* Fungi in Forest Ecosystems: Systematics, Diversity and Ecology. *Edited by* C.L. Cripps. Pp 113-123.

Bollback, J. 2006. SIMMAP: Stochastic character mapping of discrete traits on phylogenies. BMC Bioinformatics. 7: 88.

Breitenbach, J. and Kranzlin, F. 1981. Champignons de Suisse. I. Les Ascomycetes. Edition Mykologia. Switzerland.

Conant, N.F. 1937. The occurrence of a human pathogenic fungus as a saprophyte in nature. Mycologia. 29: 597-598.

Currah, R.S., Sigler, L., and Hambleton, S. 1987. New records and new taxa of fungi from the mycorrhizae of terrestrial orchids of Alberta. Canadian Journal of Botany. 65: 2473-2482.

De Hoog, G.S. 1977. *Rhinocladiella* and allied genera. Studies in Mycology. 15: 1-140.

Dennis, R.W.G. 1950. Karsten's species of *Mollisia*. Kew Bulletin. 5: 171-187.

Dennis, R.W.G. 1981. British Ascomycetes. J. Cramer Publishers. Germany.

Felsenstein, J. 1985. Confidence limits on phylogenies: an approach using the bootstrap. Evolution. 39: 783-791.

Fernando, A.A. and Currah, R.S. 1996. A comparative study of the effects of the root endophytes *Leptodontidium orchidicola* and *Phialocephala fortinii* (Fungi Imperfecti) on the growth of some subalpine plants in culture. Canadian Journal of Botany. 74: 1071-1078.

Gams, W. 2000. *Phialophora* and some similar morphologically little-differentiated anamorphs of divergent taxa. Studies in Mycology. 45: 187-199.

Greenleaf, M.A. and Korf, R.P. 1980. *Mollisia* in Macronesia: an exercise in frustration. Mycotaxon. 10: 459-472.

Grünig, C.R., Sieber, T.N., Rogers, S.O., and Holdenrieder, O. 2002. Genetic variability among strains of *Phialocephala fortinii* and phylogenetic analysis of the genus *Phialocephala* based on rDNA ITS sequence comparisons. Canadian Journal of Botany. 80: 1239-1249.

Grünig, C.R., Queloz, V., Duo, A., and Sieber, T.N. 2009. Phylogeny of *Phaeomollisia piceae* gen. sp. nov.: a dark, septate, conifer-needle endophyte and its relationships to *Phialocephala* and *Acephala*. Mycological Research 113: 207-221

Hambleton, S. and Sigler, L. 2005. *Meliniomyces*, a new anamorph genus for root-associated fungi with phylogenetic affinities to *Rhizoscyphus ericae* (≡ *Hymenoscyphus ericae*), Leotiomycetes. Studies in Mycology. 53: 1-22.

Harrington, T.C. and McNew, D.L. 2003. Phylogenetic analysis places the *Phialophora*-like anamorph genus *Cadophora* in the Helotiales. Studies in Mycology. 87: 141-151.

Huelsenbeck, J.P. and Ronquist, F. 2001. MRBAYES: Bayesian inference of phylogeny. Bioinformatics. 1 :754-755.

Jacobs, A., Xoetzee, M.P.A., Wingfield, B.D., Jacobs, K., Wingfield, M.J. 2003. Phylogenetic relationships among *Phialocephala* species and other ascomycetes. Mycologia. 95: 637-645.

Kendrick, W.B. 1961. The *Leptographium* complex. *Phialocephala gen. nov*. Canadian Journal of Botany. 39: 1079-1085.

Kobayashi, K., Tananka, F., Ui, T., and Akai, J. 1979. A new strain of *Cephalosporium gregatum*, causal fungus of brown stem rot of adzuki beans. Annals of the Phytopathological Society of Japan. 45: 409-411.

Le Gal, M. and Mangenot, M.F. 1956. Contribution à l'étude des Mollisioïdées. I. Revue de Mycologie. 21: 3-13.

Le Gal, M., and Mangenot, M.F. 1960. Contribution à l'étude des Mollisioïdées. III. Revue de Mycologie. 26: 263-331.

Le Gal, M., and Mangenot, M.F. 1961. Contribution à l'étude des Mollisioïdées. IV. Revue de Mycologie. 26: 2-214.

Maddison, W.P. and Maddison, D.R. 2009. Mesquite: a modular system for evolutionary analysis. Version 2.6. http:// mesquiteproject.org.

Melin, E., and Nannfeldt, J.A. 1934. Researches into the blueing of ground wood-pulp. Svenska Skogsvårdfören Tidskrift. 32: 397-616.

Nylander, J.A.A. 2004. MrModeltest v2. Program distributed by the author. Evolutionary Biology Centre, Uppsala University.

Prade, R.A., and Timberlake, W.E. 1993. The *Aspergillus nidulans brlA* regulatory locus consists of overlapping transcription units that are individually required for conidiophore development. The EMBO Journal. 12: 2439-2447.

Roncal, T. and Ugalde, U. 2003. Conidiation induction in *Penicillium*. Research. Microbiology. 154: 539-546.

Ronquist, F., and Huelsenbeck, J.P. 2003. MRBAYES 3: Bayesian phylogenetic inference under mixed models. Bioinformatics. 19:1572-1574.

Schmitt, I., del Prado, R., Grube, M., and Lumbsch, H.T. 2009. Repeated evolution of closed fruiting bodies is linked to ascoma development in the largest group of lichenized fungi (Lecanoromycetes, Ascomycota). Molecular Phylogenetics and Evolution. 52: 34-44.

Skinner, S. 2007. Fungal communities associated with the roots of the Betulaceae. M.Sc. Thesis. University of Alberta. Canada.

Swofford, D.L. 2002. PAUP* Phylogenetic analysis using parsimony (* and other methods). Version 4. Sunderland. Sinauer and Associates.

Timberlake, W.E. 1990. Molecular genetics of *Aspergillus* development. Annual Review of Genetics. 24: 5-36.

Vråolstad, T., Schumacher, T., and Taylor, A.F.S. 2002. Mycorrhizal synthesis between fungal strains of the *Hymenoscyphus* aggregate and potential ectomycorrhizal and ericoid hosts. New Phytologist. 153: 143-152.

Wang, C.J.K. and Wilcox, H.E. 1985. New species of extendomycorrhizal and pseudomycorrhizal fungi: *Phialophora finlandia, Chloridium paucisporum,* and *Phialocephala fortinii*. Mycologia. 77: 951-958.

Wang, W., McGhee, D., Gibas, C.F.C., Tsuneda, A., and Currah, R.S. 2009. *Phialocephala urceolata,* sp. nov., from a commercial, water-soluble heparin solution. Mycologia. 101: 136-141.

Willets, H.J. and Wong, J.A.L. 1980. The biology of *Sclerotinia sclerotiorum, S. trifolium,* and *S. minor* with emphasis on specific nomenclature. The Botany Review. 46: 101-165.

Wilson, B.J., Addy, H.D., Tsuneda, A., Hambleton, S., and Currah, R.S. 2004. *Phialocephala sphaeroides* sp. nov., a new species among the dark septate endophytes from a boreal wetland in Canada. Canadian Journal of Botany. 82: 607-617.

Table 5.1. GenBank accessions for isolates to determine patterns of character evolution in *Cadophora* and *Phialocephala*.

Species	Accession number
Ascocoryne sarcoides	AY787686
Cadophora fastigiata	AY249073
Cadophora finlandica	AF486119
Cadophora gregata	U66731
Cadophora hiberna	AF530462
Cadophora luteo-olivacea	AY249066
Cadophora malorum	DQ404350
Cadophora melinii	AY249072
Catenulifera rhodogena	DQ227259
Chloridium paucisporum	EU938675
Chloroscypha chloromela	U92311
Ciboria batschiana	AY526234
Dermea ariae	AF141158
Dermea cerasi	AF141159
Dermea hamamelidis	AF141157
Dermea padi	AF141160

Dermea acerina	AF1A1164
Dermea prunastri	AF141162
Dermea viburni	AF141163
Dicephalospora rufocornea	DQ986480
Fabrella tsugae	U92304
Hemiphacidium longisporum	AY645899
Hyaloscypha daedaleae	AY789416
Hyphodiscus hymenophilus	DQ227264
Lanzia huangshanica	DQ986485
Leotia atrovirens	EU819488
Leotia lubrica	EU819412
Leptodontidium boreale	AY129284
Leptodontidium orchidicola	AF214576
Leptondontidium elatus	AY129285
Meliniomyces variabilis	EF0931467
Meliniomyces bicolor	AY394885
Meliniomyces vraolstadiae	AJ292199

Mollisia cinerea	
Mollisia cinerella	AJ430228
Mollisia cinerella	AJ430222
Mollisia cinerella	AY259135
Mollisia dextrinospora	AY259134
Mollisia fusca	AY259138
Mollisia melaleuca	AY259136
Mollisia minutella	EU314681
*Mollisia ““rhizophila”” *	
Monilinia fructigena	FJ515891
Oidiodendron flavum	AF307763
Oidiodendron griseum	AF062796
Phaeomollisia piceae	EU434836
Phialocephala botulispora	AF083198
Phialocephala compacta	AF486125
Phialocephala dimorphospora	AF486121
Phialocephala fortinii	AY249076

Phialocephala glacialis	EU434843
Phialocephala lagerbergii	AF083197
Phialocephala repens	EU434847
Phialocephala scopiformes	AF486126
Phialocephala sphaeroides	AY524844
Phialocephala urceolata	
Phialocephala virens	AF486132
Sclerotinia sclerotiorum	FJ810516

Table 5.2. Coding of phialide complexity (reduced, single, or multiple phialides) for ancestral character reconstruction in select helotialean fungi.

Species	Coding for character reconstruction	Phialide complexity
Cadophora fastigiata	1	single
Cadophora finlandica	2	multiple
Cadophora gregata	1	single
Cadophora hiberna	2	multiple
Cadophora luteo-olivacea	1	single
Cadophora malorum	1	single
Cadophora melinii	1	single
Chloridium paucisporum	1	single
Leptodontidium orchidicola	0	reduced
Meliniomyces bicolor	0	reduced
Meliniomyces variabilis	0	reduced
Meliniomyces vraolstadiae	0	reduced
Mollisia cinerella	2	multiple
Mollisia dextrinospora	1	single
Phialocephala botulispora	2	multiple
Phialocephala compacta	2	multiple

Phialocephala dimorphospora	2	multiple
Phialocephala fortinii	2	multiple
Phialocephala glacialis	2	multiple
Phialocephala lagerbergii	2	multiple
Phialocephala repens	2	multiple
Phialocephala scopiformis	2	multiple
Phialocephala sphaeroides	2	multiple
Phialocephala urceolata	2	multiple
Sclerotinia sclerotiorum	2	multiple

Table 5.3. Posterior probabilities of character states at a given node generated by SIMMAP. Node numbers refer to those on Figure 5.6.

Node	Frequency	Probability of reduced phialides	Probability of single phialides	Probability of multiple phialides
1	0.9987	0.0221	0.9762	0.0017
2	0.988	0.0014	0.5767	0.4218
3	0.9987	0.7341	0.1549	0.111
4	0.8216	0.9962	0.0022	0.0016
5	1	0.9877	0.0018	0.0105
6	0.9987	0	1	0
7	0.9561	0	1	0
8	0.9987	0.0001	0.9999	0.0001
9	0.9987	0.0001	0.0001	0.9998
10	1	0.0001	0.0001	0.9999
11	0.7177	0	0	1
12	0.9973	0.9999	0.0001	0
13	0.5546	0.0949	0.9047	0.0004
14	0.9161	0.0158	0.9841	0.0001
15	0.996	0.2985	0.0368	0.6646
16	0.0333	0	0	1

17	0.008	0	0	1
18	0.5539	0	0	1
19	0.6951	0	0	1
20	0.9893	0	0	0.9999
21	1	0	0	1
22	0.9587	0	0	0.9999
23	0.9015	0	0	1

Table 5.4. Ascus height, paraphysis height, and ascospores size for species of *Mollisia* affiliated with *Cadophora* and *Phialocephala*.

Species	Ascus height	Paraphysis height	Average ascospore size	Reference
Mollisia cinerea	47-70 µm	51-80 µm	8x2 µm	LeGal and Mangenot 1958
Mollisia cinerella	60-67 µm	60-69 µm	9x1.6 µm	LeGal and Mangenot 1960
Mollisia fusca	47-68 µm	50-53 µm	11x1.8 µm	LeGal and Mangenot 1961
Mollisia melaleuca	52-86 µm	52-86 µm	10.5x2.3 µm	LeGal and Mangenot 1966
Mollisia minutella	49-50 µm	52-53 µm	8x2 µm	Breitenbach and Kränzlin 1981
Mollisia "rhizophila"	30-40 µm	25 µm	7.8x2 µm	Skinner 2007
Mollisia dextrinospora	unavailable	unavailable	5x2.8 µm	Greenleaf and Korf 1980

Figure 5.1 Line drawings showing phialide complexity in *Leptodontidium orchidicola, Cadophora* and *Phialocephala*.

A. Reduced/non functional phialide
B. Single phialide.
C. Complex head of phialides.

A

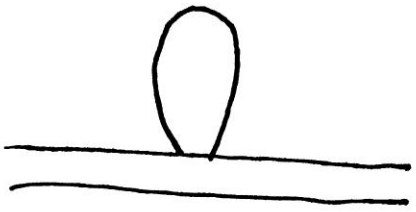

B

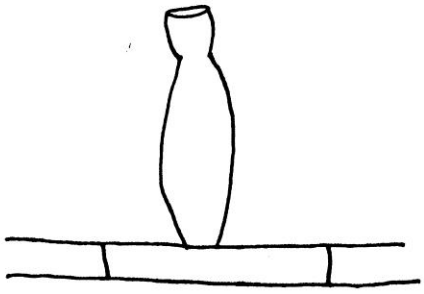

C

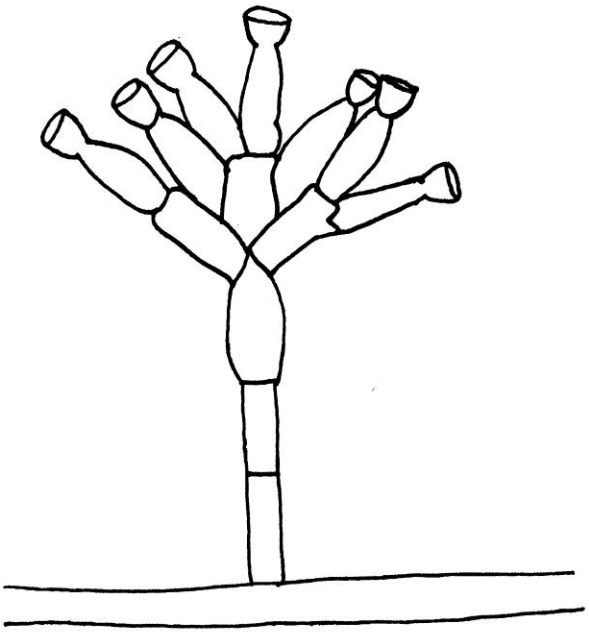

Figure 5.2. Phialides in reduced, solitary, and multiple configurations.

A. Single phialide of *C. fastigiata* UAMH 1221 with abundant conidia adhering to the sides. Bar = 30 μm.
B. SEM of a pair of phialides of *C. melinii* CBS 268.33. Bar = 3 μm.
C. Head of multiple phialides of *C. hiberna* CBS 110521. Bar = 20 μm.
D. Head of multiple phialides of *P. compacta* CBS 507.94. Bar = 30 μm.
E. SEM of head of multiple phialides of *C. hiberna* CBS 110521. Bar = 25 μm.
F. SEM of putative conidium of *L. orchidicola* UAMH 5422. Bar = 3 μm.
G. Reduced or non functional phialides produced by *C. luteo-olivacea* CBS 141.41. Bar = 20 μm.
H. Head of multiple phialides of *P. fortinii* (unaccessioned) that has broken off from the conidiophore. Bar = 30 μm.

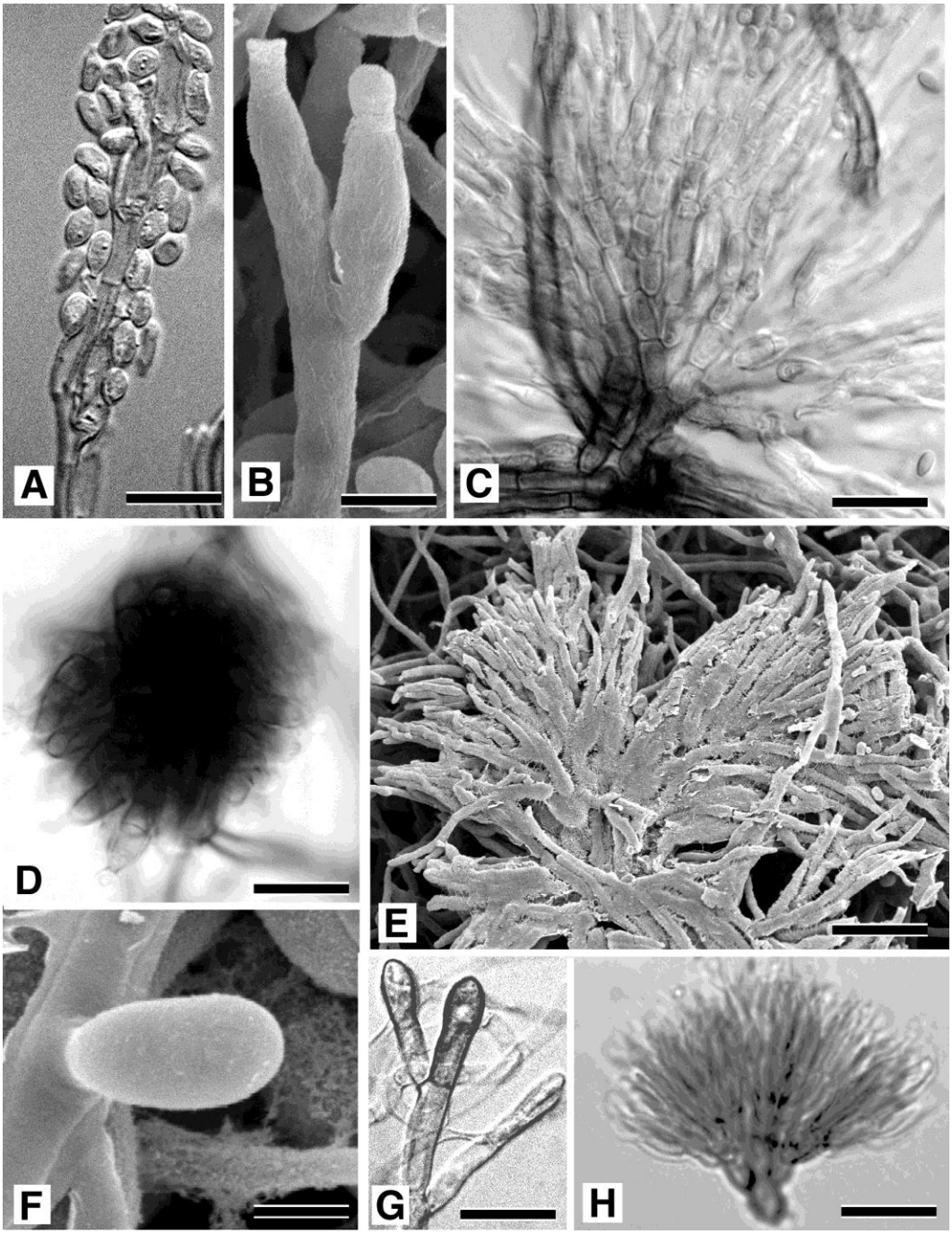
A
B
C
D
E
F
G
H

Figure 5.3. One of six most parsimonious trees showing the relationship between the target taxa and the Helotiales based on the ITS region. Lines in bold represent nodes with greater than 50% support with both bootstrap and Bayesian posterior probabilities. The trees are 2311 steps long and the CI is 0.395 and the RI is 0.593.

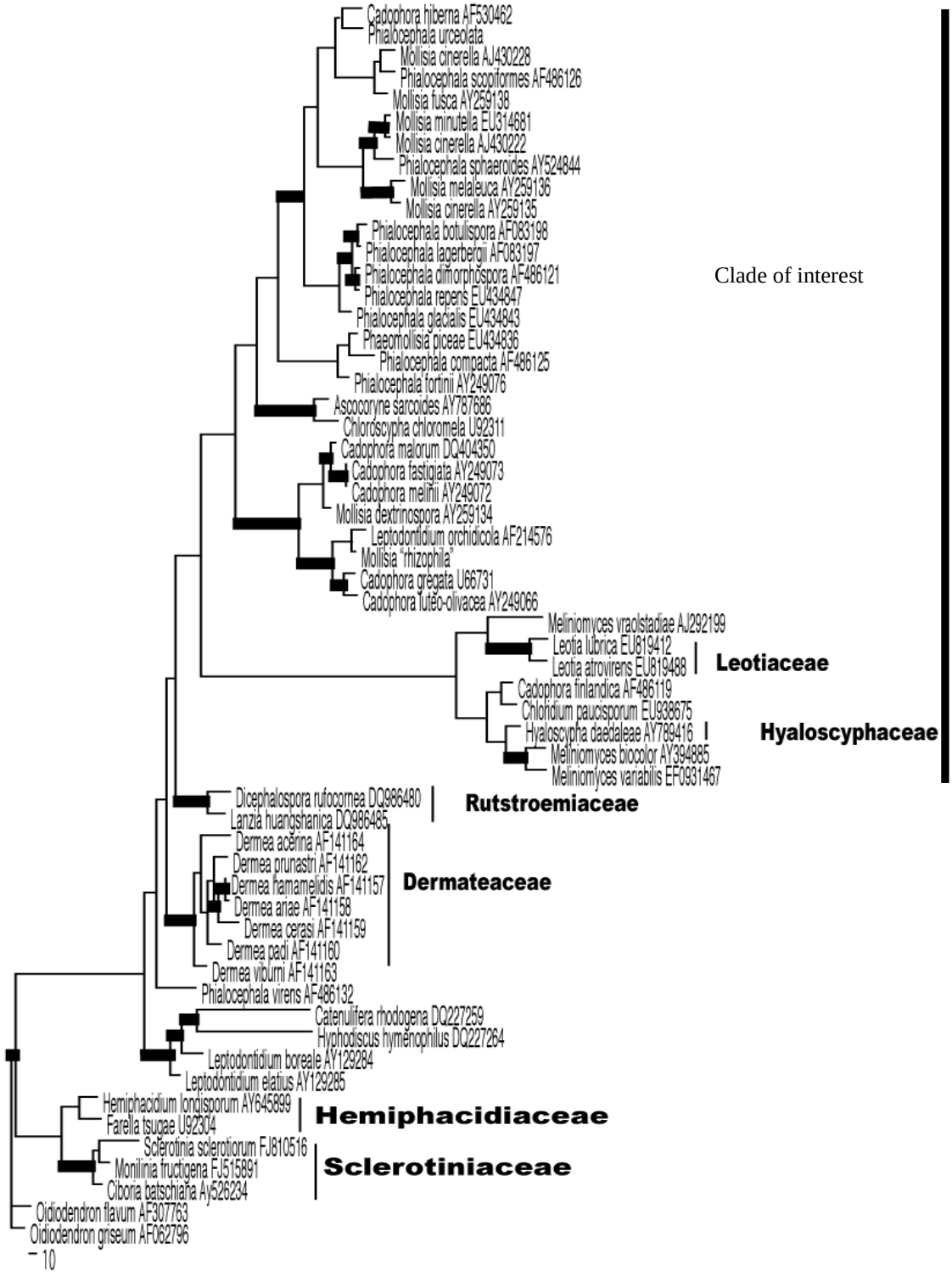
Cadophora hiberna AF530462
Phialocephala urceolata
Mollisia cinerella AJ430228
Phialocephala scopiformes AF486126
Mollisia fusca AY259138
Mollisia minutella EU314681
Mollisia cinerella AJ430222
Phialocephala sphaeroides AY524844
Mollisia melaleuca AY259136
Mollisia cinerella AY259135
Phialocephala botulispora AF083198
Phialocephala lagerbergii AF083197
Phialocephala dimorphospora AF486121
Phialocephala repens EU434847
Phialocephala glacialis EU434843
Phaeomollisia piceae EU434836
Phialocephala compacta AF486125
Phialocephala fortinii AY249076
Ascocoryne sarcoides AY787686
Chloroscypha chloromela U92311
Cadophora malorum DQ404350
Cadophora fastigiata AY249073
Cadophora melinii AY249072
Mollisia dextrinospora AY259134
Leptodontidium orchidicola AF214576
Mollisia "rhizophila"
Cadophora gregata U66731
Cadophora luteo-olivacea AY249066
Meliniomyces vraolstadiae AJ292199
Leotia lubrica EU819412
Leotia atrovirens EU819488
Leotiaceae
Cadophora finlandica AF486119
Chloridium paucisporum EU938675
Hyaloscypha daedaleae AY789416
Hyaloscyphaceae
Meliniomyces bicolor AY394885
Meliniomyces variabilis EF0931467
Clade of interest
Dicephalospora rufocornea DQ986480
Rutstroemiaceae
Lanzia huangshanica DQ986485
Dermea acerina AF141164
Dermea prunastri AF141162
Dermea hamamelidis AF141157
Dermea ariae AF141158
Dermea cerasi AF141159
Dermea padi AF141160
Dermea viburni AF141163
Dermateaceae
Phialocephala virens AF486132
Catenulifera rhodogena DQ227259
Hyphodiscus hymenophilus DQ227264
Leptodontidium boreale AY129284
Leptodontidium elatius AY129285
Hemiphacidium longisporum AY645899
Farella tsugae U92304
Hemiphacidiaceae
Sclerotinia sclerotiorum FJ810516
Monilinia fructigena FJ515891
Ciboria batschiana Ay526234
Sclerotiniaceae
Oidiodendron flavum AF307763
Oidiodendron griseum AF062796
10

Figure 5.4. One of 11 most parsimonious trees showing the relationship between the target taxa (including teleomorphs) based on the ITS region. Lines in bold represent nodes with greater than 50% support with both bootstrap and Bayesian posterior probabilities. The trees are 1186 steps long and the CI is 0.655 and the RI is 0.677.

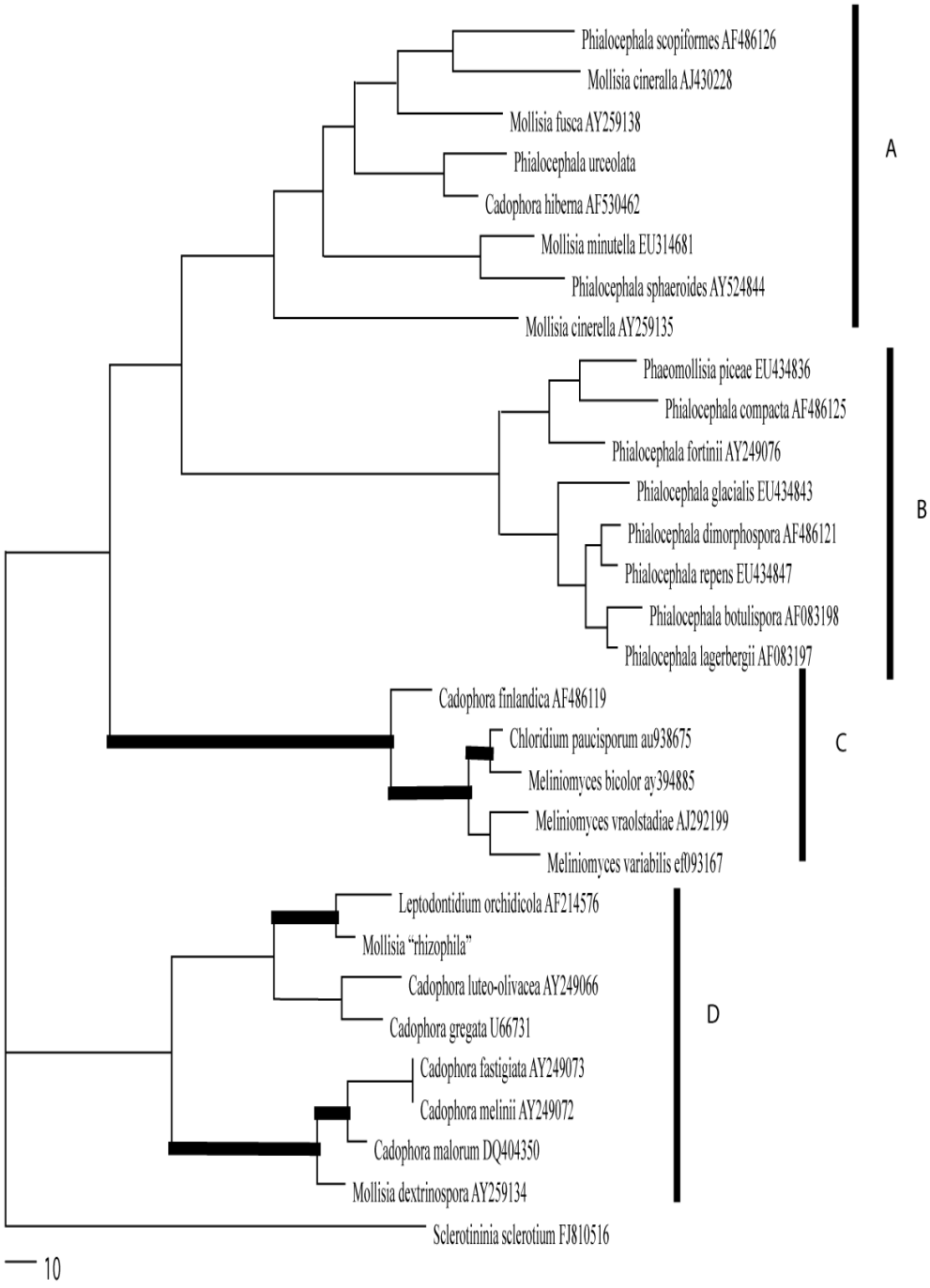
Phialocephala scopiformes AF486126
Mollisia cinerella AJ430228
Mollisia fusca AY259138
Phialocephala urceolata
Cadophora hiberna AF530462
Mollisia minutella EU314681
Phialocephala sphaeroides AY524844
Mollisia cinerella AY259135
A
Phaeomollisia piceae EU434836
Phialocephala compacta AF486125
Phialocephala fortinii AY249076
Phialocephala glacialis EU434843
Phialocephala dimorphospora AF486121
Phialocephala repens EU434847
Phialocephala botulispora AF083198
Phialocephala lagerbergii AF083197
B
Cadophora finlandica AF486119
Chloridium paucisporum au938675
Meliniomyces bicolor ay394885
Meliniomyces vraolstadiae AJ292199
Meliniomyces variabilis ef093167
C
Leptodontidium orchidicola AF214576
Mollisia "rhizophila"
Cadophora luteo-olivacea AY249066
Cadophora gregata U66731
Cadophora fastigiata AY249073
Cadophora melinii AY249072
Cadophora malorum DQ404350
Mollisia dextrinospora AY259134
D
Sclerotinia sclerotium FJ810516
10

Figure 5.5. One of five most parsimonious trees showing the relationship between the target taxa (excluding teleomorphs) based on the ITS region. Lines in bold represent nodes with greater than 50% support with both bootstrap and Bayesian posterior probabilities. The trees are 681 steps long and the CI is 0.651 and the RI is 0.722.

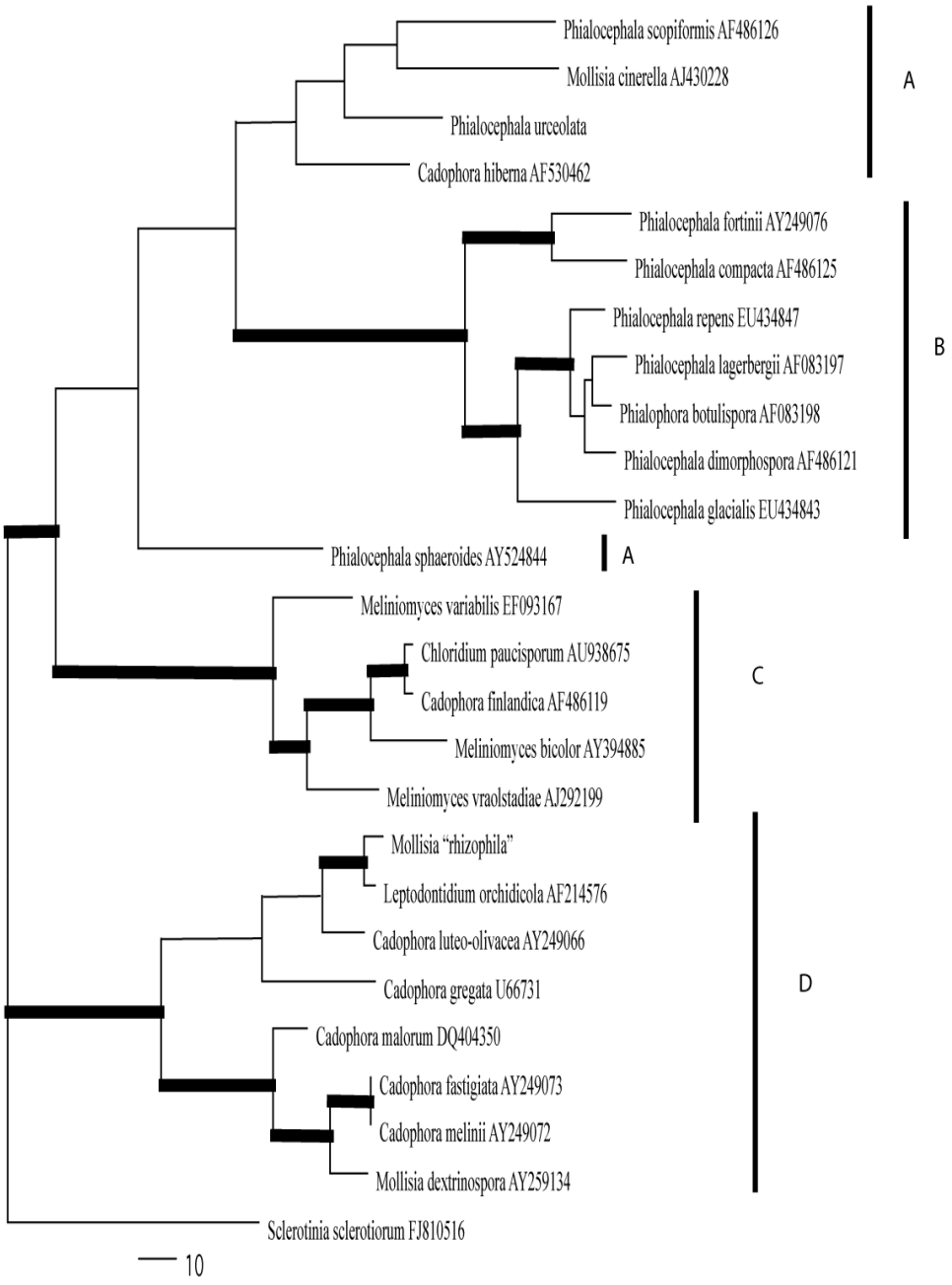
Phialocephala scopiformis AF486126
Mollisia cinerella AJ430228
Phialocephala urceolata
Cadophora hiberna AF530462
A
Phialocephala fortinii AY249076
Phialocephala compacta AF486125
Phialocephala repens EU434847
Phialocephala lagerbergii AF083197
Phialophora botulispora AF083198
Phialocephala dimorphospora AF486121
Phialocephala glacialis EU434843
B
Phialocephala sphaeroides AY524844
A
Meliniomyces variabilis EF093167
Chloridium paucisporum AU938675
Cadophora finlandica AF486119
Meliniomyces bicolor AY394885
Meliniomyces vraolstadiae AJ292199
C
Mollisia "rhizophila"
Leptodontidium orchidicola AF214576
Cadophora luteo-olivacea AY249066
Cadophora gregata U66731
Cadophora malorum DQ404350
Cadophora fastigiata AY249073
Cadophora melinii AY249072
Mollisia dextrinospora AY259134
D
Sclerotinia sclerotiorum FJ810516
10

Figure 5.6. One of five most parsimonious trees showing the ancestral character reconstruction for number of phialides. White nodes represent taxa with reduced phialides. Green nodes represent taxa with single phialides. Black nodes represent taxa with multiple phialides.

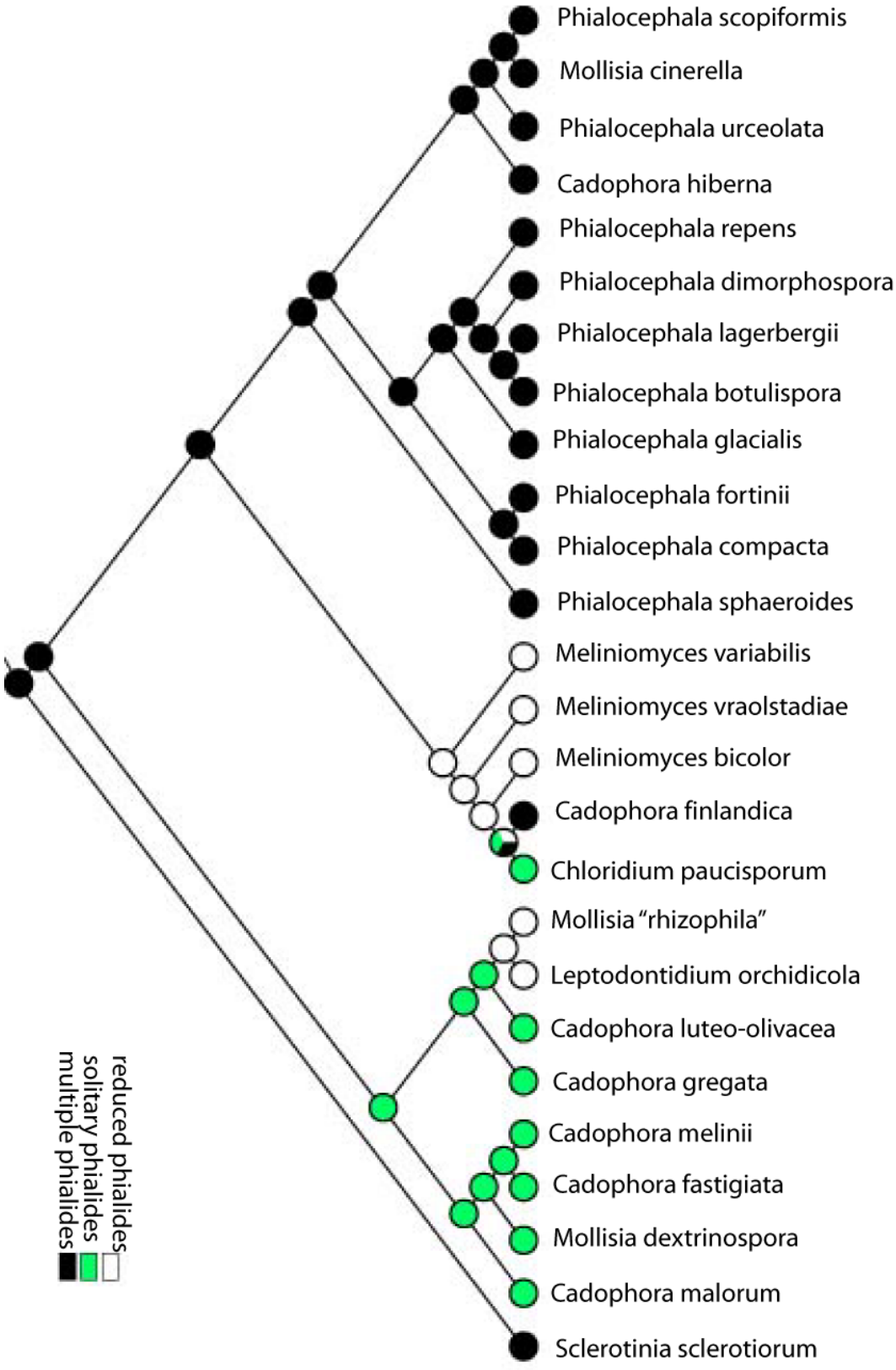
Phialocephala scopiformis
Mollisia cinerella
Phialocephala urceolata
Cadophora hiberna
Phialocephala repens
Phialocephala dimorphospora
Phialocephala lagerbergii
Phialocephala botulispora
Phialocephala glacialis
Phialocephala fortinii
Phialocephala compacta
Phialocephala sphaeroides
Meliniomyces variabilis
Meliniomyces vraolstadiae
Meliniomyces bicolor
Cadophora finlandica
Chloridium paucisporum
Mollisia "rhizophila"
Leptodontidium orchidicola
Cadophora luteo-olivacea
Cadophora gregata
Cadophora melinii
Cadophora fastigiata
Mollisia dextrinospora
Cadophora malorum
Sclerotinia sclerotiorum
reduced phialides
solitary phialides
multiple phialides

Figure 5.7. Bayesian consensus tree showing the ancestral character reconstruction of number of phialides. White nodes represent taxa with reduced phialides. Green nodes represent taxa with single phialides. Black nodes represent taxa with multiple phialides. Numbers at the nodes correspond to the nodes in Table 5.3.

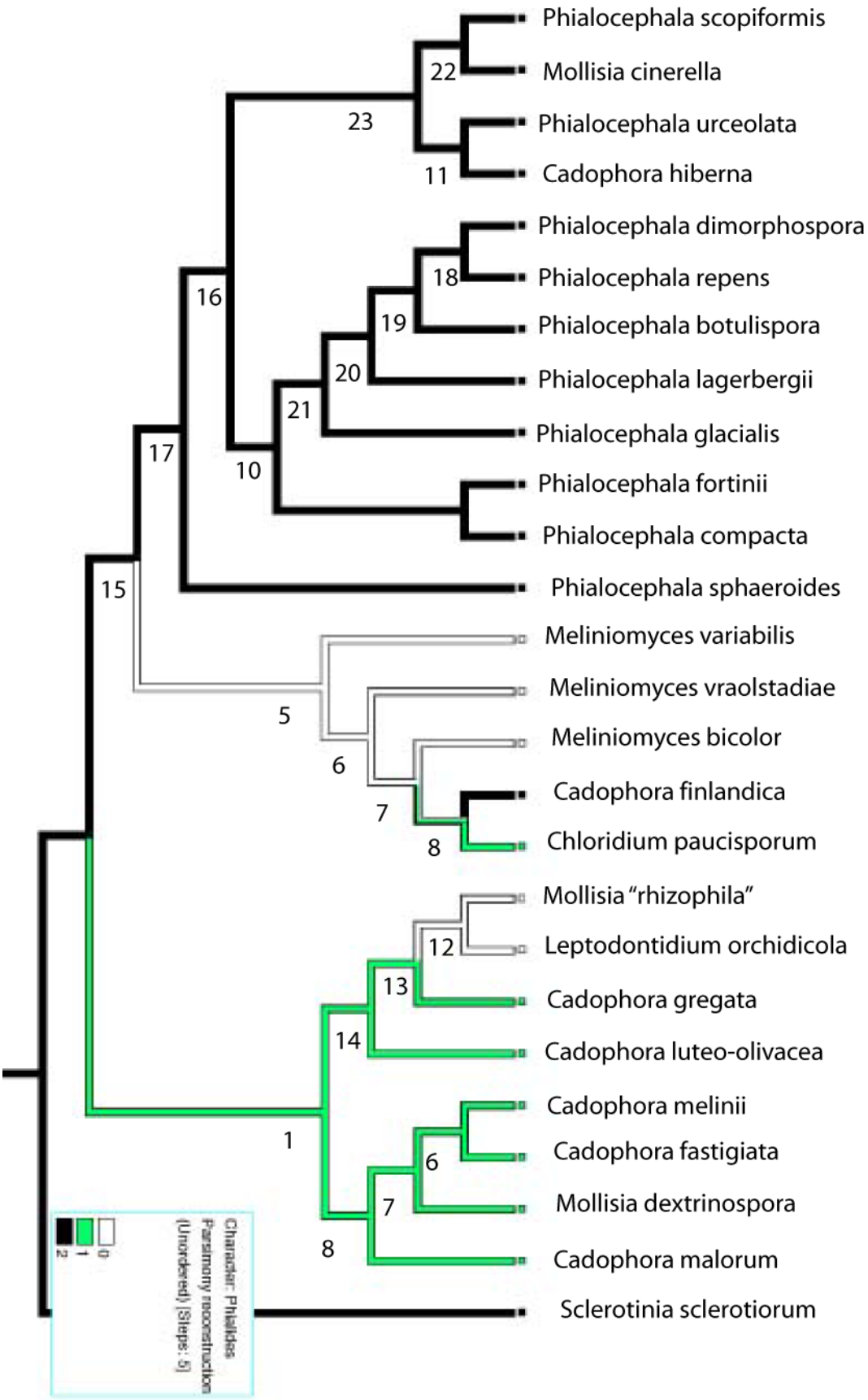
Phialocephala scopiformis
Mollisia cinerella
Phialocephala urceolata
Cadophora hiberna
Phialocephala dimorphospora
Phialocephala repens
Phialocephala botulispora
Phialocephala lagerbergii
Phialocephala glacialis
Phialocephala fortinii
Phialocephala compacta
Phialocephala sphaeroides
Meliniomyces variabilis
Meliniomyces vraolstadiae
Meliniomyces bicolor
Cadophora finlandica
Chloridium paucisporum
Mollisia "rhizophila"
Leptodontidium orchidicola
Cadophora gregata
Cadophora luteo-olivacea
Cadophora melinii
Cadophora fastigiata
Mollisia dextrinospora
Cadophora malorum
Sclerotinia sclerotiorum
22
23
11
18
16
19
20
21
17
10
15
5
6
7
8
12
13
14
1
6
7
8
Character: Phialides
Parsimony reconstruction
(Unordered) (Steps: 5)
2
1
0

Figure 5.8. Conidial lengths and widths of species of *Phialocephala* and *Cadophora*. Clades A, B, and C refer to those found in Figure 4. Cmal = *Cadophora malorum*, Clo = *Cadophora luteo-olivacea*, Cfast = *Cadophora fastigiata*, Cgreg = *Cadophora gregata*, Cmel = *Cadophora melinii*, Lo = *Leptodontidium orchidicola*, Plag = *Phialocephala lagerbergii*, Pbot = *Phialocephala botulispora*, Chib = *Cadophora hiberna*, Pglac = *Phialocephala glacialis*, Pscop= *Phialocephala scopiformis*, Prep = *Phialocephala repens*, Pcom = *Phialocephala compacta*, Pdi = *Phialocephala dimorphospora*, Purc = *Phialocephala urceolata*, Pf = *Phialocephala fortinii*, Psphaer = *Phialocephala sphaeroides*

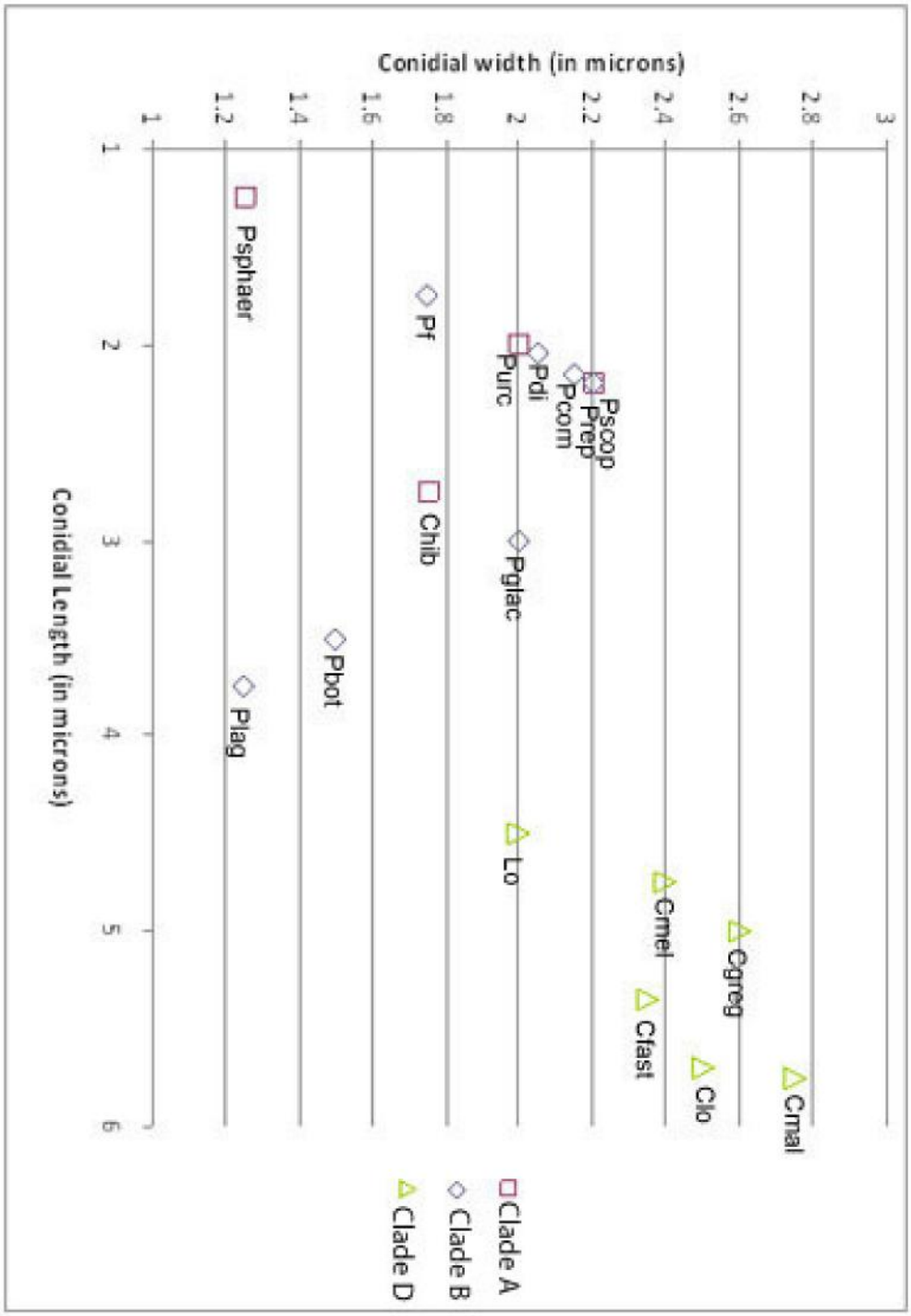
Conidial width (in microns)
3
2.8
2.6
2.4
2.2
2
1.8
1.6
1.4
1.2
1
Cmal
Cgreg
Clo
Cmel
Cfast
Pscop
Prep
Pcom
Pdi
Purc
Pf
Chib
Pglac
Lo
Pbot
Psphaer
Plag
Clade A
Clade B
Clade D
Conidial Length (in microns)
1
2
3
4
5
6

Chapter 6. Conclusion

This thesis is an account of some ecological and taxonomic aspects of a select group of dematiaceous hyphomycetes representing the Helotiales, Pleosporales, and Coniochaetales, that were deemed of potential importance to soil formation and plant establishment in post glacial environments. These orders encompassed many of the isolates from two collections of microfungi obtained from alpine and arctic habitats. I focused on two dark septate endophyte species (*Leptodontidium orchidicola, Phialocephala fortinii)*, two potential DSE species (*Cadophora luteo-olivacea* and *C. melinii*), three species isolated from bryophytes (*Ulocladium atrum, Curvularia inaequalis*, and *Coniochaeta nepalica*), and two from vascular plants (*Chalastospora gossypii* and *Monodictys arctica*) for further study. *Leptodontidium orchidicola, P. fortinii, C. luteo-olivacea,* and *C. melinii* were obtained from culture collections. I examined the nature and development of the propagules of several of these species, because of their taxonomic and ecological importance, and the ability of eight species to break down native or near-native substrates, to examine their potential roles in the humification of bryophytes, and hence soil formation, and in plant establishment.

Seven isolates from Ellesmere Island represented a new species of the hyphomycete genus *Monodictys, M. arctica*, which was in part characterised by large, multicelled, often branched conidia that resemble small sclerotia. Dark septate endophytic fungi are typically promiscuous in terms of host, yet *M. arctica* isolates were all from roots of *Saxifraga oppositifolia* even though the roots of other plants (*Cassiope tetragona, Dryas integrifolia*, and *Salix arctica*) in

the same area had also been surveyed. The closest phylogenetic relative to *M. arctica* was *Leptosphaeria dryadophila*, a loculoascomycete known from stromatic spots on the leaves and flowers of *Dryas*. *Monodictys arctica* did not produce a sexual state in culture, but a teleomorph in *Leptosphaeria* is expected. *Monodictys arctica* is unusual among other described anamorphs of *Leptosphaeria*, which are otherwise all pycnidial.

I was not able to explore the relationship between *M. arctica* and its host because the roots from which the isolates had been obtained were unavailable. Through personal communication with Kei Fujimura, the collector, I learned that all were healthy in appearance so *M. arctica* may be a DSE species as many Dothideomycetes are suspected to occupy this niche (Kadir et al. 2010). Some detailed study of the relationship of this fungus with host roots would be valuable. For instance, it would be of particular interest to see if this species forms sclerotia within roots of the host, and whether they bear any resemblance to the morphology of the conidia. In this manner, the fungus might resemble *Phialocephala fortinii*, in producing intra- and extraradical sclerotia or sclerotium-like conidiogenous structures. It would also be interesting to see if *M. arctica* could be induced to form a teleomorph so that my hypothesis about a *Monodictys-Leptosphaeria* link could be tested.

I examined the abilities of eight fungi to degrade *in vitro* the leaves and stems of the gametophyte of *Hylocomium splendens*. The species were divided into two groups, one consisting of the pleosporalean hyphomycetes *Ulocladium atrum*, *Chalastospora gossypii*, and *Curvularia inaequalis*, and the other of the

helotialean fungi *Leptodontidium orchidicola, Phialocephala fortinii, Cadophora melinii,* and *Cadophora luteo-olivacea* with *Coniochaeta nepalica* (Coniochaetales) as an additional known saprobe. For the first group i.e., the pleosporalean fungi, SEM observations were congruent with the enzymatic results (all could degrade cellulose, starch, and protein but not insoluble polyphenols) in that they were able to degrade the cellulose-rich outer cell wall but not the inner polyphenol-rich layer. Using these data to predict their action on site, I postulated that the enzymatic activities of these saprobes would cause the senescent leaves of bryophytes to disarticulate into component cells or clumps of cells that would then accumulate in the lower reaches of the grout column along with other wind- and water-borne organic particulates. In this way, these widespread fungi would be expected to play an important role in pedogenesis in post glacial areas.

The second group, consisting of four helotialean fungi and *Coniochaeta nepalica,* provided an interesting comparison with the three representatives of the Pleosporales. All fungi were able to degrade some components of the bryophyte tissues but colonisation patterns varied with *Coniochaeta nepalica, L. orchidicola,* and *C. luteo-olivacea* exhibiting the most pronounced disruption of the substrate and *P. fortinii,* and *C. melinii* the least. In addition to producing an abundant growth of mycelium, *C. nepalica* eroded the cellulose-rich cell wall layer, but not the inner layer rich in polyphenols indicating that this species is at least a potentially competent saprobe in postglacial alpine habitats. *Leptodontidium orchidicola* also formed abundant mycelium while exfoliating the outer layer of the bryophyte cell wall. In addition, my isolate also formed bore holes through the

inner layer, suggesting both cellulosic and polyphenolic components could be degraded. In contrast, the growth of *P. fortinii* was sparse and confined to junctions between adjacent cells and caused only slight thinning of the outer layer. Both *P. fortinii* and *L. orchidicola* were able to form clumps of cells, resembling sclerotia, within the bryophyte tissues supporting the suggestion that the two are capable saprobes and more likely to be weak parasites of roots rather than mycorrhizal partners.

The pattern of degradation caused by *C. luteo-olivacea* was similar to that caused by *L. orchidicola* in both the pattern of decay of the outer layer and in the formation of bore holes through the inner layer but did not form structures resembling sclerotia. Recent reports of this species from roots indicate that the species should be investigated in more detail for its role as member of the DSE. There was only scant growth produced by *C. melinii*. Either the culture used was degenerate or mostly unable to grow on the material provided.

During these studies, I found that mass loss determinations for bryophyte substrates were difficult to make consistent and reproducible. The technique was helpful because it was possible to see differences in colonisation patterns, especially with the SEM, but mass loss measurements varied dramatically due, I assume, to the physical and potential chemical heterogeneity of the substrate and the difficulty of removing hyphae from the irregular surfaces of the gametophytes. Nevertheless, I concluded that all of the species could potentially be part of a bank of endophytes in place ready to colonise post-glacial vascular plant pioneer species. *Leptodontidium orchidicola* and *Phialocephala fortinii* seemed well-

adapted to persist and disperse in windblown or water borne gametophyte fragments and the ability to sporulate abundantly would allow *Cadophora melinii* and *Coniochaeta nepalica* to disseminate from colonized materials. *Cadophora luteo-olivacea* neither sporulated nor formed sclerotia but might persist as hyphal fragments in bryophyte detritus.

In both decomposition studies, enzymatic profiles were somewhat misleading in that the positive reaction on the tannic acid medium (soluble polyphenols), indicated that most should have been capable of degrading at least some lignin-like compounds. *Leptodontidium orchidicola* and *Phialocephala fortinii* both had positive reactions on the wood guiacol medium (insoluble polyphenols), but only *L. orchidicola* created bore holes through the polyphenol rich cell wall layer.

Clearly the moss grout is a unique microcosm with intriguing interrelationships among diverse biotic and abiotic components. A detailed study of the role of a much wider range of fungi, especially including basidiomycetes, the organic particulates and organisms (e.g. pollen, and other organic detritus, fungi, bacteria, etc.) in the vertical strata of the grout would provide an interesting look at pedogenesis along a successional chronosequence. It would also be valuable to review the degradative abilities of arctic and alpine ascomycetes, which would make a valuable companion study to similar published work on the basidiomycetes.

Most published decomposition work focuses on wood decay. Investigations into the ability of fungi to degrade mosses rely heavily on

terminology from that field, and these may not be applicable (e.g. white rot, brown rot). *In situ* tests involving the same fungal species on both wood and moss would provide a basis for comparison between the two substrates and help to determine the applicability of using wood decay terminology for moss decomposition. As well, the studies on moss decomposition to date have looked at mosses with two different morphologies (i.e., *Sphagnum* vs. *Hylocomium*), and possibly cell wall components, making it difficult to determine whether the differences in decay are due to the fungi used or the substrate. Inoculating the same suite of fungal species onto many different moss species would determine the effect of the substrate on decay abilities.

During my work with *Cadophora* and *Phialocephala* in the decomposition studies, and while trying to identify the fungi comprising my collection, it became clear that the main characteristic delineating the two genera was the number of phialides per conidiophore. In the character evolution study presented in chapter 5, I found support for the assumption that the pleisomorphic state would be dense clusters of multiple phialides, characteristic of many species of *Phialocephala* and *Sclerotinia,* while the solitary phialides characteristic of most species of *Cadophora* would be derived. An interesting outcome of this work was a pattern of congruence between anamorph and teleomorph characters in that *Cadophora* anamorphs were associated with *Mollisia* states with asci larger than paraphyses, one clade of *Phialocephala* anamorphs was associated with *Mollisia* states with paraphyses larger than ascospores, and one clade of *Phialocephala* anamorphs was associated with the *Phaeomollisia*. I also rationalised why a reduction in size

of the sclerotium-like phialidic apparatus would be correlated with an increase in conidial size and perhaps number. This work provided a hypothesis about why *L. orchidicola* and *P. fortinii* are among the most frequently reported DSE. The two species have made trade-offs during their evolution to minimize the role of conidia in dissemination and to increase the role of sclerotia as structures allowing repeated infection of a host following the phenology of feeder roots. This hypothesis needs to be challenged, perhaps by studying these fungi and hosts in artificial microcosms. Any such data would contribute further to our understanding of the interrelationship of ecological and evolutionary characteristics of the dematiaceous hyphomycetes.

6.1 Literature cited.

Kadir, H.H., Eudy, D.M. Porras-Alfaro, A., Herrera, J., Natvig, D.O., and Sinsabaugh, R.L. 2010. A general suite of fungal endophytes dominate the roots of two dominant grasses in a semi-arid grassland. J. Arid Environments. 74: 35-42.

Appendix A – Glossary

Alternarioid – obpyriform with a conspicuous beak; resembles the conidia of *Alternaria.*

Anamorph – the asexually reproducing state of a fungus.

Apothecium – a saucer/disc shaped sexual fruiting body of an ascomycetous fungus.

Appressorium – a swelling in a hypha above the point of entry into a plant cell.

Ascus – cell or meiosporangium in which the sexual spores are produced in an ascomycetous fungus.

Axil – area where the leaf joins the stem in an embryophyte.

Blastic – a type of conidiogenesis cell where the conidium is blown out or through the conidiogenous cell or hypha.

Conidiogenesis – the process of forming conidia.

Conidium – a non-motile asexual spore that is not formed by free cell formation or cleavage of the cytoplasm.

Cruciseptate – forming septa in a cross-like arrangement in a single cell.

Dark septate endophyte – a darkly pigmented fungus that lives asymptomatically in the roots of vascular plants.

Dematiaceous hyphomycete – a darkly pigmented conidial fungus with exposed or unenclosed conidiophores.

Ectomycorrhiza – a type of mycorrhiza in which the fungus forms a sheath on the outer surface of the roots and surrounds the cortical cell walls to form a Hartig net.

Loculoascomycete – an artificial assemblage of fungi in which asci develop inside locules which are enzymatically formed in a stroma.

Microsclerotium – a small, darkly pigmented, mass of swollen cells formed in the roots of vascular plants by some dark septate endophytes.

Monilioid – a hypha which is regularly constricted to form a “string of pearls” like configuration.

Mycorrhiza – an association between plant roots and fungi in which there is a presumed reciprocal transfer of nutrients.

Obpyriform – upside down pear shaped.

Paraphysis – sterile hair found among the asci in some ascomata.

Perithecium – a flask shaped sexual fruiting body produced by some members of the Ascomycota.

Phialide – a conidiogenous cell with a fixed conidiogenous locus through which conidia are produced basipetally.

Poikilohydric – the ability to desiccate and rehydrate with no impairment of cell function.

Pseudoparaphylia – the hair-like projections on the stems of some moss gametophytes.

Pycnidium – a flask shaped structure formed of fungal hyphae in which the phialides are found.

Rhexolytic dehiscence – breaking away of a conidium by means of breaking the transverse walls of the subtending cell.

Sclerotial head – a dense cluster of phialides that resembles a sclerotium.

Sclerotium – a multi-hyphal, resting/dissemintive body often impregnated with melanins.

Septum – cross wall.

Teleomorph – the sexual state of a fungus.

Toruloid – cylindrical cells with swellings at the septum so the cell resembles a knucklebone